



## A review for phase change materials (PCMs) in solar absorption refrigeration systems



Mohammed Mumtaz A. Khan<sup>a</sup>, R. Saidur<sup>a,c,\*</sup>, Fahad A. Al-Sulaiman<sup>a,b</sup>

<sup>a</sup> Center of Research Excellence in Renewable Energy (CORE-RE), Research Institute, King Fahd University of Petroleum & Minerals, Dhahran 31261, Saudi Arabia

<sup>b</sup> Mechanical Engineering Department, King Fahd University of Petroleum & Minerals, Dhahran 31261, Saudi Arabia

<sup>c</sup> Research Centre for Nano-Materials and Energy Technology (RCNMET), School of Science and Technology, Sunway University, No. 5, Jalan Universiti, Bandar Sunway, 47500 Petaling Jaya, Malaysia

### ARTICLE INFO

#### Keywords:

Phase change materials  
Solar absorption system  
Thermal energy storage  
Latent heat

### ABSTRACT

Energy storage has become an important part in renewable energy technology systems. Solar thermal systems, unlike photovoltaic systems with striving efficiencies, are industrially matured, and utilize major part of sun's thermal energy during the day. Yet, it does not have enough (thermal) backup to keep operating during the low or no solar radiation hours. New materials are selected, characterized, and enhanced in their thermo-physical properties to serve the purpose of a 24 h operation in an efficient thermal energy storage system (TESS). Solar absorption refrigeration system requires a continuous operation in many of its applications (food storage, space cooling etc), which in turn requires an efficient TES system utilizing material with high heat of fusion, eg. phase change materials (PCMs). This review is a comprehensive evaluation of suitable PCM selection, methodologies of integration, enhancements and challenges for operating temperatures of each component in a single-effect solar absorption system affecting its performance. Observations and lessons from previous studies are discussed in detail. Recommendations based on investigation results, advantages and drawback of PCMs, PCM enhancement options, energy, exergy and cost analysis are made for the future research direction.

### 1. Introduction

Increasing global population demanding for a better life has given rise to numerous inventions for comfort livings. As a result, problems like global warming and greenhouse effect contributed to imbalance the nature. Therefore, we realized how to make use of nature without exploiting it. Renewable energies like solar radiation, ocean waves, wind, hydel, biogas etc. has been playing a major role in reforming the natural balance and providing the needs of growing population demand [1].

Although renewable energy technologies contribute to about 1% of world energy supply, numerous efforts are being made to shift the paradigm of power source from fossil fuel to environment-friendly alternatives [2]. Parabolic trough and concentrated solar collectors are renewable based technologies integrated with power generation system. Direct steam generation is one such area which has been explored by researchers extensively [3]. Similarly, photovoltaic, wind and solar-MED technologies are mostly integrated in water desalination industry [4]. Although photovoltaic technology is continuously pushing its limits

[5], further improvements are needed for its better performance.

One of the applications which became a necessity rather than a luxury is air-conditioning and refrigeration systems, as predicted and explored by Tabor [6] in 1962. Since then, numerous attempts [7–13] were made to develop new technologies and optimize them for better living. This review analyses suitable usage of PCM technology in absorption cooling system. Grossman [14] compared different trends in studying closed and open cycle solar air conditioning and dehumidification systems. He concluded that absorption cycles are more promising over heat-powered cycles. He also mentioned that higher COPs can be achieved with double-effect LiBr-water absorption chillers whereas quality air-conditioning with independent temperature and humidity control can be achieved by open cycle systems. Balaras et al. [15] surveyed and analyzed over 50 solar powered cooling projects in Europe to evaluate the future needs of solar cooling technology. They found that solar assisted cooling systems can save 40–50% primary energy with 0.07€/kW. Lamp and Ziegler [12] studied the research trends leading to innovations in solar assisted air cooling. Their study revealed that research was focused towards cheaper collectors with

\* Corresponding author at: Center of Research Excellence in Renewable Energy (CORE-RE), Research Institute, King Fahd University of Petroleum & Minerals, Dhahran 31261, Saudi Arabia.

E-mail addresses: [saidur912@yahoo.com](mailto:saidur912@yahoo.com), [saidur@kfupm.edu.sa](mailto:saidur@kfupm.edu.sa) (R. Saidur).

<http://dx.doi.org/10.1016/j.rser.2017.03.070>

Received 3 April 2016; Received in revised form 13 February 2017; Accepted 10 March 2017

Available online 17 March 2017

1364-0321/© 2017 Elsevier Ltd. All rights reserved.

higher output temperatures, and efficient chillers to work at low-grade heat. They mentioned that intermittent solar radiation is one of the major constraints solar powered cooling systems. The use of thermal storage, although initially, couldn't provide effective backup, but helped the system to thermally stabilize. Consequently, thermal storage made its place in solar assisted thermal systems [16]. Since then, studying thermal energy storage technologies, usability and affect of both sensible and latent heat storage (PCM) in numerous applications increased, leading to a number of reviews [17–23]. These reviews focused only on one side (cold or hot) or component of the system or integral mechanism in it. Moreover, the studies could only cover one temperature range in either hot or cold side, irrespective to the systems requiring various temperature ranges (cooling and refrigeration). For example, Pintaldi et al. [24] reviewed thermal energy storage technologies and control approaches for solar cooling system. They mainly focused on types of thermal storages used in solar cooling applications, with emphasis on higher temperatures ( $> 100\text{ }^{\circ}\text{C}$ ). Tian and Zhao [25] compiled various types of research in solar collectors and thermal energy storages used for solar thermal applications. Joybari et al. [26] compiled a review on PCM for cold storage for the application of domestic refrigeration i.e., evaporator side only. Oró et al. [27] also compiled a review of PCM for cold storage covering all types and applications used till 2011. Their study covered ice-storage and air-conditioning separately. However, there are complete absences of reviews on topics like: the affect of PCM at condenser; and PCM in solar cold storage. Various designs, methodologies, and enhancements have been conducted that were never compiled to understand how solar absorption system performance can be enhanced. Likewise, there are other reviews [28–35] briefly mentioning classifications of PCM, suitable applications, integration and related generalized issues separately, but none focused with respect to a specific application. The present study focuses on how and what PCMs can be used at each component of a solar powered absorption refrigeration system operating a various temperature ranges throughout the cycle. The present review is intended to bring forth a detailed evaluation of selection criteria, methods of integration, enhancement techniques, challenges and solutions of using PCM in various components (with various operating temperatures) in a solar absorption system. The review congregates the investigations performed in the temperature range of  $-15\text{--}150\text{ }^{\circ}\text{C}$  with PCM throughout various cooling and heating applications, and then classifying their applicability with respect the system in focus and present the effect on performance. The review is expected to provide selection preferences, basis of approach, and a scholarly guide in using PCM to its fullest advantage in enhancing the performance of the systems, specifically, aqua-ammonia ( $\text{NH}_3\text{-H}_2\text{O}$ ) and lithium bromide-water ( $\text{LiBr-H}_2\text{O}$ ) absorption systems.

In order to apply suitable PCM between different elements of a refrigeration cycle, a brief of absorption cycles and different approaches are presented in the next section.

Refrigeration through solar power can be obtained electrically or thermally. Thermal approach can either be thermo-mechanical or sorption. Adsorption, absorption, chemical adsorption and desiccant cooling are various types of sorption cooling techniques. Other methods like Electro-Chemical and Ejector Refrigeration are also under this category [36]. An illustration of the classification for electrical and thermal methods can be seen in Fig. 1. All approaches reject heat in more than one stage of operation, which affects the COP of the system. COP as a function of heat rejection temperature for different systems can be seen in Fig. 2, which illustrates various opportunities for rejected heat management using PCM and further work needed in this avenue.

## 2. Absorption systems

Although there are numerous absorption refrigeration cycles (like half, single or multi-effect absorption systems; absorption heat trans-

former, absorption refrigeration cycle with GAX or absorber-heat-recovery, sorption-resorption cycle; diffusion, self-circulation, osmotic membrane, combined ejector and combined vapor absorption systems), only a few are studied extensively due to their promising outcomes [37]. Ullah et al. [38] compiled various solar thermal refrigeration systems with emphasis on absorption and adsorption refrigeration systems. The current study focuses on aqua-ammonia and LiBr-water absorption systems (operating temperatures) due to plentiful investigations and diversified techniques used.

In recent years, the most researched cooling system is the single effect (solar) absorption refrigeration system due to higher energy efficiency and economic feasibility [39,40]. This system, unlike a compressor in vapor compression cycle, uses a generator and an absorber to produce the cooling effect [41]. The generator is heated by an external source, i.e., either by solar collector circuit or an auxiliary heating unit, to heat the low pressure strong solution of the refrigerant from absorber and turn it into pure vapor at high pressure for the condenser [42]. This process of generating pressurized refrigerant by absorption consumes far less or no electrical energy than the conventional vapor compression method [16]. There are two most widely used absorption refrigeration cycles; continuous operation and intermittent operation. These cycles are explained in the following section:

### 2.1. Continuous operation system

It is a system where the generation and absorption takes place simultaneously, with a system operation cycle time of less than a day ( $< 24\text{ h}$ ). An electrical pump circulates the solution in the system. The system components are generator, condenser, evaporator, expansion valves, solution pump and the absorber as shown in Fig. 3(a).

As shown in Fig. 3(a), the generator (GEN) is heated through solar collectors subjected to varying solar radiation levels. Constant heat supply can only be maintained by either running an auxiliary heating unit or through thermal storage system. The heat then flows through the dephlegmator (DEPH) where the water is condensed from the weak solution vapor and goes back to the generator. The condensation process here needs a lower temperature water vapor to exchange heat. This vapor is taken from the strong solution coming from the absorber. Condenser (COND) rejects heat to the atmosphere cooling the refrigerant at high pressure. The refrigerant then enter the evaporator (EVAP) through the expansion valves. The heat is absorbed from the load and the refrigerant continues towards the absorber (ABS) through a refrigerant pre-cooler (RPC) located ahead of the expansion valves.

Although the first developed solar absorption system by Worsøe-Schmidt [44] was based on solid-absorption ( $\text{CaCl}_2/\text{NH}_3$ ) cycle, later, the two most studied solar absorption refrigeration systems were based on liquid cycle; aqua-ammonia ( $\text{NH}_3\text{-H}_2\text{O}$ ) and LiBr-water absorption systems, where the latter is used for air-conditioning buildings and the former is used for refrigeration purpose with subzero operating temperatures.

In aqua-ammonia absorption systems, water acts as an absorbent and pure ammonia as a refrigerant, whereas in LiBr-water absorption system, water acts as a refrigerant and lithium as the absorbent. Nonetheless, in both cases of continuous operation cycles, the operating temperatures differ with a value suitable for the required application. Similarly, different temperature ranges are required from various solar thermal heat input technologies for single, double and triple-effect systems and accordingly higher COPs and evaporator temperatures are obtained [14].

Brendel et al. [45] used flat plate heat exchangers to develop a 10 kW aqua ammonia absorption system with a COP of 0.58–0.74. Later in 2012, Lostec et al. [46] developed a similar 10 kW system operating at COP of 0.6 at much lower generator temperatures. Consequently, their evaporator temperature was higher than that of Brendel et al. [45] and couldn't go lower due to design constraints. Li

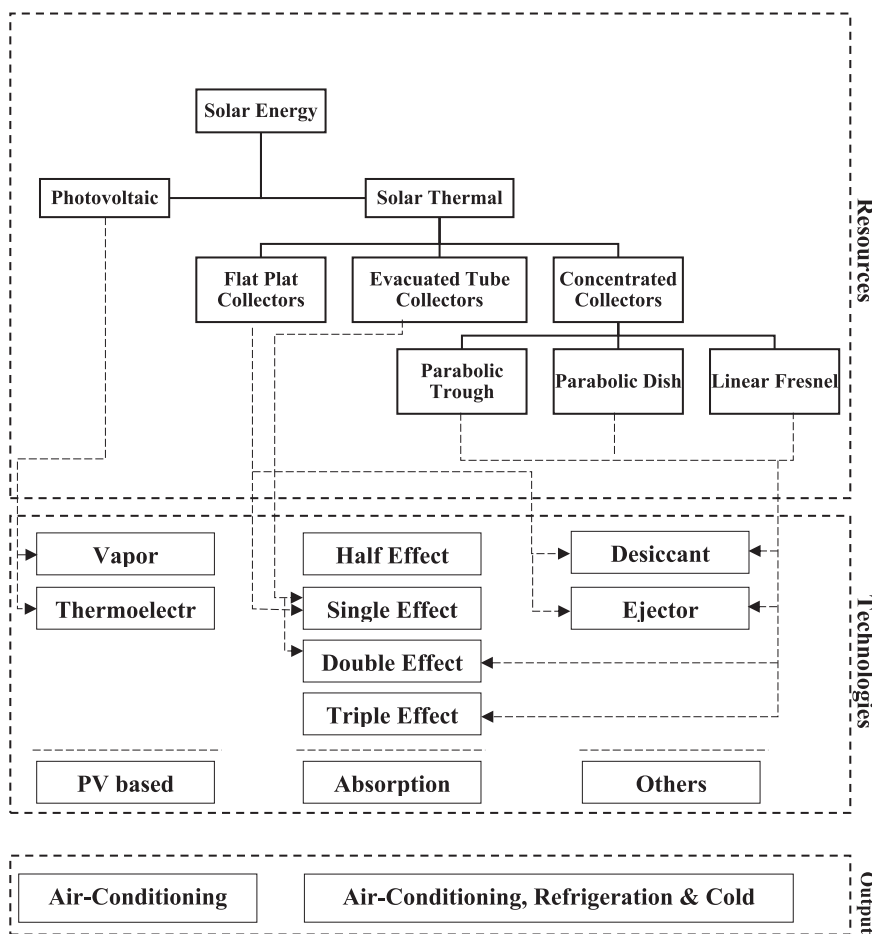


Fig. 1. Different combinations of solar integrated cooling technologies.

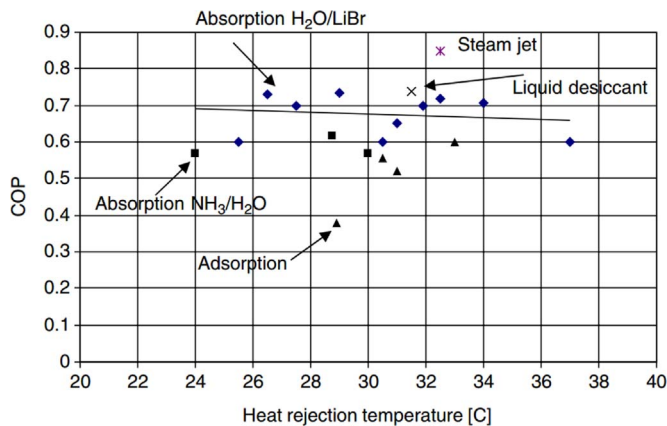


Fig. 2. COP as a function of heat rejection medium temperature [15].

et al. [47] experimentally studied the performance of a 4.7 kW LiBr-H<sub>2</sub>O absorption chiller with a specially designed hot water storage tank giving 15% higher COP. Syed et al. [48] also used a 2 m<sup>3</sup> hot water storage tank for their 35 kW single effect LiBr-H<sub>2</sub>O absorption chiller. They reported a daily average solar cooling ratio (cooling produced divided by incident solar energy) of 11%. A similar 35 kW single effect LiBr-H<sub>2</sub>O absorption chiller was designed and installed by Pongtornkulpanich et al. [49]. They oversized the chiller to analyze the possible extent to replace conventional energy sources by evacuated tube collectors. They reported that annually 81% of thermal energy can be obtained through solar collectors, and the remaining 19% was supplied by LPG-fired backup heating unit. Asdrubali and Grignaffini [50] experimentally simulated single stage LiBr-H<sub>2</sub>O absorption plant

with input generator temperatures as low as 65–70 °C suggesting it an optimum choice for future commercialization. Another 4.5 kW LiBr-H<sub>2</sub>O absorption chiller was designed by Agyenim et al. [51] at an average COP of 0.58 with a cold storage of 1000 ltr for chilled water at almost 7 °C. They made a critical analysis on each component of the system with daily measurements of thermodynamic properties and suggested to use 60–90 ltr of cold storage per square meter of vacuum tube collectors, or 80–150 ltr of for every kW chiller capacity to produce chilled water. Recently, He [52] modified the system with additional thermal storage unit with PCM (Erythritol) to enhance the COP of the system. He reported that the only disadvantage of using erythritol is low thermal conductivity. He also suggested that longitudinal and multitubes are most suitable for charging and discharging of erythritol. Kherris et al. [53] proposed a system with 0.46 COP. Their working fluids were water and ammonia, with hydrogen as an inert gas. Said et al. [54] developed a system with COP 0.6, which allows uninterrupted supply of building cooling in the Kingdom of Saudi Arabia using the same working fluids but without hydrogen gas. Recently, they performed a simulation of the same system and increased its COP to 18% by including a waste heat recovery from the dephlegmator and utilizing a refrigerant storage unit [55]. In an experimental investigation, they designed and studied a 10.1 kW NH<sub>3</sub>-H<sub>2</sub>O absorption chiller with a COP of 0.69 at a generator inlet, condenser/absorber inlet and evaporator outlet temperature of 114 °C, 23 °C and –2 °C, respectively [56]. Balghouthi [57] used two tanks for storage and drain-back storage in a 16 kW double-effect LiBr-H<sub>2</sub>O system and obtained a COP of 0.8–0.9 at evaporator temperature of 8 °C. They claimed that 3000 kg of CO<sub>2</sub> emission can be avoided during a cooling season. More recently, Raja and Shanmugam [58] developed a 5.25 kW single-effect LiBr-H<sub>2</sub>O system with a maximum

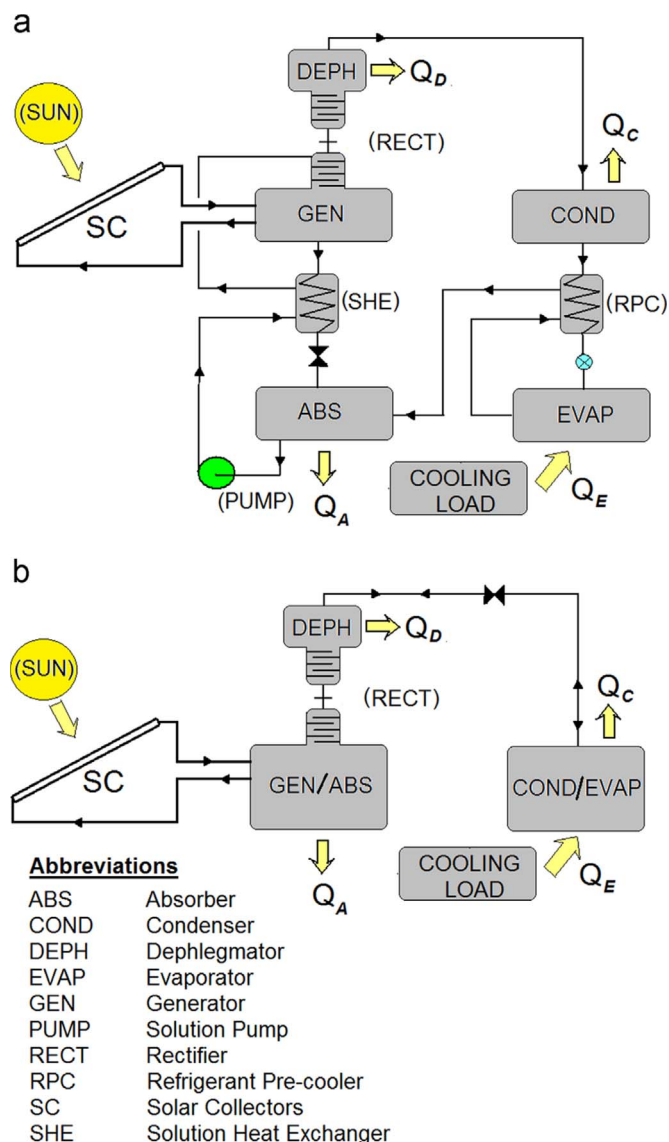


Fig. 3. (a) Continuous-cycle solar absorption system (b) Intermittent-cycle solar absorption system [43].

COP of 0.9 and lowest evaporator temperature of 16 °C. They designed the system to have reasonably low initial and operating cost. They also reported a heat loss when the designed value of maximum capacity was lower than the average heat capacity on a particular day. Ozgoren et al. [59] studied hourly performance of a solar (evacuated tube collectors) assisted NH<sub>3</sub>-H<sub>2</sub>O absorption system with COP ranging from 0.243 to 0.454 at generator temperatures equivalent to 110 °C. They also calculated the required collector area for evaporator capacities ranging from 2.5 to 4 kW. Their most important observation was that the atmospheric temperature is very important in SAR system for cooling, and that it is proportional to the generator rate of heat transfer. More recently, Pintaldi et al. [60] numerically evaluated thermal energy storage options for a triple effect solar absorption system. They compared sensible and latent heat storage using transient simulation and finally reported a high storage efficiency for latent heat materials.

Although, absorption systems are becoming common in applied research, they are not completely away from challenges. A length of 23 years is the payback time for a 7 kW aqua-ammonia system with COP 0.42 [61]; and with a condition that the collector output temperature is higher than the cut off temperatures in their 5.7 kW, 0.6 COP NH<sub>3</sub>-H<sub>2</sub>O absorption system [62]. Sometimes, commercially available brazed solution heat exchangers were underperforming ( $\eta_{\text{heat exchanger}}=0.16$ )

| Year | Cooling load | Temperatures |           |              | COP       | Results  | Ref. |
|------|--------------|--------------|-----------|--------------|-----------|--|------|
|      |              | Generator    | Condenser | Absorber     |           |  |      |
| 2000 | 2 kW         | 106          | -10       | 34           | 0.426     | Economically analyzed the feasibility of the system. Results indicated that the payback time of approximately 23 years for the chiller   | [61] |
| 2002 | 2 kW         | 150          | 35        | Not reported | 0.05      | Absorption chiller utilizes concentrating collectors and uses a transfer tank instead of a pump. They suggested the inefficient operation of the transfer tank being responsible for such a low COP of their system                      | [65] |
| 2010 | 10 kW        | 80–120       | 30–45     | 30–45        | 0.58–0.74 | Developed an experimental setup with plate heat exchangers for all components except generator. Generator fabricated as helical coil heat exchanger in a cylindrical shell   | [45] |
| 2009 | 5.27 kW      | 60 to 98     | 23 to 39  | 23 to 39     | 0.6       | Most of the components of the chiller were constructed as shell and tube heat exchangers. 10 m <sup>2</sup> evacuated tube solar collectors was used in the operation  | [62] |
| 2012 | 10 kW        | 68 to 75     | 24 to 29  | 24 to 29     | 0.6       | Plate heat exchangers were used in this investigation. Their results indicated a significant decrease in COP when decreasing the evaporator temperature. They reported over feeding of the evaporator causing drop in COP of the system. | [46] |
| 2012 | 4.2 kW       | 80           | 27        | 27           | 0.65      | Chiller components were constructed using the industrially available brazed plate heat exchangers. Their system used 0.735 kg of water and 2.4 kg of ammonia. They reported poor operation of solution heat exchanger in their system    | [63] |

Table 1  
Component-wise thermal variations in few solar absorption systems.

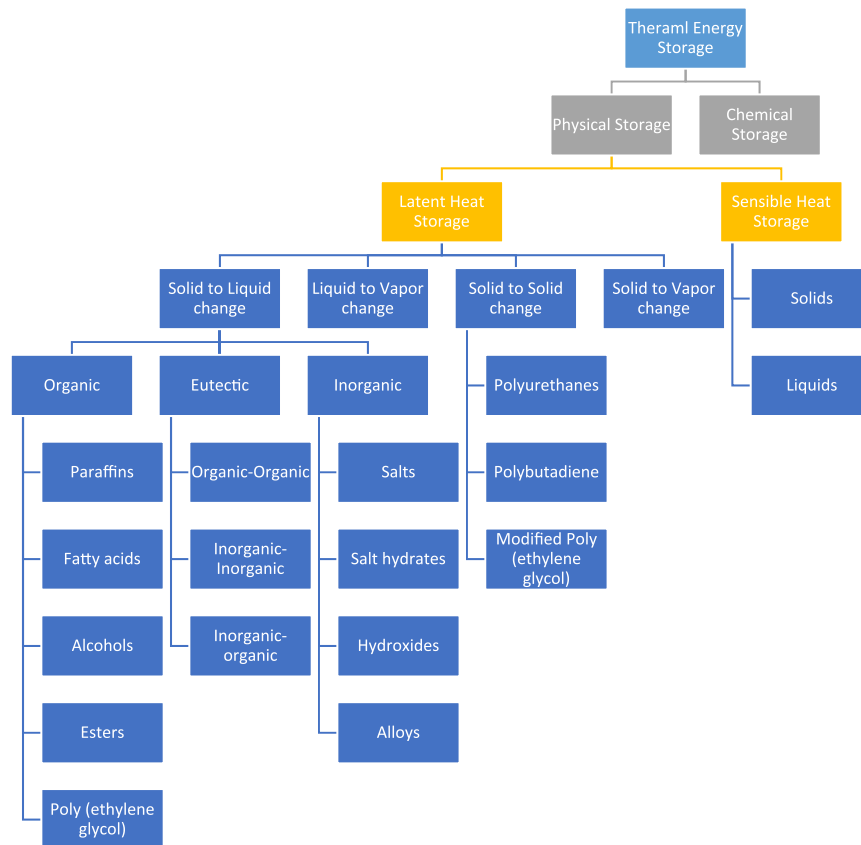


Fig. 4. Classification of thermal energy storage materials.

in a 0.65 COP 5 kW NH<sub>3</sub>-H<sub>2</sub>O absorption system [63]. Lostec et al. [46] were not able to attain proper cooling ( $T_{\text{evap}} = 16\text{ }^{\circ}\text{C}$ ) at the evaporator due to decreasing COP with increasing generator temperature. They attributed the non-compliance behavior to the design specifications is mainly due to the overfeeding of the evaporator. A similar phenomenon was observed by Albers and Ziegler [64] and Asdrubali and Grignaffini [50] at higher generator temperatures, suggesting a critical parametric review while designing the system. Table 1 shows various attempts to develop a solar absorption system with component wise temperatures and a few highlights.

## 2.2. Intermittent operation system

The intermittent operation system has two main differences compared to continuous operating system. In this system, instead of a solution pump (PUMP), the pressure is generated by isochoric heating of the refrigerant solution in the generator. The second variation is the absence of a separate absorber; instead, the generator and absorber are a single component (GEN/ABS) which acts as a generator during the daytime and absorber during the night in an open cycle. Such a cyclic operation takes a complete day (24 h) for a single cycle to complete and practically no electrical energy is required in its operation (Fig. 3(b)). Intermittent operation systems have not been extensively investigated due to its low coefficient of performance (half or one-third) compared to continuous operation system.

Rivera and Rivera [66] modeled an intermittent absorption refrigeration system operating with ammonia-lithium nitrate mixture using a compound parabolic concentrating (CPC) collector. Theoretically, they obtained an efficiency of 0.15–0.4 and were able to produce a maximum of 11.8 kg of ice with generator temperature of 120 °C. Later in 2011, Riever et al. [67] performed an experimental study on a similar system with a CPC collector and were able to reach as low temperature as  $-11\text{ }^{\circ}\text{C}$  at the evaporator at a COP of 0.083 at 50%

refrigerant concentration. They observed that the increase in solution concentration decreases the initial generator temperature and increase the maximum operating pressure. Again, in 2012, they experimentally tested and compared the same system with and without water as an absorbent. They observed that water in the working fluid mixture gave a 24% higher solar coefficient of performance [68]. In the same year, they applied direct and inverse artificial neural network (ANN and ANNi) approach to run the system at required COP by obtaining the input variables of the system. The configuration 6-6-1 (6 inputs, 6 hidden and 1 output neurons) presented an excellent agreement ( $R > 0.986$ ) between experimental and simulated values [69]. Tangka and Kamnang [70] experimentally tested another simple intermittent absorption system with a COP of 0.487 and an average lowest refrigeration temperature of 4 °C. They recommended shielding the solar collector at the end of the generating cycle and keeping the refrigeration cabinet covered and protected from the day light in order to avoid adding more heat to the system.

## 3. Thermal energy storage technologies

Due to intermittency in availability and constant variation in the solar radiation, thermal energy storage (TES) found its place in thermodynamic systems. TES not only reduces the discrepancy between the demand and supply by conserving energy, but also improves the performance and thermal reliability of the system. Therefore, designing efficient and economical TES systems is of high importance. However, only few solar thermal plants in the world have employed TES at a large scale. Utilization of TES systems in various domestic solar applications are even investigated today [71]. Designing using computational fluid dynamic approach is also a vastly used method to save money, where Fluent® software seems to be successfully used at different engineering applications [72].

Thermal energy storages are broadly classified into sensible and



**Table 2**  
Properties of sensible heat storage materials.

| S No. | Material  | Density ( $\rho$ ), kg/m <sup>3</sup> | Sp. Heat ( $C_p$ ), kJ/kgK | Heat Capacity (C), kJ/m <sup>3</sup> K | Melting point ( $^{\circ}$ C) | Thermal conductivity (k), W/mK | Thermal diffusivity $\alpha = k/\rho c \times 10^6$ (m <sup>2</sup> /s) |
|-------|-----------|---------------------------------------|----------------------------|--|-------------------------------|--------------------------------|---|
| 1     | Sand      | 1555                                  | 0.8                        | 1244                                   | 1500                          | 0.15–0.25                      | 1.172   |
| 2     | Rock      | 2480                                  | 0.84                       | 2086.6                                 | 1800                          | 2–7                            | 1.45  |
| 3     | Concrete  | 2240                                  | 0.75                       | 1680–1800                              | 1000                          | 1.7                            | 0.356–0.514   |
| 4     | Granite   | 2640                                  | 0.82                       | 2164                                   | 1215                          | 1.7–4.0                        | 0.799–1.840   |
| 5     | Brick     | 1698                                  | 0.84                       | 1426                                   | 1800                          | 1.04                           | 0.484   |
| 6     | Aluminium | 2707                                  | 0.896                      | 2425                                   | 660                           | 204                            | 84.10   |
| 7     | Cast iron | 7900                                  | 0.837                      | 6612                                   | 1150                          | 29.3                           | 4.431   |

latent energy storages. Sensible storage being without any transformation in their physical state is either solids or liquid. On the other hand, latent heat storage often changes their state from solid to liquid or liquid to vapor. Moreover, latent heat storage materials store 5–14 times more heat per volume than the former type of materials. However, certain thermophysical and chemical properties must be exhibited for such materials to be employed as latent heat storage systems (LHSS) [18]. Water is the most common sensible heat storage medium and has good thermal characteristics. Latent heat storage materials are gaining popularity due to their diversity, capacity and performance in thermal applications. A more detailed classification is shown in Fig. 4.

Sensible heat storages store thermal energy by utilizing the heat capacity of the solid or liquid. This is during both charging and discharging the storage system. The thermophysical properties necessary to focus in a sensible heat storage material are specific heat, volume and change in the temperature of the materials. Table 2 shows the most used sensible heat storage materials and their properties [73].

Latent heat storage (LHS) materials are also known as Phase Change Materials (PCMs) due to their property of releasing or absorbing energy with a change in physical state; liquid to solid or solid to liquid. However, the main advantage of using LHS over SHS is their capacity of storing heat at almost similar temperature range. Initially, these materials act similar to sensible heat storage materials where the temperature rises linearly with the system enthalpy, but later, heat is absorbed or release at almost constant temperature with a change in physical state (Fig. 5). Hence, properties like thermophysical, kinetic and chemical are critically measured before appropriate usage of the materials for the various applications.

Important properties of a latent heat storage materials are thermal, physical, kinetic, chemical and economic. A derived illustration of sub-properties of these essential features is shown in Fig. 6 [18,75]. A crude illustration of various thermal storage technologies with respect to their working temperatures is given in Fig. 7 [76].

### 3.1. PCM classification

Latent heat storage materials are used in thermal applications since

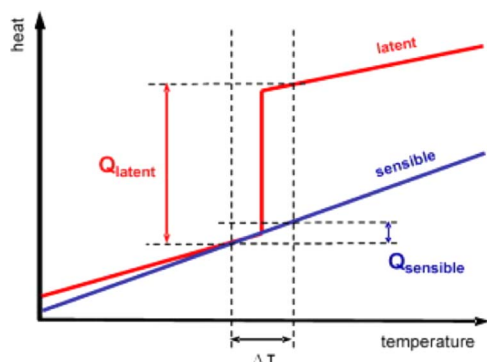


**Fig. 5.** Comparison between latent and sensible heat storage [74].

few decades ago. They are broadly classified based on their physical transformation for heat absorbing and desorbing capabilities. As seen from Fig. 4, a wide classification of solid-liquid phase change materials which are further classified into organic, inorganic and eutectic materials are presented. A few advantages and disadvantages of organic and inorganic PCMs and their influence on solar cooling application are listed in Table 3.

Organic PCMs have stable phase change temperatures without phase segregation, no super-cooling, and usually non-corrosive properties [78] which are highly desirable in solar cooling technologies. Organic materials are classified into paraffins and non-paraffins, where paraffins have many good qualities with few crucial undesirable qualities. Similarly, non-paraffins like fatty acids, alcohols, glycols and esters which constitute the largest group for latent heat storage materials also exhibit few undesirable properties. Table 4 lists advantages and disadvantages of both paraffins and non-paraffins. Details of thermal properties, applications and limitations of fatty acids are discussed in [79] and that of sugar alcohols/polyols are found in [80,81]. Thermal stability is very crucial in cyclic loads and super-cooling is the most undesirable property which completely dampens the thermal performance.

Inorganic PCMs are (mostly) used in high temperature solar applications and one of the most reported challenges with them is the maintenance. At lower temperature they freeze and at high temperatures difficult to handle. They are salts, salt hydrates and metal alloys. Salts and salt hydrates are the most studied PCMs in inorganic solid-liquid PCMs. They have high latent heat of fusion per unit volume, higher thermal conductivity and smaller thermal stresses (less volume change in phase transition). However, the ratio of anhydrous salt dissolving in its water varies during the melting process. This is classified as congruent, incongruent and semi-congruent melting [30]. Mohamed et al. [82] listed few crucial drawbacks of inorganic salts in their review of which includes, change of volume, low thermal conductivity, subcooling (salt hydrates), corrosive, and costly.

Low melting point metals and their alloys have high thermal conductivity suitable as liquid metals in latent heat storage materials. They also have small volume change, high electrical conductivity and low heat of fusion per unit weight, which makes them better than traditional PCMs in heat transfer capacity [83]. The main reason for such material's usage in solar applications is their ability to operate for high demands of large capacity power plants.

Inorganic and organic eutectic materials are a combination of two or more low melting materials with similar (congruent) melting and freezing points. The weight percentage of each material can be varied in order to obtain a variation in melting point of the resulting eutectic mixture [18]. This gives the resulting mixture a unique property of tuned melting point temperature according to the requirement. There are new properties that emerge and a vast scope is revealed in applying these materials for solar cooling applications.

Nonetheless, organic PCMs have many advantages over inorganic PCMs except being flammable and low at thermal conductivity. On the other hand, inorganic PCMs are cheaper, abundant, non-flammable and have high heat storage capacity and thermal conductivities. Two

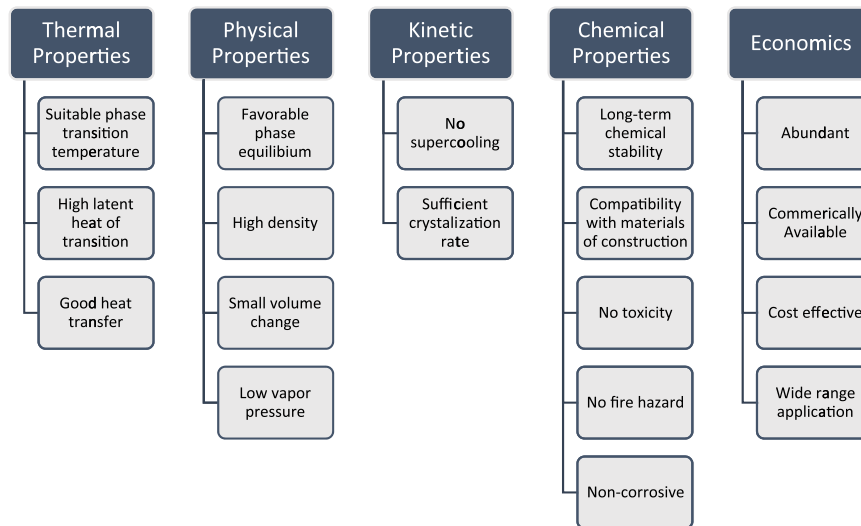
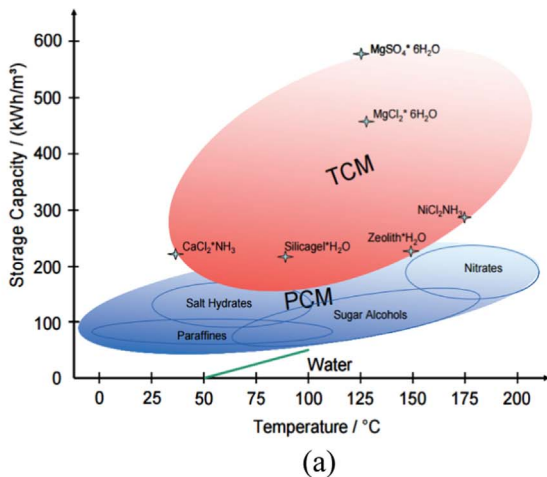
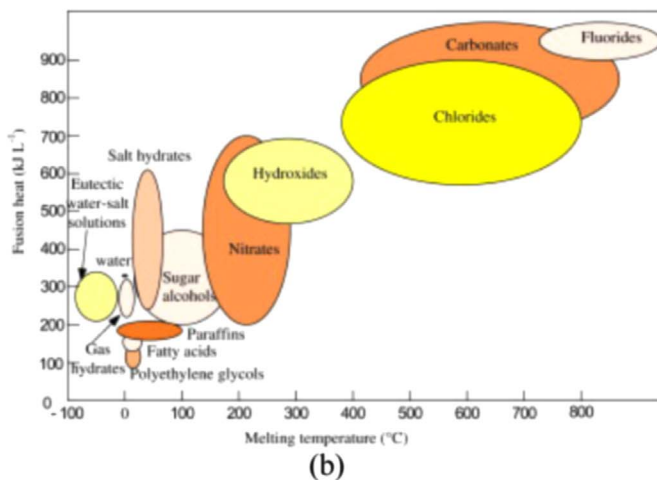


Fig. 6. Characteristics properties of a latent heat storage material.



(a)



(b)

Fig. 7. (a) PCM with respect to storage capacity [76] (b) PCM with respect to heat of fusion [77].

concerns with inorganic PCMs are subcooling and phase segregation. Eutectic PCMs take advantage here in being able to adjust their melting point by combining different wt% of components, without subcooling or phase segregation; and have high thermal conductivities and densities. However, they have low latent and specific heat capacities [84]. PCMs are classified based on suitable temperature range as well.

In fact, temperature range is one of the main criterions for the suitability of the PCM in any application. There are numerous applications which use PCM as thermal energy storage, all fitting a particular range suitable for their optimum thermal performance [85]. Fig. 8 shows a brief classification based on melting temperatures helpful to choose PCM for specific application. A more detailed application based analysis is presented in next chapters.

#### 4. Solar collectors

The applicability of PCM in solar collectors depends largely upon the operating temperature and the mass flow rate of the heat transfer fluid. The operating temperature helps in selecting the PCM with appropriate melting points, and the mass flow rate of the heat transfer fluid (along with heat load) decides the charging and discharging time of the heat storage system. With intermittent heat source, solar absorption system inevitably needs a thermal storage to provide heat during dark hours. The low-medium temperature PCM can handle the requirements of an absorption chiller for few hours, which can effectively influence the system performance.

##### 4.1. Classification

Depending upon the required heat from the absorption chiller capacity, the solar collectors are selected. The requirement can also be escalated considering thermal void of charging the thermal storage unit. Solar collectors are either stationary or single/two-axis tracking. Depending upon their motion capabilities and concentration ratio, the indicative temperature range varies. Flat plate collectors used in half effect absorption cycles have low thermal capacities, unlike most absorption cycles use collectors with higher output temperatures and lesser heat loss targeting higher COPs [36]. Kalogirou [86] compiled types of collectors and their output indicative temperature ranges in Table 5. Use of different types of collectors and relative efficiencies for different solar thermal technologies are given in Fig. 9(a) indicating evacuated tube collectors most suitable for single and double effect absorption cycles. Sabiha et al.[87] recently studied evacuated tube solar collectors and their applications, finding its huge potential in energy producing industries with better performance using nanofluids as heat transfer fluid. Licuona et al. [88] studied the optimum hot water temperature required for a 4.5 kW single effect LiBr-H<sub>2</sub>O absorption system using a modified characteristic equation model to empirically calculate the performance of a real chiller. They studied various hot water temperatures and corresponding system COPs along with solar

**Table 3**  
Comparison of organic and inorganic materials for heat storage [17].

| Organic   | Effect on Solar Cooling system                             | Inorganic  | Effect on solar cooling system                   |
|---|--|--|--|
| <b>Advantages</b><br>Non corrosives<br>Low or no undercooling<br>Chemical and thermal stability   | good<br>crucial<br>important                               | <b>Advantages</b><br>Greater phase change enthalpy   | good   |
| <b>Disadvantages</b><br>Lower phase change enthalpy<br>Low thermal conductivity<br>Inflammability | bad<br>Crucial (in condenser and generator)<br>undesirable | <b>Disadvantages</b><br>subcooling<br>Corrosion<br>Phase separation<br>lack of thermal stability | crucial<br>undesirable<br>undesirable<br>crucial |

**Table 4**  
Properties of paraffins and non-paraffins.

|               | Advantages   | Disadvantages   |
|---------------|--|---|
| Paraffins     | Safe<br>Reliable<br>Predictable<br>Less expensive<br>Non-corrosive<br>Low vapor pressure   | Low thermal conductivity<br>High volume change with phase change<br>Non-compatibility with plastic container<br>Moderately inflammable  |
| Non-paraffins | Thermal stability<br>Chemical durability<br>Non-corrosiveness<br>Non-toxicity<br>Easy availability<br>Little/no subcooling<br>Narrow temperature range | Highly inflammable<br>Low heat of fusion<br>Low thermal conductivity<br>Low flash point<br>Toxicity<br>Instability at high temperatures |

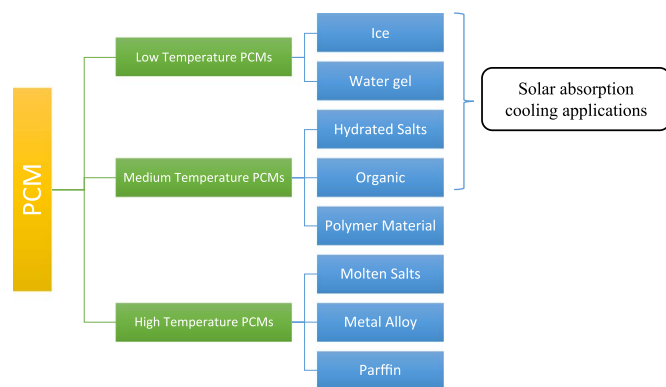


**Fig. 8.** Category of PCM based on melting point [83].

coefficient of performance for the solar collector field as shown in Fig. 9(b).

4.2. Methodologies

Approach of integrating PCM in solar thermal collector goes back to

**Table 5**  
Solar energy collectors and their output temperatures [86].

| Motion               | Collector type                     | Absorber type | Concentration ratio | Indicative temperature range (°C) |
|----------------------|------------------------------------|---------------|---------------------|-----------------------------------|
| Stationary           | Flat plate collector (FPC)         | Flat          | 1                   | 30–80                             |
|                      | Evacuated tube collector (ETC)     | Flat          | 1                   | 50–200                            |
|                      | Compound parabolic collector (CPC) | Tubular       | 1–5                 | 60–240                            |
| Single-axis tracking | Linear Fresnel reflector (LFR)     | Tubular       | 10–40               | 60–250                            |
|                      | Parabolic trough collector (PTC)   | Tubular       | 15–45               | 60–300                            |
|                      | Cylindrical trough collector (CTC) | Tubular       | 10–50               | 60–300                            |
| Two-axes tracking    | Parabolic dish reflector (PDR)     | Point         | 100–1000            | 100–500                           |
|                      | Heliostat field collector (HFC)    | Point         | 100–1500            | 150–2000                          |

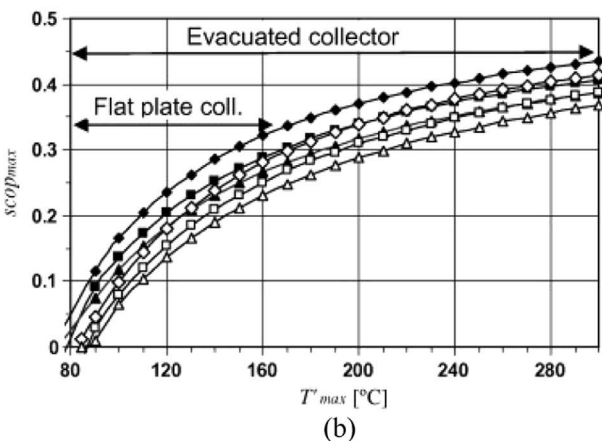
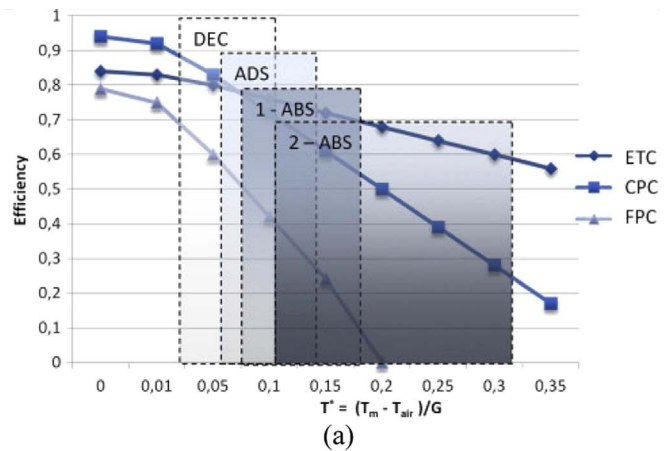


**Fig. 9.** (a) Comparison of three types of solar collector for different cooling systems production. ETC (evacuated tube) – CPC (parabolic) – FPC (flat plate) for Desiccant (DEC), adsorption (ADS) and absorption (ABS) cooling technologies [89], (b) SCOP<sub>max</sub> as a function of collector output temperatures for  $\eta_{generator} = 0.6$  [88].

as early as 1987. Salt hydrate PCM within a plastic container of flat plate collector with reflector was theoretically and experimentally investigated by Rabin et al. [90]. Their system and the numerical



model was intended only to find the thickness of PCM required and the location of solid/liquid interface. Mettawee and Assassa [91] submerged the solar absorber inside solid paraffin wax to create a customized compact PCM solar collector. They found that the average heat transfer coefficient increases sharply during the charging process due to natural convection, but during the discharge, only an increase in water mass flow rate can increase the useful heat gain. The melting temperature of the paraffin wax was 53.5 °C. In a 30 kW LiBr/H<sub>2</sub>O single-effect absorption cooling system with 90 m<sup>2</sup> of double glazed flat-plate collectors, Praene et al. [89] simulated and experimentally investigated the performance of the system with 1500 L hot-water storage to ensure stable supply of hot water. Eames and Griffiths [92] used a transient finite volume model to predict heat collection and retention in a flat plate solar collector (1 m long, 0.125 m deep at 30 ° to the vertical) with water and various concentrations (10–15–20–25–30%) of PCM slurries at melting temperature of 65 °C. They reported an improved solar saving fraction due to the use of PCM slurry (heat retention for longer time), but at the cost of reduced solar collection efficiency. This was due to the lower specific heat capacity of the PCM than that of water. Similar reports of lower thermal performance and repressed heat transfer of PCM integrated solar collector than that of water-in-glass evacuated tube solar collector was found by Sheng [93]. Naghavi et al. [94] mathematically investigated an evacuated tube heat pipe solar collector with PCM in the overhead tank that acts as a latent heat storage system. This tank also contains finned heat exchanger to transfer heat to flowing water. This way they made the header as LHES attached to heat pipes of evacuated tube collectors. The new system thermal performance was better than the baseline system and the efficiency did not decrease with increasing flowrate. They suggested further parametric research on the concept.

#### 4.3. Materials selection

Materials selection is the core and most important step in designing latent heat thermal energy storage. PCM is selected based upon its melting temperature and heat of fusion. The parameters necessary to identify the material is the temperature range required for the application and heat requirements. Then, the type of PCM is selected for its physical and chemical properties, considering the drawbacks. There are different temperature ranges according to application as shown in Table 4. Numerous studies have been done to list various PCMs and their thermophysical properties which can be used in suitable applications. One of the most reliable method of laboratory thermal analysis is heat flux differential scanning calorimeter (hf-DSC) to test heat storage capacity of PCM with constant heating/cooling rate [95]. Based on the temperature range required, various PCMs were used in application of solar cooling.

Brancato et al. [96] recently investigated few PCMs with melting temperatures between 80 and 100 °C for application of solar cooling. They found that those PCM (with high latent heat) characterized by them still have some issues like subcooling, incongruent melting, allotropic phase transition; and that the commercially available (PlusIce A82, S83 & S89) eutectic mixtures are much stable with lower heat of fusion. They found that Gil et al. [97] selected Hydroquinone and D-mannitol as PCMs for a temperature range of 140–200 °C. Their basis of storage temperature range was the maximum collector output and minimum chiller input temperatures. The minimum heat of fusion was set to 150 kJ/kg. Several PCMs from the literature were chosen and tested in their laboratory (Table 6), where hydroquinone was selected based on high phase change enthalpy and negligible subcooling. D-mannitol was also selected based on suitable melting range and high heat of fusion. Their selection criteria were based primarily upon the high heat of fusion and suitable melting temperature. They later repeated the properties tests after finalizing the two PCMs. Similarly, Agyenim et al. [98] selected PCMs in the temperature range of 100–130 °C. They used Erythritol as PCM to

**Table 6**

Materials tested with possibility to work as PCM in solar cooling [97].

| Material              | Experimental phase change temperature (°C) | Experimental phase change enthalpy (kJ/kg) |
|-----------------------|--|--|
| Salicylic acid        | 159.1 (m)/113.3 (s)                        | 161.5 (m)/109.4 (s)                        |
| Benzanilide           | 163.6 (m)/136.1 (s)                        | 138.9 (m)/129.4 (s)                        |
| D-mannitol            | 166.8 (m)/117 (s)                          | 260.8 (m)/214.4 (s)                        |
| Hydroquinone          | 172.5 (m)/159.5 (s)                        | 235.2 (m)/178.7 (s)                        |
| Potassium thiocyanate | 176.6 (m)/156.9 (s)                        | 114.4 (m)/112.5 (s)                        |

(m = melting, s = solidification).

improve the efficiency of a domestic LiBr–H<sub>2</sub>O solar absorption cooling system. The driving criteria in their experiment was the temperature required on the hot side of the system for efficient operation. The generator operating temperature for LiBr absorption system was determined to be less than 120 °C and erythritol was chosen for its suitable melting temperature of 117.7 °C. Their selection criteria included high energy density and ability to deliver near constant heat source. The PCM was integrated with Thermomax vacuum tube solar collectors for a temperature range of 90–120 °C [99]. Agyenim [52] tested three PCMs (Erythritol, RT100 and Magnesium chloride hexahydrate) in four different types (no fin, circular and longitudinal finned and multitube systems) of storage unit/heat exchanger set-ups in a 4.5 kW LiBr–H<sub>2</sub>O solar absorption cooling system. His study revealed that multitube design is best for melting/charging in short time; whereas longitudinal fin design yields more uniform melting and is suitable for discharging with no subcooling. He also calculated the suitable quantity of PCM required to meet 4 h of peak load. Therefore, the criteria of selection of PCM implied from the literature seems to depend mainly upon the suitable melting temperature, high heat of fusion and design characteristics. Minor subcooling properties can be overlooked when high latent heat values look promising.

Table 7 lists investigations in solar thermal application with PCMs and a brief of their finding on the usage of LHTES system. Schweigler et al. [100] used calcium chloride hexahydrate as PCM in a LiBr–H<sub>2</sub>O absorption chiller at low operating temperatures with a maximum COP of 0.8. They found that usage of PCM helped maintain a low operating temperature of solar collectors with positive effect on the heat gain. In general, nitrites exhibited high heat capacities at comparatively lower costs. Similarly, Serale et al. [101] numerically studied a slurry PCM based flat plate collector with an efficiency improvement of +0.08 compared to conventional water based technology. A 20%–40% improvement in heat conversion was seen on average, throughout the year. Their concern with the 50% or more concentration of PCM was not possible due to increased demand in pumping energy (design constrain).

#### 4.4. Storage tank design

The design of the storage tank is responsible for efficient charging and discharging of the PCM when required. Shell and tube heat exchanger is the most common type of (PCM) storage unit, with PCM on the shell side. A bundle of 49 U-shaped tubes distributed in square pitch; and an identical second storage tank incorporating 196 transversal square fins were tested [103]. When fins were used in the storage system, the available volume to place PCM was decreased and therefore the PCM mass had to be reduced from 170 kg with no fins to 155 kg with fins, in the storage system. Table 8 shows the main characteristics of storage tanks designed highlighting the main differences of increased heat transfer area by using fins, and decreased PCM volume. The heat required by the system is the primary criteria to design the storage unit size (Fig. 10), while an effort must be made to keep the size as small as possible for economic and handling feasibilities. Another important criterion of design is the thermal

**Table 7**  
Literature on phase change materials used with solar collectors.

| Author                  | Year | Type of Study | System                           | Solar Collector       | PCM                                       | Melting temp.      | Type of Storage system | Important findings   | Remarks  |
|-------------------------|------|---------------|----------------------------------|-----------------------|---|--------------------|------------------------|--|--|
| Elbhajaoui [102]        | 2014 | Numerical     | -                                | Flat plate            | Paraffin wax                              | 47                 | Rectangular tubes      | Optimum values of PCM mass, M, aspect ratio, flow rate, and number of rectangular tubes during storage mode were estimated | Long time to begin phase change during early hours                           |
| Agvenim et al. [99]     | 2007 | Experimental  | LiBr/H <sub>2</sub> O Absorption | Thermomax vacuum tube | Erythritol                                | 117.7              | Shell-and-tube         | A 100 l of PCM can provide 4.4 h of peak load cooling (13.2kWh heat) at COP 0.7  | Testing of more PCMs in the temperature range                                |
| Schweigler et al. [100] | 2007 | Experimental  | LiBr/H <sub>2</sub> O Absorption | Flat plate            | calcium chloride hexahydrate              | 27–29              | Capillary tubes        | Introduction of PCM reduces the oversizing of collector field.   | The size, cost and maintenance were reduced for commercial feasibility       |
| Gil et al. [97]         | 2013 | Experimental  | -                                | -                     | hydroquinone and D-mannitol               | 168–173<br>162–170 | Shell-and-tube         | Low operating temperature and positive solar gain  | D-mannitol can store more energy, it showed subcooling every time was tested |
| Serale et al. [101]     | 2013 | Numerical     | -                                | Flat plate            | Microencapsulated n-eicosane paraffin wax | 35–39              | -                      | the heat that is given by the HTF during the charging process is recovered when the discharging occurs                     | Pump energy demand limits PCM concentration to below 50%                     |

**Table 8**  
Storage tank dimensions and characteristics [103].

|                          | Unit           | Tank without fins | Tank with fins |
|--------------------------|----------------|-------------------|----------------|
| Tank width               | mm             | 527               | 527            |
| Tank height              | mm             | 273               | 273            |
| Tank depth               | mm             | 1273              | 1273           |
| HTF pipes average length | mm             | 2500              | 2500           |
| Heat transfer surface    | m <sup>2</sup> | 6.6               | 26.7           |
| Dimensions of fins       | mm             | -                 | 250 × 250      |
| Thickness of fins        | mm             | -                 | 0.5            |
| Distance between fins    | mm             | -                 | 10             |
| PCM mass                 | kg             | 170               | 155            |

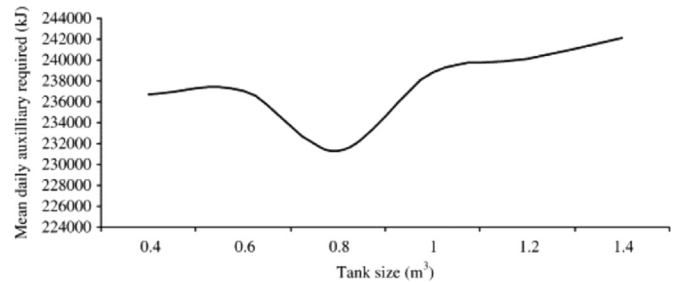


**Fig. 10.** Size of storage tank with respect to auxiliary heat required [106].

capacity to be delivered. This is estimated by comparing the required heat to the heat of fusion of PCM, HTF thermal capacity & flow rate, heat exchanger efficiency and design characteristics of the thermal storage unit. The auxiliary heat required by an absorption system for various volumes of storage was also calculated as 230,000 kJ hence a tank size of 0.8 m<sup>3</sup> was chosen (Fig. 10). Nonetheless, to increase the reliability of a system, a thermal storage tank is necessary [104]. Lorente et al. [105] numerically designed and analyzed two new type of latent heat storage unit. They made a single and double coaxial spiral tubes (heat source) inside a cylindrical PCM storage tank and studied the effect of geometrical features such as helix diameter and pitch on the overall performance. Doing so, they found the lowest volumetric ratio of the heated tank and tube with time to reach melting fraction 1 for the PCM with complete geometry of helical tubes as heat source. Their design was modified until the dictating criterion of PCM melting fraction of one was reached. Such design modifications are essential to fully-charge the thermal storage while extracting maximum heat during discharging process.

**4.5. Heat loss**

Heat loss is a major concern when designing any thermodynamic system, especially when the attention is given to thermal storage units. In solar absorption cooling system, heat is gained as well as rejected. The rejected heat is fully controlled and any uncontrolled heat loss changes the performance parameters. Improper insulation can not only increase the energy loss, but also drastic reduction in exergy efficiency. A 24 cm thick rock wool was placed surrounding the storage tank to minimize the heat losses, while 45 cm of Foamglass™ was installed between the bottom of the tank and the ground [103], yet reading were taken from the centrally located thermocouples in the tank as the heat loss is more near the boundaries. Solidification/crystallization process of the PCM was studied by Suarez et al. [107]. They used a computational fluid dynamics model to simulate molten salt (60% sodium nitrate and 40% potassium nitrate) storage tanks to analyze the cooling process during standby periods. They concluded that more than 3 days long standby period could cause freezing problems. They also mentioned a linear relation between the charging level of the storage tank and the onset of crystallization. They suggested to charge the tank to an

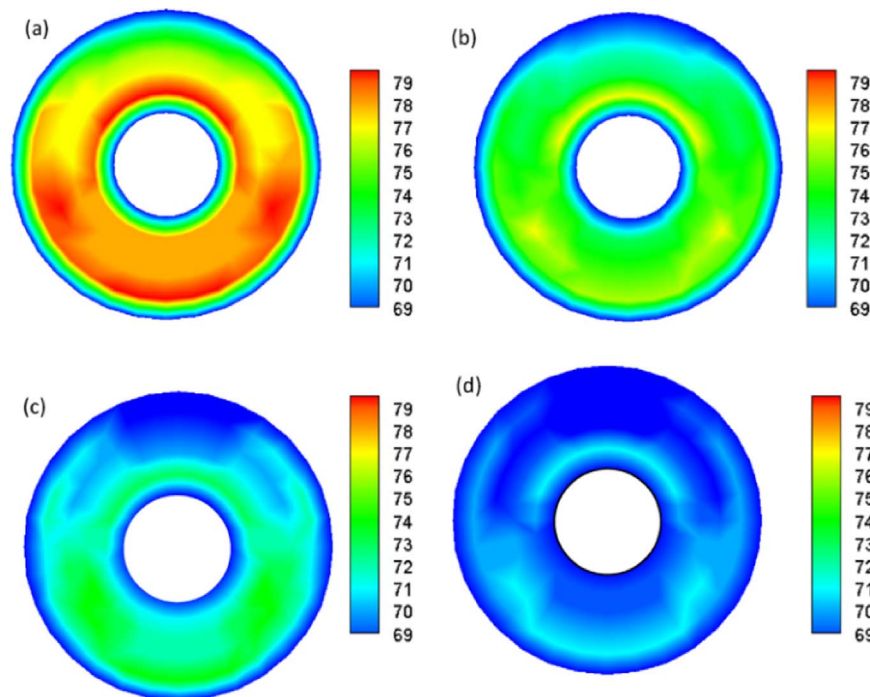


**Fig. 11.** Temperature contour of PCM during solidification, average discharging temperature ( $T_i = 68$  o°C); (a)  $t = 15$  min, (b)  $t = 30$  min, (c)  $t = 45$  min, (d)  $t = 60$  min [108].

adequate level, based on operation temperature and standby duration in order to avoid the risk of freezing.

#### 4.6. Thermal behavior

Heat propagation and distribution in latent storage is one of the primary concerns when selecting a PCM and designing the heat exchanger (storage) unit. The thermal behavior of the PCM includes the melting and freezing profiles in the PCM container. This largely depends upon the thermal conductivity of the material used. Often, thermal conductivity is increased by reducing the space between tubes containing the heat transfer fluid (in a shell and tube design), or by adding heat transfer enhancements like fins on the heating surface. The effect of design of the storage container, mass flow rate, insulation, gravity, known issues with the material (phase segregation) and suspension of nano-particles play a major role in heat propagation during the charging/discharging process. Al-Abidi et al. [108] studied the charging/discharging behavior in a triplex tube heat exchanger with internal and external fins for both steady and unsteady HTF inlet temperatures (see Fig. 11). They found that for HTF mass flow rate and inlet temperature, the charging time is reduced to 58% and 86%, respectively, indicating a higher influence of the HTF inlet temperature on the PCM melting process than that of the HTF mass flow rate. Murray et al. [109] simultaneously charged and discharged a vertical cylinder with Dodecanoic acid as PCM under various scenarios and flow rates. Natural convection in melted PCM facilitated direct heat exchange between the two extreme temperatures, while PCM thermal conductivity was the primary barrier to reach higher performances. When Eames et al. [92] numerically studied various concentrations of PCM filled in a flat plate collector. They observed that a significant volume of PCM has an average higher temperature with higher concentration. The overall stored energy was however higher for water than that of all the PCM concentrations due to increased viscosity and heat loss at higher temperatures. When Qarnia [110] tested three phase change materials with solar hot water heater, he found that two of the three PCMs were not attaining a melting fraction of one in the given period of time. During discharging process, a part of PCM remains liquid, indicating that thermal behavior as a crucial factor in selecting

and testing a PCM for the required output temperatures. A comprehensive review of PCM melting in containers (rectangular, spherical, cylindrical and annular shaped) and their thermal behavior analysis is done recently by Dhaihan and Khodadadi [111]. PCM enhancement techniques and portability of PCM in the system and its effects is reviewed in detail by Tay et al. [21].

Stefan or moving boundary problems also need attention in the study of thermal interface behavior during the charging/discharging process. Analytical and numerical approach to study the solid-liquid interface were also made [112]. but, a more detailed study with a possible empirical relation for the interface behavior is needed in order to design the TES system in a more efficient way.

#### 4.7. Enhancements

PCM enhancements are useful techniques to increase the heat transfer rate during charging and discharging process. There are many approaches to achieve the results; viz, design modification of the heat exchanger, or physical composition of the PCM itself. Nonetheless, such modifications come at a cost, generally resulting in heat transfer rate proportional to cost, time and energy.

#### 4.8. Encapsulation

Thermophysical properties of PCMs can be changed by altering their chemical composition or by physical modification. PCM encapsulation is encapsulating PCM at micro levels to increase the heat transfer surface area and decrease the possibility of phase segregation. It also enhances thermal conductivity (heat transfer rate), decrease PCM interaction with the outside environment, and significantly controls the volume change of PCM with increase in operating temperature preventing leakage during phase change [113]. PCM encapsulation has been used extensively in building cooling systems where air is passed through flat containers of PCM [114]. The effect of encapsulated PCM has a good scope in enhancing the performance of LHTS systems [115] used in solar absorption cooling system.

Hawladar et al. [116] prepared and characterized encapsulated paraffin wax to study its efficiency, energy storage and release

capacities. They found higher energy storage and release capacities (145–240 J/g) for the microcapsules and suggested that the efficiency depends upon core-to-coating ratio, emulsifying time and cross-linking agent. Shell material used for encapsulation also plays an important role, primarily due to its ease of fabrication. Materials used in microencapsulation and macroencapsulation for high temperature thermal stability are listed by Jacob and Bruno [117]. Organic PCMs can be encapsulated physico-mechanically, chemically and physico-chemically. Various approaches to prepare the encapsulated PCM (organic) as a new kind of TES medium have been extensively developed and can be manufactured to suit the desired properties [118]. The morphology of each particle in encapsulated PCM plays a key role in defining its mechanical strength, chemical and thermal stability [84]. Su et al. [119] microencapsulated paraffin wax with Melamine-formaldehyde (MF-3) resin to develop five types of encapsulations and found enhanced thermal stability values using thermogravimetric technique. Binary emulsifiers were key factor for thermal stability. The usage of such materials in the thermal storage systems is yet to be seen in future. An extensive review on applications, types and techniques of microencapsulation can be found in [120]. A unique bibliometric worldwide trend analysis on encapsulated PCM can be referred [121] to know the current status and future roadmap of this technical approach.

#### 4.9. Heat transfer enhancement

Heat transfer enhancement techniques by modifying the PCM container design was mentioned in earlier section. This section reviews few investigations in this direction. Tairi et al. [122] studied the effect of natural convection, heat pipe spacing, fin length, number of fins in a thermal energy storage unit with several fins attached to single and multiple heat pipes. A heat flux of 40 kW/m<sup>2</sup> was given to the heat pipe evaporator to reach the melting point (608 K) of the PCM (KNO<sub>3</sub>) with 0.5 thermal conductivity. They performed a two-dimensional transient finite volume model using enthalpy-porosity technique to study the performance. They found that the natural convection reduces the charging time of the system by 30% with more uniform temperature distribution; decreasing the heat pipe spacing increases the melting rate of the PCM; temperature difference within the PCM is inversely proportional to the fin length, and the number of fins do not significantly affect the system performance. Gil et al. [97] reported a similar effect of fins after testing two shell and tube PCM tanks, one with fins and another without fins. They found that fins are useful when there is a partial charging and discharging processes is expected, not when complete melting is needed. Their argument was that increasing fins consumes more money, time and space, reducing the quantity of actual PCM in the container. Investigating longitudinal fins in a double pipe heat exchanger containing PCM, Hosseini et al. [123] also suggested that higher (lengthier) fins reduce the PCM quantity, affecting overall performance by increasing the weight. They also found that increasing Stefan number results vortices development at a more rapid rate in higher fins, which are also the reason for blockage of vortices merger. Rathod and Banerjee [124] also experimentally studied the effect of longitudinal fins in a double pipe with PCM. They reported that at 85 °C inlet temperature, a decrease in solidification and melting processes by 43.6% and 24.5%, respectively is observed. A similar study was done by Prabhakar et al. [125] where they studied both annular and longitudinal fins in a double pipe. They reported that for the same volume percentage, longitudinal fins perform better than annular fins, and that the heat transfer increases with the fin width and that it should be optimized according to the application. Enhancing shell-and-tube double pipe latent heat storage unit was also studied by Tao and He [126]. They compared the results of four cases in which a helically-finned enhanced (outer) tube with multiple PCMs significantly enhanced the melting fraction and heat storage capacity. Employing finned tubes has been however extensively

used in enhancing heat transfer in charging and discharging of PCMs [127–132]. Use of metal matrix and metal foams as thermal conductivity enhancers (TCE) was done extensively where an increase in temperature distribution is evident [133–135]. Further study on thermal energy storage arrangement and heat exchange under specific operating conditions can be found in [136]. The porosity effecting the maximum thermal diffusivity in metal foams was also studied where smaller pore size can have lesser temperature gradient during charging and discharging, but occupying larger volume of matrix affects the overall latent heat capacity of the thermal storage system [137]. In circular concentric tubes, multitubes give higher melting rate but with subcooling; while longitudinal fins are known to give uniform heat transfer escaping the subcooling phenomenon [52].

#### 4.10. Nano-fluids

Nano-fluids have been extensively studied to achieve efficient phase change properties as well as to enhance the absorption capacity of solar collectors [138]. Hajare and Gawali [139] mixed Al<sub>2</sub>O<sub>3</sub> and TiO<sub>2</sub> nanoparticles in paraffin wax (melting point at 59.2 °C), with oleic acid (C<sub>17</sub>H<sub>35</sub>COOH) as solvent. They observed 6% reduction in melting time with addition of 0.05% of TiO<sub>2</sub> and concluded that the percentage of nanoparticles and the location of the encapsulated PCM spheres in the storage tank plays important role in the enhancement. Chaichan et al. [140] also performed investigation on same base-PCM (paraffin wax) and nanoparticles (Al<sub>2</sub>O<sub>3</sub> and TiO<sub>2</sub>), but with different mass fractions (1%, 2%, 3%, 4% and 5%). They observed similar reduction in melting time and reported that 5% Al<sub>2</sub>O<sub>3</sub> and TiO<sub>2</sub> relatively enhanced 65% and 40% with mass fraction, respectively. Nano-particle size and shape distribution can be varied to selectively enhance the volumetric absorption offering a unique advantage over conventional collectors [141]. Mettawee and Assassa [142] in their custom built PCM integrated solar collector, used 80 μm sized aluminium powder particles with different mass fractions with paraffin wax. They reported a 60% decrease in charging time and a significant increase in useful heat gain with aluminium additives instead of pure wax.

Effective latent heat of aqueous nano-fluids were tested by Lee et al. [143]. They experimentally determined that the latent heat of vaporization can be manipulated substantially up to ± 30% depending upon the (graphite or silver) nano particle. Graphite nanoparticles increase thermal storage capacity and in some cases, photo-thermal performance [144]. The most promising nano-additives seems to be the carbon based nanostructure with high aspect ratio due to enhanced thermo-physical properties as compared to the metal and metal oxide nanomaterials [113]. Nanocomposite PCM are also known to charge the material faster and discharge slower, that is, high retention ability [145]. Li et al. [146] characterized and studied the thermal performance of nitrate mixture/SiC ceramic honeycomb composite phase change materials (KNO<sub>3</sub>/NaNO<sub>3</sub>; 50:50 mol%) for thermal energy storage. The melting temperatures for pure and composite PCMs were 222.6 and 223.4 °C with a significant reduction in latent heat of melting and freezing temperatures in composite PCM. They reported a directly proportional relation between the heat storage and release rates of the composite PCM and the mass fraction of SCH making nitrate mixture/SCH composite PCM a promising PCM in latent heat thermal storage system. Recently, Abdollahzadeh and Esmaeilpour [147] numerically studied the sinusoidal surface waviness (0–0.4) and nanoparticle dispersion inside a vertical enclosure for various Grashof number. They found that the geometry can enhance and control the thermal process where low Grashof number and increased waviness delays the solidification, while the use of nanoparticles promotes the solidification process at the cost of reduced capacity of energy storage/release in the phase change material. Recently, Kardam et al. [148] reported heat transfer characteristics of PCM (Mg(NO<sub>3</sub>)<sub>2</sub>·6H<sub>2</sub>O) with carbon nanotubes (CNT) and nanographites under conventional heating and solar illumination. They observed ultrafast (in seconds) melting



**Table 9**  
Solar thermal nanofluid comparison table [151].

| Type     | vol%   | Surfactant, vol% | 1 M NaOH, vol% (achieve pH 9–10) | Sonication time, min | Collector depth, cm | Approximate cost, \$/L |
|----------|--------|------------------|----------------------------------|----------------------|---------------------|------------------------|
| Graphite | 0.0004 | 0.5              | 0.003                            | 45                   | 10                  | 0.52                   |
| Al       | 0.001  | 0.25             | 0.003                            | 30                   | 10                  | 0.64                   |
| Copper   | 0.004  | 0.25             | 0.003                            | 30                   | 10                  | 1.85                   |
| Silver   | 0.004  | 0.25             | 0.003                            | 30                   | 10                  | 3.65                   |
| Gold     | 0.004  | 0.25             | 0.003                            | 30                   | 10                  | 233                    |

\*Assumes pure water base—where water + stabilizer = \$0.5/L.

and solidification rate increase by 77% for CNT-PCM composite (at 0.2 wt%). They concluded that CNT gives better heat transfer performance than nanographites to collect and store solar energy in thermal energy storage systems. In general, CNT are known to enhance thermal conductivity, mostly without compatibility issues [149]. Jin et al. [150] added expanded graphite (EG 300  $\mu\text{m}$ ) to paraffin wax and significantly improved heat transfer performance and thermal stability of the composite PCM at little cost of latent heat of fusion. Optical properties of nano-fluids were studied and an absorption of > 95% of heat from the sun was claimed by Taylor et al. [151]. They tested graphite, Al, Cu, Ag and Au nanofluids prepared by simple model with approximation of the effective extinction coefficient of the nanofluids (Table 9). Their results agreed well with the experimental values. They also concluded that graphite and aluminium nano-fluids can relatively find their way to real direct absorption solar collectors.

To summarize, the use of nanofluids has improved the efficiency of solar thermal applications [152]. Direct absorption collectors (DAC) have improved outlet temperature and thermal efficiencies [153–155], with a minimal effect on optical properties [156]; whereas in other types of solar collectors, they improved the convective heat transfer coefficient [157], and specific heat, with lower environmental damage cost [158]. Nanofluids increase photo-thermal conversion efficiency at precise wt% of nano-particles [152], and few hybrid nanofluids have higher efficiencies [159]. Stability sometimes comes at the cost of efficiency [160] which needs more study. TiO<sub>2</sub>, Al<sub>2</sub>O<sub>3</sub> and CuO are the most investigated nanoparticles [161]; and the most solar spectrum absorptivity is seen more in CNT (up to 100%) [162]. The use of direct absorption is hardly seen in solar absorption cooling; and work on the use of nano-refrigerants in generators is needed [163]. Compact design and efficiency enhancement are the two major advantages DAC but, due to long payback period, the economic feasibility might be weak in developing countries [164]. Low cost systems with about 70% efficiency and low concentration sunlight (10 suns) with water based carbon black nanofluids might be a good alternative [165]. More discussion on types of enhancements and their effects on thermal energy storage systems are discussed in a recent review by Liu et al. [166]. A review on nanoparticle enhanced PCM and their effect on thermophysical properties of PCM can be found in [167].

#### 4.11. Energy-exergy analysis

Mahfuz et al. [168] theoretically studied the thermodynamic performance of a PCM integrated solar power plant. They found that the overall exergy efficiency for the parabolic trough collector system can be increased from 10% to 30% using PCM, and that higher the PCM melting temperature, higher is the exergetic efficiency. The output temperature from the collector field was 265.65 °C at 505 kPa. Koca et al. [169] studied another energy exergy analysis of a latent heat storage system with PCM CaCl<sub>2</sub>·6H<sub>2</sub>O for an in-house built solar collector and calculated the energy and exergy efficiencies to be 45% and 2.2%, respectively. Koroneos et al. [170] investigated the applicability of a 70 kW LiBr/H<sub>2</sub>O absorption system with hot water tank size of 50 l/m<sup>2</sup> of collector area (11,500 l), in installation and working on a medical center. They reported a payback time period of 24 years

without national subsidies which can reach up to 50% (2010). However, they recommended a detailed investigation with regards to economic potential, commercial maturity and presence of technological barrier.

## 5. Heat exchangers

Heat exchangers are devices facilitating flow of thermal energy between two fluids at different temperatures. Hence, in an absorption system, the generator, condenser, and evaporator fall into two broad classification of heat exchangers: liquid-liquid (generator, absorber and other), and liquid-vapor (condenser and evaporator) heat exchangers. The only two thermofluid differences between the generator and the absorber liquid-liquid heat exchangers are the mass flow rates and effective temperature difference of the fluids. The specific heat of the fluids in question also play an important role, but it is concerned with material selection rather than a factor affecting the performance of the heat exchanger. A brief integration of PCM with various types of heat exchangers is shown in Fig. 12.

### 5.1. Generator

Generator was named due to its primary function of generating heat to evaporate the refrigerant. Later, integration of solar thermal technology with absorption refrigeration systems evolved to make use of an effective heat exchanger serving the same purpose.

### 5.2. Effect of generator temperature on system COP

Numerous investigations and optimization on component-wise thermodynamic modeling of absorption cooling systems have been done to study the appropriate component temperatures for better performance [172–179]. For generator temperatures, corresponding system COP and evaporator temperatures have been identified in order to store the excess heat when the sun is down. Table 10 lists few investigations on absorption cooling systems with various thermodynamic properties of generator.

### 5.3. Methodologies

There are a number of ways to provide heat to the generator. A heat storage tank in the hot-side of the system is the most common source, but it still needs power to pump the HTF. Ponshanmugakumar et al. [187] numerically investigated a vertical generator integrated with PCM (Erythritol) for forced convective boiling in a NH<sub>3</sub>-H<sub>2</sub>O solar absorption air-conditioning system connected to concentrating parabolic collector field. They developed a TRNSYS model to simulate a real stainless steel generator with coaxial tubes of 1 m length. The hot water charging the PCM tubes in the generator as shown in the Fig. 13, is also connected to a hot water storage tank and an auxiliary boiler. They found that the use of PCM can decrease the auxiliary heating source demand during the peak load and low radiation hours. Lorente et al. [105] numerically and analytically studied melting of PCM (paraffin wax) in a cylindrical tank with vertical spiral tube(s) as a heater. The



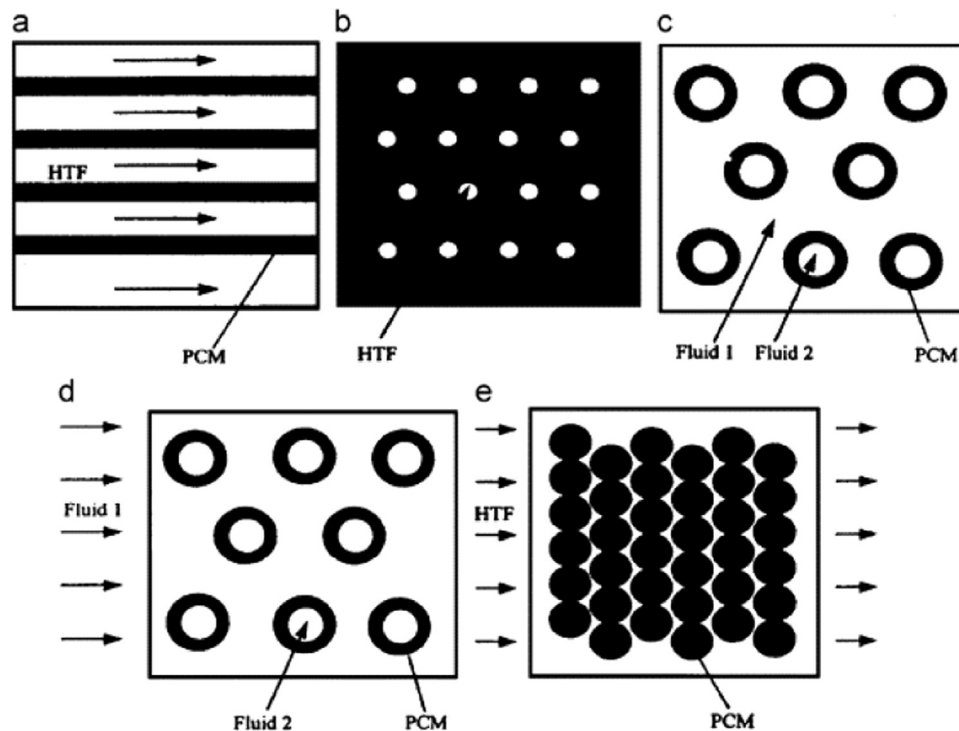


**Fig. 12.** Schematic of typical LHTS system [171]: (a) flat-plate; (b) shell and tube with internal flow; (c) shell and tube with parallel flow; (d) shell and tube with cross flow; (e) sphere packed bed.

helix radii were changed and properties like melting fraction, temperature distribution were studied with varying tube geometry. They suggested that scale analysis combined with numerical simulation is a powerful method to advance in the design (Fig. 14). Similar attempts have been seen in boiling binary mixtures in advanced vapor compression heat pump systems [188,189] and in preheating the weak solution entering the generator [190]. Hence, there is a scope of research in the applicability of heat exchangers as generators in absorption systems. Heat exchangers with PCM is also not a new idea to pursue [191–193], but with the perspective of using it as a generator in solar absorption system is a new application and investigations are needed in this direction. Nonetheless, the melting temperatures and enthalpy of a suitable PCM can serve to be an integral part of the generator and effectively act as an alternative heat source with proper generator design.

#### 5.4. Material selection

It is clear from section 5.1.1, that the evaporator temperature demand is directly proportional to the generator temperature. Moreover, it is observed that most generators for a single effect absorption cooling system work best between 80 and 120 °C for subzero (0–10 °C) temperatures at the evaporator, and 60–105 °C for cooling performances. Even with non-conventional refrigerants ( $Zn_2Cl_5/NH_3$  or  $NaSCN/NH_3$ ) the COPs seems to be affected similarly with varying values.

PCM melting temperature is the primary filter to select the PCM for a particular application. Furthermore, the enthalpy of the system and thermal conductivity of the PCM also play an important role in effective performance of the generator in generating vapor refrigerant. Tables below lists selected organic, inorganic and eutectic mixtures with potential ability to be used as PCM compiled by Zalba et al. [17]. Table 11 list the materials that can be used in generators of absorption cooling systems (60–105 °C), Table 12 lists the materials (without redundancy) for refrigeration absorption system (80–120 °C), and Table 13 contains few of the commercially available PCMs and their

properties claimed. The materials used in manufacturing the generator is mostly stainless steel. This gives us the advantage of using inorganic PCM neglecting their corrosive nature. Nonetheless, the primary criteria to select the material can be deduced from Table 3 and focus be given on:

- High heat of fusion for stable as well as sufficient delivery of heat when required.
- No phase segregation or inflammability due to high temperatures involved.

Temperatures can go higher than expected in some time of the year. Materials like Hydroquinone (168–173 °C), Potassium thiocyanate (173 °C) and D-mannitol (162–170 °C) are successful choices and can be used for higher range of thermal storage [97]. In the current study, generator temperatures are in focus, hence the limit (120 °C). Any excess heat is obvious to be stored to TES system attached to the system which require calculations based on the amount of time and heat required as a standby.

#### 5.5. Absorber

Absorber is the most important component of the absorption refrigeration and cooling system. The most commonly used absorber is the falling film absorber where the refrigerant vapor is absorbed by the falling film of solution over cooled horizontal tubes [37]. The solution flow rate is directly proportional to the heat transfer rate in the absorber [194,195]. The process of absorption releases heat and reduces the performance for the absorber, but the cooling pipes absorb the heat to increase the rate of absorption, therefore, an absorber is a chemical and physical heat exchanger mechanism to absorb vapor into a liquid. Hence, the cooler the absorber, better is the performance. In Fig. 15, absorber temperatures are illustrated from the data provided by Siddiqui and Said [43] on various solar powered absorption systems. Also, a general understanding of absorber temperatures (25–35 °C) with various working fluids can be gained from Table 13.

**Table 10**  
Absorption cooling systems with various generator thermodynamic properties.

| Author                   | Study        | Capacity | System          | Generator temperature, $T_g$ (°C) | COP | Maximum                                       | Feature   |
|--------------------------|--------------|----------|-----------------|-----------------------------------|-----|---|---|
| Said et al. [55]         | Numerical    | 10 kW    | $NH_3-H_2O$     | 90–145                            |     | 0.53 at $T_g=70$ °C, $T_{abs}=T_{cond}=25$ °C | COP almost constant for $T_g=70$ –80 °C, and declines above $T_g=80$ °C                       |
| Said et al. [56]         | Experimental | 10.1 kW  | $NH_3-H_2O$     | 90–145                            |     | 0.71 at $T_g=114$ °C                          | COP almost constant for $T_g=138$ –141 °C, and increase as $T_g$ drops to 125 °C              |
| Abdulateef et al. [180]  | Numerical    | 19 kW    | $NH_3-H_2O$     | 70–120                            |     | 0.5 at $T_g=80$ °C                            | COP almost constant from $T_g=80$ –120 °C   |
| Raghuvanshi et al. [181] | Numerical    | –        | $NH_3-H_2O$     | 90–100                            |     | 0.225 at $T_g=100$ °C                         | COP drastically decreases from 0.15 at $T_g=110$ °C to 0.075 at $T_g=120$ °C                  |
| Said et al. [54]         | Numerical    | 5 kW     | $NH_3-H_2O$     | 120                               |     | 0.65 at $T_g=80$ °C                           | COP gradually decrease at the rate of ave. 7% with every 5 °C increase in ambient temperature |
| Bangotra et al. [182]    | Analytical   | 10.5 kW  | $NH_3-H_2O$     | 120                               |     | 0.2   | COP can be enhance by using liquid-liquid heat exchangers                                     |
| Caciula et al. [183]     | Numerical    | 100 kW   | $NH_3-H_2O$     | 70–150                            |     | 0.2 at $T_g=90$ °C                            | COP gradually decreases to 0.19 at $T_g=150$ °C ( $T_{evap}=-3$ °C)                           |
| Chen et al. [184]        | Numerical    | –        | $Zn_2Cl_6/NH_3$ | 110–230                           |     | 0.54 at $T_g=130$ °C                          | COP gradually decreases to 0.47 at $T_g=230$ °C ( $T_{evap}=-10$ °C)                          |
| Kaynakli et al. [185]    | Numerical    | –        | LiBr- $H_2O$    | 75–105                            |     | 0.82 at $T_g=85$ °C                           | COP almost constant upto $T_g=97$ °C (Crystallization temperature).                           |
| Francisco et al. [65]    | Experimental | 2 kW     | $NH_3-H_2O$     | 85–130                            |     | 0.53 at $T_g=95$ °C                           | COP gradually decreases to 0.4 at $T_g=130$ °C  |
| Sözen [186]              | Numerical    | 1 kW     | $NH_3-H_2O$     | 50–130                            |     | 0.71 at $T_g=65$ °C ( $T_{cond}=28$ °C)       | COP gradually decreases to 0.65 at $T_g=130$ °C   |

### 5.6. Working fluid

The COP of the system depends on both thermophysical and thermochemical properties of the working fluid. Apart from miscibility of the two fluids in the range of operating temperatures required, certain factors like non-toxicity, non-corrosive, non-explosive, easily separable, large boiling point differential, favorable diffusion, viscosity, and thermal conductivity should also be considered carefully [196]. From over 200 absorbents and 40 refrigerant compounds [197], Table 14 lists a few investigations with corresponding maximum coefficient of performances reached.

### 5.7. Material section

Irrespective of the main function of the absorber which is to absorb the refrigerant, it rising in temperature on doing so. The heat release is generally disposed by a cooling water connection. This waste heat can also be collected for other suitable applications. A list of suitable PCMs that can be used to store this energy at corresponding temperature ranges are listed in Table 15. Paraffin materials are more suitable in this temperature range due to their high heat of fusion and non-corrosive nature and possible applications that may utilize the heat. Moreover, as the maximum temperature released from the absorber is ~40 °C (Fig. 15), which may only be used in space cooling application in cold countries, the system needs little requirement to store energy.

### 5.8. Applications

Although absorber works in a temperature range of various tropical climates, if properly use, these temperatures can be used for various applications with respect to local necessity. For example, in cold geographical locations, warm water can be used just from absorber without involving the solar collector circuit. Phase change materials can be used when the utility is less or as need arises while the system is not working. Various applications requiring the precise temperature control can utilize PCM for storing the heat that absorber rejects.

### 5.9. Condenser

Condenser is type of heat exchanger responsible to reduce the temperature of the refrigerant by forced convection (air-cooled) at constant pressure. During this process of condensation, latent heat of the refrigerant is given out, lowering the temperature of the sub-cooled refrigerant and stabilizing the superheat. Using PCM at condenser is intended to reduce the temperature of the condensing refrigerant as much as possible. Although, significant increase in performance of a refrigeration system is seen upon the use of PCM at condenser, little attention has been given in recent years to investigate this approach. This might be due to few undesirable outcomes like, extended heat rejection process and frequent compressor ON/OFF [202–204] which drastically affects the compressor lifetime.

Wang et al. in their three part study (Part-1 [205], Part-2 [206] and Part-3 [207]) extensively investigated, both experimentally and numerically, the effect of PCM on refrigeration plant performance. They also tested a novel control purpose of using PCM in the refrigeration system by placing a shell-and-tube PCM structure at various locations in a refrigeration cycle. In Part-1, they tested a cooling split system model placing eutectic PCMs at three different locations. PCM-A was located between the compressor and the condenser and PCM-B was located between the condenser and the thermostatic expansion valve (TEV). They did a thorough measurement calibration, testing and uncertainty and error analysis. They found that placing PCM-B between condenser and TEV with 21 °C melting temperature and 220 kJ/kg latent heat gives better COP (8% increase) than placing the same PCM-A between the compressor and the condenser (6% increase in COP). The temperature difference in the refrigerant at TEV

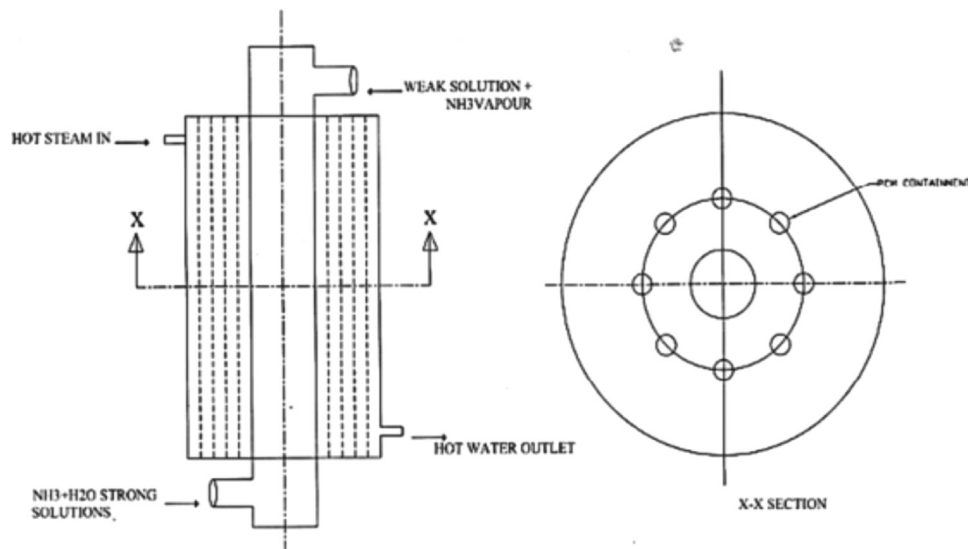


Fig. 13. Hot water charging the PCM in generator [187].

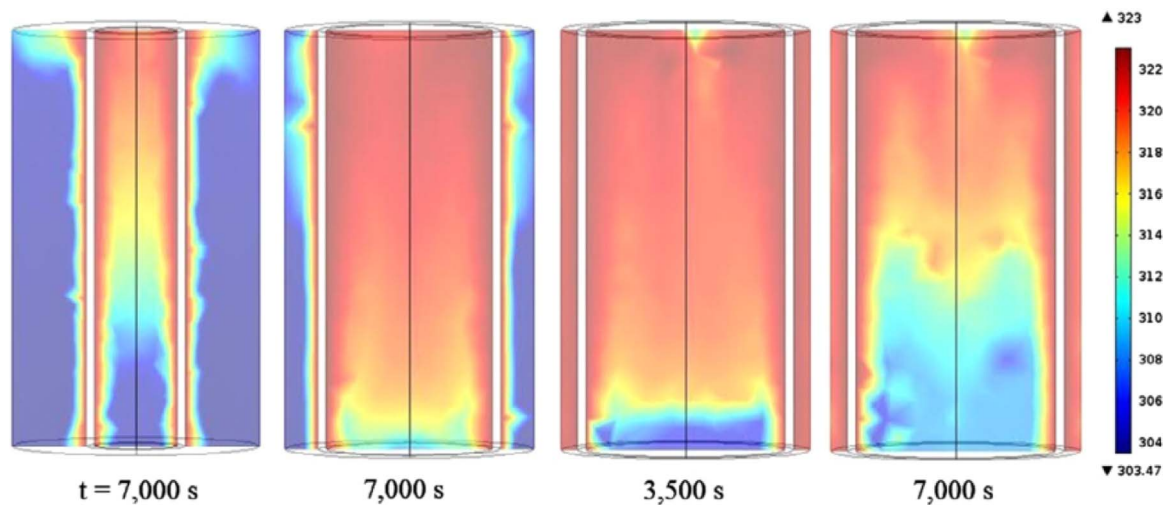


Fig. 14. Temperature distribution in vertical cut with various helical heating tube diameter  $R_{H1} = 100$  mm, 200 mm, 240 mm, and 240 mm [105].

with and without PCM-B was about  $10\text{ }^{\circ}\text{C}$ , whereas the same different was about  $5\text{ }^{\circ}\text{C}$  for PCM-A. In part-2, they developed a dynamic mathematical model to design and optimize the performance of a refrigeration system coupled with PCM and variable frequency compressor. To improve the accuracy of the model at low compressor speed, liquid refrigerant flash into the gas region of the condenser was conceptualized. The model was in a good agreement with the test data with a parametric prediction of 8%. However, due its nature, the model assumed average parameters rather than spatial distribution parameters, which made it less precise in predicting the superheating and sub-cooling. Hence, in part-3, they introduced a tank into the refrigeration system to control the fluctuations in the cooling load and help in system stabilization. They placed the PCM tank between the evaporator and the compressor due to its proven results in their previous study [205,206]. The main advantage of placing PCM at this location is to reduce the refrigerant average and peak inlet temperature. They controlled the condenser pressure by not only using PCM-A between the compressor and the condenser, but also an additional PCM heat exchanger in the bypass to control minimum condenser temperature at low ambient temperatures. They suggested that these controls contribute to saving energy to a great extent. Finally, they significantly stabilized the condenser pressure and temperatures, even at low ambient temperatures.

Cheng et al. [204] tested shape-stabilized paraffin/high density polyethylene (HDPE) composite phase change material with two additives, graphite powder (GP) and expanded graphite (EG). They found that the thermal conductivity of PCM with EG increase 4 times ( $0.31\text{--}1.36\text{ W/mK}$ ). They used this enhanced PCM with a household refrigerator as a heat storage, charging when the compressor is ON, and discharging the condenser heat when the compressor is OFF [202]. The condenser midpoint temperature was decrease to  $2.3\text{ }^{\circ}\text{C}$  and the condenser outlet temperature was decrease by  $6.3\text{ }^{\circ}\text{C}$ , resulting an overall energy efficiency increase of 12% at the cost of more frequent starts of the compressor. Later, they used the data to validate a dynamic numerical model proving an increase of COP by about 19% [203]. However, higher overall heat leakage per 24 h was observed due to full charging of the PCM and decreased heat dissipation the ambient in off-time period. They suggested more study on various components of the refrigeration system with various amount and dimensions of PCM in relation to cost and energy in future.

Recently, Sonnenrein et al. tested standard heat storage components (water and paraffin as well as PE-HD foil and aluminium-compound film) and block copolymer fixed organic paraffin derivative as two PCM to integrate in a regular household refrigerator.  $5\text{ }^{\circ}\text{C}$  and  $8\text{ }^{\circ}\text{C}$  reduction in condenser outlet temperature was observed with water and copolymer compound, respectively. A 10% decrease in power

**Table 11**  
List of materials suitable for generator temperatures in single-effect absorption cooling systems (60–105 °C).

| Type   | Compound  | Melting temp. | Heat of fusion          | Thermal conductivity    |
|--|---|---------------|-------------------------|-------------------------|
| Inorganic  | Zn(NO <sub>3</sub> ) <sub>2</sub> ·2H <sub>2</sub> O  | 54            | n.a.                    | n.a.                    |
|  | NaOH·H <sub>2</sub> O   | 58            | n.a.                    | n.a.                    |
|  | Na(CH <sub>3</sub> COO)·3H <sub>2</sub> O   | 58            | 264                     | n.a.                    |
|  |   | 58.4          | 226                     |                         |
|  | Cd(NO <sub>3</sub> ) <sub>2</sub> ·4H <sub>2</sub> O  | 59.5          | n.a.                    | n.a.                    |
|  | Fe(NO <sub>3</sub> ) <sub>2</sub> ·6H <sub>2</sub> O  | 60            | n.a.                    | n.a.                    |
|  | NaOH  | 64.3          | 227.6                   | n.a.                    |
|  | Na <sub>2</sub> B <sub>4</sub> O <sub>7</sub> ·10H <sub>2</sub> O   | 68.1          | n.a.                    | n.a.                    |
|  | Na <sub>3</sub> PO <sub>4</sub> ·12H <sub>2</sub> O   | 69            | n.a.                    | n.a.                    |
|  | Na <sub>2</sub> P <sub>2</sub> O <sub>7</sub> ·10H <sub>2</sub> O   | 70            | 184                     |                         |
|  | Ba(OH) <sub>2</sub> ·8H <sub>2</sub> O  | 78            | 265.7                   | 0.653 (liquid, 85.7 °C) |
|  |   |               | 267                     | 0.678 (liquid, 98.2 °C) |
|  |   |               | 280                     | 1.255 (solid, 23 °C)    |
|  | AlK(SO <sub>4</sub> ) <sub>2</sub> ·12H <sub>2</sub> O  | 80            | n.a.                    | n.a.                    |
|  | KAl(SO <sub>4</sub> ) <sub>2</sub> ·12H <sub>2</sub> O  | 85.8          | n.a.                    | n.a.                    |
|  | Al <sub>2</sub> (SO <sub>4</sub> ) <sub>3</sub> ·18H <sub>2</sub> O   | 88            | n.a.                    | n.a.                    |
|  | Al(NO <sub>3</sub> ) <sub>3</sub> ·8H <sub>2</sub> O  | 89            | n.a.                    | n.a.                    |
|  | Mg(NO <sub>3</sub> ) <sub>2</sub> ·6H <sub>2</sub> O  | 89            | 162.8                   | 0.490 (liquid, 95 °C)   |
|  |   | 90            | 149.5                   | 0.502 (liquid, 110 °C)  |
|  |   | 95            | 269                     | n.a.                    |
| (NH <sub>4</sub> )Al(SO <sub>4</sub> ) <sub>2</sub> ·6H <sub>2</sub> O | 97.5  | n.a.          | n.a.                    |                         |
| Na <sub>2</sub> S·½5H <sub>2</sub> O                                   |   |               |                         |                         |
| Inorganic eutectic   | 58.7% Mg(NO <sub>3</sub> ) <sub>2</sub> ·6H <sub>2</sub> O+41.3% MgCl <sub>2</sub> ·6H <sub>2</sub> O             | 59            | 132.2                   | 0.510 (liquid, 65.0 °C) |
|  |   | 58            | 132                     | 0.565 (liquid, 85.0 °C) |
|  |   |               |                         | 0.678 (solid, 38.0 °C)  |
|  |   |               |                         | 0.678 (solid, 53.0 °C)  |
|  | 53% Mg(NO <sub>3</sub> ) <sub>2</sub> ·6H <sub>2</sub> O+47% Al(NO <sub>3</sub> ) <sub>2</sub> ·9H <sub>2</sub> O | 61            | 148                     | n.a.                    |
|  | 14% LiNO <sub>3</sub> +86% Mg(NO <sub>3</sub> ) <sub>2</sub> ·6H <sub>2</sub> O                                   | 72            | > 180                   | n.a.                    |
|  | 66.6% urea+33.4% NH <sub>4</sub> Br   | 76            | 161                     | 0.331 (liquid, 79.8 °C) |
|  |   |               | 1548 (solid, 24 °C)     |                         |
|  |   |               | 0.324 (liquid, 92.5 °C) |                         |
|  |   |               | 0.649 (solid, 39.0 °C)  |                         |
|  |   |               | 0.682 (solid, 65 °C)    |                         |
| Inorganic non-eutectic   | Mg(NO <sub>3</sub> ) <sub>2</sub> ·6H <sub>2</sub> O/Mg(NO <sub>3</sub> ) <sub>2</sub> ·2H <sub>2</sub> O         | 55.5          | n.a.                    | n.a.                    |
|  | KOH·H <sub>2</sub> O/KOH  | 99            | n.a.                    | n.a.                    |
| Organic  | Paraffin C <sub>22</sub> –C <sub>45</sub>   | 58–60         | 189                     | 0.21 (solid)            |
|  | Paraffin wax  | 64            | 173.6                   | 0.167 (liquid, 63.5 °C) |
|  |   |               | 266                     | 0.346 (solid, 33.6 °C)  |
|  |   |               |                         | 0.339 (solid, 45.7 °C)  |
|  | Polyglycol E6000  | 66            | 190.0                   | n.a.                    |
|  | Paraffin C <sub>21</sub> –C <sub>50</sub>   | 66–68         | 189                     | 0.21 (solid)            |
|  | Biphenyl  | 71            | 119.2                   | n.a.                    |
|  | Propionamide  | 79            | 168.2                   | n.a.                    |
|  | Naphthalene   | 80            | 147.7                   | 0.132 (liquid, 83.8 °C) |
|  |   |               |                         | 0.341 (solid, 49.9 °C)  |
|  |   |               |                         | 0.310 (solid, 66.6 °C)  |

**Table 12**  
lists the materials for refrigeration absorption system (80–120 °C).

| Type      | Compound  | Melting temp. | Heat of fusion        | Thermal conductivity   |
|-----------|---|---------------|-----------------------|------------------------|
| Inorganic | CaBr <sub>2</sub> ·4H <sub>2</sub> O                                | 110           | n.a.                  | n.a.                   |
|           | Al <sub>2</sub> (SO <sub>4</sub> ) <sub>3</sub> ·16H <sub>2</sub> O | 112           | n.a.                  | n.a.                   |
|           | MgCl <sub>2</sub> ·6H <sub>2</sub> O                                | 117           | 168.6                 | 0.570 (liquid, 120 °C) |
|           |   | 115           | 165                   | 0.598 (liquid, 140 °C) |
|           | 116   |               | 0.694 (solid, 90 °C)  |                        |
|           |   |               | 0.704 (solid, 110 °C) |                        |
| Organic   | Erythritol  | 118.0         | 339.8                 | 0.326 (liquid, 140 °C) |
|           |   |               |                       | 0.733 (solid, 20 °C)   |
|           | High-density polyethylene (HDPE)                                    | 100–150       | 200                   | n.a.                   |

consumption was also observed with variation according the condenser loading. They stated no need of encapsulation of copolymer compound due to their stable spatial dimensions. They concluded recommending

copolymer compound as a cost effective PCM in reducing power consumption of a household refrigerator. In their later study, they equipped two evaporator types and a standard wire and tube condenser with PCM used in their previous study and specific graphite (THERMOPHIT GFG, SGL GROUP) to increase the thermal conductivity. The power consumption was reduced by 17% and further research on designing control algorithm was suggested. Table 16 lists few of the features and noticeable outcomes of investigations conducted on enhancing performance of condenser using phase change materials.

### 5.10. Summary

A condenser is required to dissipate the refrigerant temperature efficiently in less time. In general, a PCM reduces this thermodynamic nature of a heat exchanger, unless, a PCM with low melting temperature absorbs the heat quicker and dissipates it in the off-time of the compressor. This way the ambient where the heat is lost can be simulated at much lower temperatures and controlled for required performances. Condenser-PCM integration has been done on small domestic refrigerators. The advantages are more than the side-effects and interesting thermal behaviors are pointing the research to explore more options (Table 17). More work is needed to be done on larger capacity plants. Effect of PCM on bigger condensers, higher tempera-

**Table 13**  
A few commercially available materials.

| PCM name     | Type of product | Melting temperature (°C) | Heat of fusion (kJ/kg) | Source           |
|--------------|-----------------|--------------------------|------------------------|------------------|
| ClimSel C 70 | n.a.            | 70                       | 194                    | Climator         |
| PCM72        | Salt hydrate    | 72                       | n.a.                   | Merck KgaA       |
| RT80         | Paraffin        | 79                       | 209                    | Rubitherm GmbH   |
| TH89         | n.a.            | 89                       | 149                    | TEAP             |
| RT90         | Paraffin        | 90                       | 197                    | Rubitherm GmbH   |
| RT110        | Paraffin        | 112                      | 213                    | Rubitherm GmbH   |
| PCM-OM65P    | Organic         | +65                      | 210                    | RGEES            |
| PureTemp 151 | –               | 151                      | 217                    | PureTemp         |
| PureTemp108  | –               | 108                      | 180                    | PureTemp         |
| S117         | Salt hydrate    | 117                      | 160                    | PCM Products Ltd |
| S89          | Salt hydrate    | 89                       | 151                    | PCM Products Ltd |
| S83          | Salt hydrate    | 83                       | 141                    | PCM Products Ltd |
| A118         | Organic         | 118                      | 340                    | PCM Products Ltd |
| A95          | Organic         | 95                       | 205                    | PCM Products Ltd |
| X120         | –               | 120                      | 180                    | PCM Products Ltd |
| H115         | –               | 114                      | 100                    | PCM Products Ltd |
| H120         | –               | 120                      | 120                    | PCM Products Ltd |

tures and pressures is unknown. The design of PCM heat exchanger, controlling algorithm and use of various enhanced PCM thermal properties are needed in future to equip solar thermal technology with an upgrade.

### 6. Evaporator

The primary goal of improving solar absorption system is to obtain efficient cooling at the evaporator. Numerous cycles with varying technologies are industrially operating and research-wise studied [211]. PCM in cooling is not a new combination to investigate, in fact, PCM is now used commercially in domestic refrigerators both on cooling and freezing side.

#### 6.1. PCM in domestic evaporators

Evaporator is responsible to take the heat load by exchanging heat during the process of refrigerant evaporation. Evaporator is attached with a fan coil unit (FCU) to induce forced convection to mobilize and maximize the effect. Phase change materials have already made a significant contribution in space cooling of building technology creating a comfortable environment to live and work between 22 and 26 °C [212]. It is to be noted that the PCM temperature is kept much lower (0–15°C) so as to store more energy and last longer when used [213]. A further reduced operating cooling temperature (subzero) is used in refrigeration applications for domestic and industrial purposes. Depending upon the ambient temperature, PCM type and thermal

**Table 14**  
Absorber temperatures in various working pairs.

| Author                     | Working pair                  | Capacity           | Absorber Temp. | COP    |
|----------------------------|-------------------------------|--------------------|----------------|--------|
| Rivera and Rivera [66]     | Lithium nitrate–ammonia       | 11.8 kg of ice/day | 40–44          | 0.36   |
| Quintanar et al. [68]      | Lithium nitrate–ammonia–water | 8 kg of ice/day    | –              | 0.0956 |
| El-Ghalban [198]           | Lithium chloride–water        | 20 W               | 40             | 0.19   |
| Rasul and Murphy [199]     | Calcium chloride–ammonia      | 0.08–0.204 kW      | 20–30          | 0.65   |
| Aman et al. [200]          | Ammonia–water                 | 10 kW              | 30             | 0.6    |
| Abbaspour and Saraei [201] | Lithium bromide–water         | 0.25 kW            | 20–40          | 0.81   |

load, 2–74% enhancement in COP can be achieved by the application of PCM at domestic refrigerator evaporator [26], but there are few common advantages and disadvantages observed. For example, Wang et al. [214] claimed that, in vapor compression evaporation system, both peak energy and power can be reduced to as much as 35% by the use of PCM in cooling tower circuit charging at night and cooling the condenser during the day. Besides this, there are other advantages of using PCM at the evaporator (Table 18) obtained through observations of numerous investigations [215–221] done on improving domestic refrigerator performance. A brief overview of studies done on refrigerator performance using PCM at evaporator can be seen in Table 19.

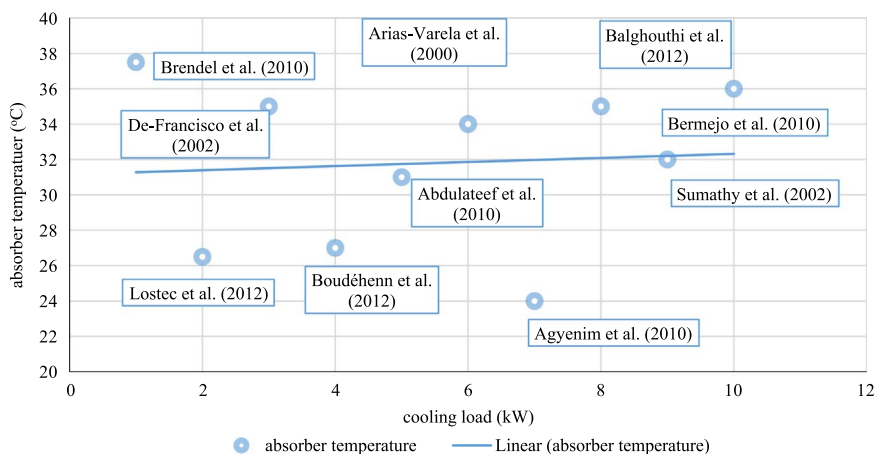


**Fig. 15.** Experimental absorber temperatures for NH<sub>3</sub>-H<sub>2</sub>O and LiBr-H<sub>2</sub>O systems.



**Table 15**

List of materials suitable for absorber waste heat collection.

| Type   | Compound  | Melting Temp. | Heat of fusion | Thermal Conductivity    |                         |
|--|---|---------------|----------------|-------------------------|-------------------------|
| Inorganic  | Na <sub>2</sub> CrO <sub>4</sub> ·10H <sub>2</sub> O  | 18            | n.a.           | n.a.                    |                         |
|  | KF·4H <sub>2</sub> O  | 18.5          | 231            | n.a.                    |                         |
|  | Mn(NO <sub>3</sub> ) <sub>2</sub> ·6H <sub>2</sub> O  | 25.8          | 125.9          | n.a.                    |                         |
|  | CaCl <sub>2</sub> ·6H <sub>2</sub> O  |               | 29             | 190.8                   | 0.540 (liquid, 38.7 °C) |
|  |   |               | 29.2           | 171                     | 0.561 (liquid, 61.2 °C) |
|  |   |               | 29.6           | 174.4                   | 1.088 (solid, 23 °C)    |
|  |   |               | 29.7           | 192                     |                         |
|  |   |               | 30             |                         |                         |
|  |   | 29–39         |                |                         |                         |
|  | LiNO <sub>3</sub> ·3H <sub>2</sub> O  | 30            | 296            | n.a.                    |                         |
|  | Na <sub>2</sub> SO <sub>4</sub> ·10H <sub>2</sub> O   |               | 32.4           | 254                     | 0.544                   |
|  |   |               | 32             | 251.1                   |                         |
|  |   |               | 31–32          |                         |                         |
|  | Na <sub>2</sub> CO <sub>3</sub> ·10H <sub>2</sub> O   |               | 32–36          | 246.5                   | n.a.                    |
|  |   |               | 33             | 247                     |                         |
|  | CaBr <sub>2</sub> ·6H <sub>2</sub> O  | 34            | 115.5          | n.a.                    |                         |
|  | Na <sub>2</sub> HPO <sub>4</sub> ·12H <sub>2</sub> O  |               | 35.5           | 265                     | n.a.                    |
|  |   |               | 36             | 280                     |                         |
|  |   | 35            | 281            |                         |                         |
|  |   | 35.2          |                |                         |                         |
| Zn(NO <sub>3</sub> ) <sub>2</sub> ·6H <sub>2</sub> O |   | 36            | 146.9          | 0.464 (liquid, 39.9 °C) |                         |
|  |   | 36.4          | 147            | 0.469 (liquid, 61.2 °C) |                         |
| Inorganic eutectics                                  | 66.6% CaCl <sub>2</sub> ·6H <sub>2</sub> O+33.3% MgCl <sub>2</sub> ·6H <sub>2</sub> O                             | 25            | 127            | n.a.                    |                         |
|  | 48% CaCl <sub>2</sub> +4.3% NaCl+0.4% KCl+47.3% H <sub>2</sub> O  | 26.8          | 188.0          | n.a.                    |                         |
|  | 47% Ca(NO <sub>3</sub> ) <sub>2</sub> ·4H <sub>2</sub> O+33% Mg(NO <sub>3</sub> ) <sub>2</sub> ·6H <sub>2</sub> O | 30            | 136            | n.a.                    |                         |
|  | 60% Na(CH <sub>3</sub> COO)·3H <sub>2</sub> O+40% CO(NH <sub>2</sub> ) <sub>2</sub>                               |               | 31.5           | 226                     | n.a.                    |
|  |   |               | 30             | 200.5                   |                         |
| Organic  | Paraffin C <sub>16</sub> –C <sub>18</sub>   | 20–22         | 152            | n.a.                    |                         |
|  | Polyglycol E600   | 22            | 127.2          | 0.189 (liquid, 38.6 °C) |                         |
|  |   |               |                | 0.187 (liquid, 67.0 °C) |                         |
|  | Paraffin C <sub>13</sub> –C <sub>24</sub>   | 22–24         | 189            | 0.21 (solid)            |                         |
|  | 1-Dodecanol   | 26            | 200            | n.a.                    |                         |
|  | Paraffin C <sub>18</sub>  | 28            | 244            | 0.148 (liquid, 40 °C)   |                         |
|  |   | 27.5          | 243.5          | 0.15 (solid)            |                         |
| Fatty acids  | 1-Tetradecanol  | 38            | 205            | 0.358 (solid, 25 °C)    |                         |
|  | Capric–lauric acid (45–55%)   | 21            | 143            | n.a.                    |                         |
|  | Dimethyl sebacate   | 21            | 120–135        | n.a.                    |                         |
|  | 34% Mistic acid+66% Capric acid   |               | 24             | 147.7                   | 0.164 (liquid, 39.1 °C) |
|  |   |               |                |                         | 0.154 (liquid, 61.2 °C) |
|  | Vinyl stearate  | 27–29         | 122            | n.a.                    |                         |
| Capric acid  |   | 32            | 152.7          | 0.153 (liquid, 38.5 °C) |                         |
|  |   | 31.5          | 153            | 0.152 (liquid, 55.5 °C) |                         |
|  |   |               |                | 0.149 (liquid, 40 °C)   |                         |

Further discussion on cold thermals storage materials heat transfer and performance enhancements can be cited in [222].

### 6.2. Evaporator temperatures in absorption cycles

Comparing evaporator temperatures for single, half, double and triple effect absorption cycle was studied by few researchers [224–227]. Table 20 shows these studies, both experimental and numerical, to deduce optimum evaporator temperature of a single effect absorption system for our case study. It can be concluded from the Table 19 and few more studies [45,46,48–51,54,55,57,61–63,66–68,70,224,228,229] that the single-effect absorption cycle is the simplest and has the capability to produce low temperatures (–10 to 7 °C) at evaporator with generator temperature as low as 60 °C and condenser temperatures between 30 and 40 °C at a COP of about 0.7. Also, from Section 6.1, it is clear that the selection of PCM largely depends upon the system being used and the application.

### 6.3. Material selection

Subzero temperatures or cold storage generally make use of solid-liquid or liquid-solid phase changer materials. The selection criteria of PCM for subzero temperatures are [230]:

- Correct phase change temperature and pressure.
- High heat of fusion
- Good cycling stability
- Good thermal conductivity
- Low/no subcoolingsubcooling
- Stable chemical properties: environmental impact and corrosion
- Easy manufacturing and low price

Other specific properties of a cold (ice) thermal storage system include: specific heat of about 2 kJ/kg K, latent heat of fusion of about 300 kJ/kg, charging temperature between –6 to –3 °C, discharging between 1 and 3 °C, with a cost of about 14–20 \$/kWh. Deciding and choosing a suitable PCM for the application depends on its financial and thermal properties. A visual combination of important thermal properties (Fig. 16) of few types of PCM was produced by Li et al. [230]. Furthermore, phase change materials and their thermal properties suitable for air-conditioning applications can be found with Li et al. [230].

### 6.4. PCM selection in cold storage applications

Study of PCM in cold storage methods and the associated challenges (multidimensional freezing, phase-segregation, super-cooling, corrosion, crystallization and agglomeration etc.) have been in research

**Table 16**  
Literature on enhancing the condenser performance by applying PCM.

| Author (s)              | Study                    | Capacity                      | Condenser Temp (°C)      |                                     | PCM/location   | Features  | Outcomes   |
|-------------------------|--------------------------|-------------------------------|--------------------------|-------------------------------------|--|---|--|
|                         |                          |                               | Without PCM              | With PCM                            |  |   |  |
| Wang et al. [205]       | Experimental             | 5 kW                          | 27<br>38                 | 22<br>34                            | Ahead of condenser<br>After condenser  | Quantifying the benefits of using PCM heat exchangers in a real plant<br>Dynamic testing and error analysis of thermocouples, pressure transducers and COP                              | 6% higher COP<br>8% higher COP   |
| Wang et al. [207]       | Numerical                | 5 kW                          | Inlet = 105, Outlet = 50 |                                     | PCM ahead of condenser   | A novel control purpose of using PCM in refrigeration systems<br>discuss some parameters which affect the performance of these three systems  | Most of the desuperheating is done in the PCMA (before the condenser) heat exchanger and this enables the condenser to operate more efficiently<br>PCMB (after the condenser) gives higher COP (8%) and energy saving<br>Location of PCM after evaporator stabilizes refrigerant temperature<br>Overall heat-transfer performances of the condensers could be significantly improved, which resulted in a lower condensation temperature, a higher evaporation temperature and a much larger subcooling degree at the condenser outlet<br>cycle time and the ratio of on-time to the total cycle time of the novel refrigerator were much smaller<br>Lower energy consumption<br>Increase of energy efficiency by about 12%<br>COP increased about 19%<br>Ambient temperature increasing and the freezer temperature decreasing can increase the energy saving effect<br>Second phase change temperature region with the peak temperature about 49 °C of SSPCM results in the minimum energy consumption<br>PCM lowers the condenser temperature<br>significant reduction of power consumption |
| Cheng et al. [202]      | Experimental             | 0.45 kWh                      | 16–32                    | 2.5–28                              | Heat conduction enhanced SSPCM (HCE-SSPCM) - Paraffin+HDPE composite+Enhanced Graphite (paraffin/HDPE/EG) prepared in Ref. [204] | Condensation heat was stored in the shape-stabilized PCM during the on-time and discharged to the environment while the compressor was off  |  |
| Cheng et al. [203]      | Numerical                | 0.44 kW                       | 17–32                    | 0–28                                | SSPCM (shape-stabilized phase change material)   | Dynamic simulation model of Ref [202]   |  |
| Sonnenrein et al. [208] | Experimental             | 0.011 kW                      | 39 (water)               | 34 (water), 31 (copolymer compound) | Macro-encapsulations (PE-HD foil and aluminium-composite film)   | A standard wire-and-tube condenser is equipped with different heat storage elements (containing water, paraffin or copolymer compound)  |  |
| Sonnenrein et al. [209] | Experimental             | 0.085 kW                      | 48                       | 40                                  | Copolymer fixed organic paraffin derivative  | Two evaporator types and a standard wire-and-tube condenser tested copolymer-bound PCM<br>Influence of PCM on power consumption and fresh-food compartment temperatures was studied     | PCM can be optimized through modifications of the control strategy to achieve different targets: (a) Power consumption can be significantly reduced by increasing the evaporator and decreasing the condenser temperature. (b) Temperature fluctuations in the refrigerator's fresh-food compartment during the cooling cycle can be reduced from 4 °C to 0.5 °C. (c) The cooling cycle duration can be tripled without compromising the fresh-food compartment conditions.<br>17% decrease in power consumption when PCM is used at evaporator and condenser.<br>25.6% increase in COP<br>Effectiveness is generally higher than 0.5.<br>Optimum fin height in the PCM heat exchanger can be designed depending upon the load capacity  |
| Zhao et al. [210]       | Experimental & Numerical | 3.95 kW<br>3.63 kW<br>2.89 kW |                          | 45<br>40<br>35                      | PCM (RT22) in a separate loop with the condenser cooling system.   | A mathematical model using effecting thermal conductivity of charging process developed and validated with experimental values<br>Used water and air as two HTF for day and night time. |  |

**Table 17**  
Advantages and disadvantages of using PCM at condenser.

| Advantages   | Disadvantages   |
|--|---|
| <ul style="list-style-type: none"> <li>● Higher COP</li> <li>● Shorter compressor global ON-time ratio</li> <li>● Lower energy consumption</li> <li>● Continuous heat rejection from condenser even during compressor OFF period</li> <li>● Smaller starting compressor power due to higher refrigerant temperature in condenser</li> <li>● Faster stable condition of refrigeration system</li> <li>● Lower condensation temperature and pressure</li> <li>● Higher sub-cooling degree</li> <li>● Lower heat gain from condenser to compartment during ON time</li> </ul> | <ul style="list-style-type: none"> <li>● More frequent compressor ON/OFF</li> <li>● Higher heat gain from condenser to compartment during OFF Time</li> <li>● More refrigerant displacement losses</li> </ul> |

**Table 18**  
Advantage and disadvantages of using PCM at evaporator [26].

| Advantage  | Disadvantage  |
|--|---|
| <ul style="list-style-type: none"> <li>✓ Higher COP</li> <li>✓ Shorter compressor global ON-time ratio</li> <li>✓ Longer compressor OFF time</li> <li>✓ Slower compartment temperature changes</li> <li>✓ More controlled temperature at compressor inlet</li> <li>✓ More stable condition against thermal load variations</li> <li>✓ Higher refrigerant density at compressor inlet</li> <li>✓ Assistance in case of power outage</li> <li>✓ Helpfulness for damping defrost and door opening temperature increase</li> </ul> | <ul style="list-style-type: none"> <li>✓ Higher condensation temperature</li> <li>✓ Longer compressor ON time during a cycle</li> </ul> |

since decades [230–233]. As mentioned earlier, the melting temperature of the PCM is about 5–10 °C lower than the operating temperature in case of hot side of the system. PCM at the evaporator (cold side) also need to have freezing temperature lower than the average output temperature. In the case of hot-side, especially in solar applications, a continuous variation in solar irradiation cause minor fluctuations within minutes and major fluctuations within hours or passage of the day. With the use of thermal storage system, the input temperatures can be stabilized so as to achieve a stable output evaporator temperature. For air-conditioning and refrigeration (ice storage), temperatures from –5 to 15 °C is optimum for thermal storage [216,217,219,220,223,234–236], but at lower temperatures, latent heat storage materials are better than sensible heat storage materials (like water). Some of the PCMs available in the literature in the temperature range of –10 to 15 °C are shown in Table 21, and commercially available products are shown in Table 22. The selection criteria of PCM at evaporator primarily depends upon its subcooling property, besides two characteristics: heat of fusion and melting point. It is very important to know if the PCM solidifies below its melting temperature, or else, subcooling can drastically reduce the thermal capacity of the system. Organic materials have an advantage in this application as they exhibit no subcooling and phase segregation.

## 7. Challenges

Despite many desirable properties, PCM have various challenges in

its usage. Some of the thermophysical issues faced are: phase separation, subcooling, low thermal conductivity, corrosion and thermal stability. Although solid-liquid PCMs are most studied and used, solid-solid PCM are more favorable in terms of leakage problems, containment and design flexibility [29].

### 7.1. Subcooling

Supercooling/Subcooling/Undercooling is the phenomena of PCM temperature reaching below its freezing temperature, but without solidification. This delays the phase change and latent heat storage capability of the system. Furthermore, lower phase change temperature means lesser difference between the evaporator and the PCM temperature, which reduces the heat transfer rate and prolongs the compressor ON time as the PCM acts more like a load than a charging energy storage unit. In *n*-eicosane paraffins, the convective heat transfer coefficient in the presence of subcooling is 10–15% lower than that of PCM without subcooling [237]. Agyenim [52] indicated subcooling in his multi-tubes storage system at the start of discharge whereas longitudinal fins performed the best in uniform discharging. This made him to suggest a combination of the two designs for desired features. Therefore, low or no subcooling and high rate of crystallization is an indication of a good PCM. When Xue [93] investigated the PCM (Ba(OH)<sub>2</sub>·8H<sub>2</sub>O) with evacuated tube solar collector, he observed serious subcooling while discharging. Gil et al. selected hydroquinone as PCM for their solar absorption refrigeration system due to its low subcooling and high enthalpy properties. Barreneche et al. [238] and Pitkanen et al. [239] studied D-mannitol for its polymorphism and thermos-analysis, and found subcooling behavior.

Paraffins and fatty acids not only show wide range of melting temperatures, but they are also known to freeze with little or no subcooling [240,241]. Salt hydrates and clathrate hydrates have poor nucleating properties, hence form liquid salt hydrates before freezing [236]. Eutectic water-salt solutions also have subcooling problems but with high latent heat and desirable melting temperature [242]; while non-eutectic water-salt solutions do not exhibit very high subcooling [242]. In general, inorganic PCMs subcool and organic don't, so severely [243].

Subcooling is minimized by adding a nucleating agents (like carbon nanofibers, of similar crystal structure [18,244,245], using “cold finger” [246] or using rough metallic heat exchanger surface to promote heterogeneous nucleation [240]. Critical information on factors influencing degree of subcooling, triggering mechanisms and the effect on output capacity are discussed in [247].

Microencapsulated PCM (MEPCM) is made to enhance its thermal conductivity and physical interaction capability during the melting process. Subcooling increases in MEPCM due to higher heat transfer rate and more contact surface; and it is minimized by (a) controlling the encapsulation size [248], (b) adding nucleating agents or metal additives [249–252], (c) optimizing the composition and structure of the shell [253,254] or, by (d) changing the fill volume in the encapsulation [255].

### 7.2. Stability

Repeated charging and discharging of PCM without an excessive change in its thermos-physical and chemical properties is called thermal stability/thermal reliability. Complete thermal cycling can occur one or more times in a 24 h time period, implying at least a 1000 cycles for a 3 years life of a PCM storage. This cyclic charging and discharging of PCM is very important for its thermal reliability and commercialization of LHSS in solar applications. Usually, materials with little or no subcooling are stable [27]. Paraffins are mostly stable and chemically inert, and have very low subcooling [242]. Solé et al. [256] studied the thermal stability of D-mannitol, myo-inositol and galactitol. Authors reported that Myo-inositol showed good cyclic

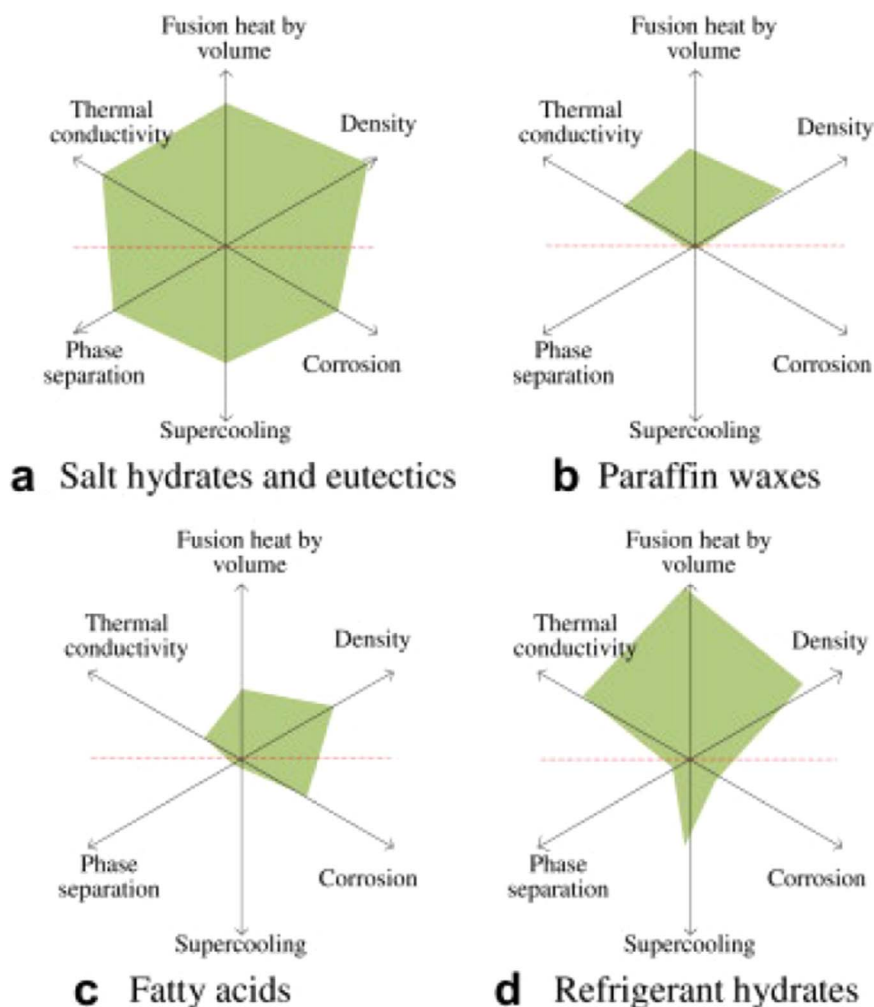
**Table 19**  
A brief overview of literature on PCM at evaporator.

| Author (s)           | Study                      | Load     | PCM   | PCM melting temp. | Features   | Outcomes/Findings   |
|----------------------|----------------------------|----------|---|-------------------|--|---|
| Oró et al. [221]     | Experimental               | 628 W    | Climsel-18  | -18 °C            | Thermal performance improvements under door openings and electrical power failure  | During 3 h of electrical power failure, the use of PCM maintained the freezer temperature 4–6 °C lower temperature fluctuations   |
| Gin and Farid [215]  | Experimental               | 0.044 kW | eutectic composition of water and ammonium chloride | -15.4 °C          | PCM) panels placed against the internal walls of a freezer during repeated power loss every 24 h over a 2 week period<br>Measured the drip loss in 1 × 1 cm cubes of bovine muscle ( <i>Musculus semimembranosus</i> ) and the ice crystal size in 1 L blocks of vanilla ice cream   | Drip loss in meat was found to be lower and ice crystal sizes in the ice cream were found to be smaller   |
| Azzouz et al. [216]  | Experimental               | 34 W     | eutectic aqueous solution                           | -3 °C             | PCM is located on the back side of the evaporator<br>Tested with water and with a eutectic mixture   | temperature rise during loss of power is limited<br>10–30% increase in COP depending upon the thermal load<br>Continuous operation with PCM is 5–9 h compared to that of without PCM (1–3 h)  |
| Azzouz et al. [217]  | Numerical                  | 0.018 kW | eutectic aqueous solution                           | -9–0 °C           | added a PCM slab on the outside face of a refrigerator evaporator<br>A dynamic model of the vapor compression cycle including the presence of the phase change material and its experimental validation is presented   | model predicts a 5–15% increase in the coefficient of performance   |
| Khan and Afroz [223] | Experimental               | 0.13 kW  | Water and Eutectic solution                         | 0 and -5 °C       | Effect on the energy efficiency of the refrigerator of various designs and operating condition is also studied<br>PCM container on the outside face of a refrigerator evaporator at different thermal loads  | 20–27% COP improvement depending upon the type of PCM and thermal load<br>With the increase of the quantity of PCM (0.003–0.00425 m <sup>3</sup> ) COP increases about 6%<br>average compressor running time per cycle is reduced significantly and it is found about 2–36%<br>horizontal PCM configuration produces lower compartment temperatures |
| Marques et al. [219] | Experimental and numerical |          | Eutectic mixtures (water+salt)                      | -2 to -6 °C       | characterize the airflow and temperature distribution in a natural convection thermal energy storage refrigerator<br>PCM orientation, PCM temperature and compartment designs were tested<br>temperature distribution with a horizontal PCM was tested experimentally and the results were in agreement with the CFD predictions | Eutectic with a phase change temperature below 0 °C must be employed to maintain the compartment temperature within acceptable limits<br>energy savings of 19%  |

**Table 20**

Evaporator temperatures for most used working pairs.

| Author (s)                     | Study   | Single-effect $T_{\text{evap}}$                  | Half-effect $T_{\text{evap}}$ | Double-effect $T_{\text{evap}}$ | Triple-effect $T_{\text{evap}}$ |
|--------------------------------|---|--|-------------------------------|---------------------------------|---------------------------------|
| Domínguez-Inzunza et al. [224] | Numerical for $\text{NH}_3\text{-LiNO}_3$ absorption system | -50 to -10 °C for COP 0.1–0.65 @ $T_A=T_C=30$ °C | -50 to 0 °C for COP 0.15–0.3  | -35 °C, max. COP 1.12           | 0 °C, max. COP 1.22             |
| Gomri [228]                    | Numerical for $\text{LiBr-H}_2\text{O}$ absorption system   | 4–10 °C at COP 0.7–0.75                          | -na-                          | 4–10 °C at COP 1.2–1.3          | 4–10 °C at COP 1.63–1.8         |

**Fig. 16.** Thermal properties of various phase change materials [230].

stability. D-mannitol reacted with oxygen during the test, resulting in an unstable material with low storage capacity. It was recommended to design the heat storage unit considering D-mannitol's reaction to oxygen (vacuum storage). Behzadi and Farid [257] tested two commercial organic PCMs Rubitherm 21 and mixed esters (propyl stearic and palmitate mixture). Rubitherm-21 after 120 days at 55 °C shifted its melting temperature from 21 to 28 °C with an increase of 27% in latent heat of fusion while the ester mixture showed no change in mass and good thermal stability. Thermal enhancement up to 37 °C can be achieved in thermal stability of 160 °C heat-treated microcapsules of *n*-octadecane with a urea-melamine-formaldehyde copolymer shell containing 8.8% cyclohexane [258].

Tang et al. [259] improved thermal conductivity of (hybrid form-stable PCM) PEG/SiO<sub>2</sub>-Al<sub>2</sub>O<sub>3</sub> by 12.8% for 3.3 wt% Al<sub>2</sub>O<sub>3</sub>. An excellent thermal stability was observed when the temperature was

below 290 °C. Cai et al. [260] prepared and improved ultrafine composite fibers of lauric acid and polyamide using carbon nanofibers (CNF) when they observed maximum weight loss and temperature and charred residue at 700 °C. Fauzi et al. [261] studied thermal reliability of two eutectic PCMs, myristic acid/palmitic acid/sodium myristate (MA/PA/SM) and myristic acid/palmitic acid/sodium palmitate (MA/PA/SP) and found no chemical degradation and small irregular changes in their thermal properties. A detailed review of thermal stability on organic, inorganic and eutectic materials can be found in the work done by Rathod and Banerjee [262].

### 7.3. Characterization and testing

It is important to know the reliability of the PCM before its application. Thermal cycling is conducted for specific parameters



**Table 21**  
Materials suitable for single-effect evaporator temperature range (–10 to 15 °C).

| Type   | Material   | Melting point °C                                   | Fusion heat kJ/kg |        |
|--|--|--|-------------------|--------|
| emulsion (tetradecane/water)                         | Tetradecane: water (10:90 wt %)                                  | 4.36   | 18.69             |        |
|  | Tetradecane: water (20:80 wt %)                                  | 4.57   | 31.56             |        |
|  | Tetradecane: water (30:70 wt %)                                  | 4.51   | 73.47             |        |
| Eutectic   | Na <sub>2</sub> SO <sub>4</sub> /NaCl/KCl/H <sub>2</sub> O       | 4  | 234               |        |
|  | CuSO <sub>4</sub> /H <sub>2</sub> O                              | –1.6   | 291               |        |
|  | FeSO <sub>4</sub> /H <sub>2</sub> O                              | –1.8   | 287               |        |
|  | Na <sub>2</sub> CO <sub>3</sub> /H <sub>2</sub> O                | –2.1   | 310               |        |
|  | KNO <sub>3</sub> /H <sub>2</sub> O                               | –2.8   | 296               |        |
|  | NaF/H <sub>2</sub> O   | –3.5   | 314               |        |
|  | Na <sub>2</sub> SO <sub>4</sub> /H <sub>2</sub> O                | –3.6   | 285               |        |
|  | MgSO <sub>4</sub> /H <sub>2</sub> O                              | –3.9   | 264               |        |
|  | NiSO <sub>4</sub> /H <sub>2</sub> O                              | –4.2   | 259               |        |
|  | NaCl/H <sub>2</sub> O  | –5.0   | 289               |        |
|  | KHCO <sub>3</sub> /H <sub>2</sub> O                              | –5.4   | 269               |        |
|  | Sr(NO <sub>3</sub> ) <sub>2</sub> /H <sub>2</sub> O              | –5.8   | 243               |        |
|  | ZnSO <sub>4</sub> /H <sub>2</sub> O                              | –6.5   | 236               |        |
|  | BaCl <sub>2</sub> /H <sub>2</sub> O                              | –7.8   | 246               |        |
|  | NaH <sub>2</sub> PO <sub>4</sub> /H <sub>2</sub> O               | –9.9   | 214               |        |
|  | Diethylene glycol  | –10  | 247               |        |
| Eutectic Organic                                     | Tetradecane + octadecane   | –4.02  | 227.52            |        |
|  | 91.67% tetradecane + 8.33% hexadecane                            | 1.7  | 156.2             |        |
|  | Tetradecane + docosane   | 1.5–5.6  | 234.33            |        |
|  | Tetradecane + geneicosane  | 3.54–5.56  | 200.28            |        |
|  | Tetrahydrofuran (THF)  | 5  | 280               |        |
|  | Pentadecane + heneicosane  | 6.23–7.21  | 128.25            |        |
|  | Pentadecane + octadecane   | 8.5–9.0  | 271.93            |        |
|  | Pentadecane + docosane   | 7.6–8.99   | 214.83            |        |
|  | Inorganic eutectic   | Na <sub>2</sub> SO <sub>4</sub> (31 wt%)           | 4                 | 234    |
|  |  | 6 wt% KCl + H <sub>2</sub> O                       | –10               | –      |
| Inorganic  | 16.5 wt% KHCO <sub>3</sub> + H <sub>2</sub> O                    | –6   | –                 |        |
|  | 20.5 wt% NaCO <sub>3</sub> + H <sub>2</sub> O                    | –3   | –                 |        |
|  | LiClO <sub>3</sub> ·3H <sub>2</sub> O                            | 8.1  | 253               |        |
|  | ZnClO <sub>2</sub> ·3H <sub>2</sub> O                            | 10   | –                 |        |
|  | H <sub>2</sub> O   | 0  | 333               |        |
|  | LiClO <sub>3</sub> ·3H <sub>2</sub> O                            | 8.1  | 253               |        |
|  | ZnCl <sub>2</sub> ·3H <sub>2</sub> O                             | 10   | –                 |        |
|  | eutectic water–salt solutions                                    | NaH <sub>2</sub> PO <sub>4</sub> /H <sub>2</sub> O | –9.9              | 214.25 |
|  |  | BaCl <sub>2</sub> /H <sub>2</sub> O                | –7.8              | 246.44 |
|  |  | ZnSO <sub>4</sub> /H <sub>2</sub> O                | –6.5              | 235.75 |
| Sr (NO <sub>3</sub> ) <sub>2</sub> /H <sub>2</sub> O |  | –5.75  | 243.15            |        |
| KHCO <sub>3</sub> /H <sub>2</sub> O                  |  | –5.4   | 268.54            |        |
| NiSO <sub>4</sub> /H <sub>2</sub> O                  |  | –4.15  | 258.61            |        |
| Na <sub>2</sub> SO <sub>4</sub> /H <sub>2</sub> O    |  | –3.55  | 284.95            |        |
| NaF/H <sub>2</sub> O                                 |  | –3.5   | 314.09            |        |
| NaOH/H <sub>2</sub> O                                |  | –2.8   | 265.98            |        |
| MgSO <sub>4</sub> /H <sub>2</sub> O                  |  | –3.9   | 264.42            |        |
| Organic  | KNO <sub>3</sub> /H <sub>2</sub> O                               | –2.8   | 296.02            |        |
|  | Na <sub>2</sub> CO <sub>3</sub> /H <sub>2</sub> O                | –2.1   | 310.23            |        |
|  | FeSO <sub>4</sub> /H <sub>2</sub> O                              | –1.8   | 286.81            |        |
|  | CuSO <sub>4</sub> /H <sub>2</sub> O                              | –1.6   | 290.91            |        |
|  | C <sub>14</sub> H <sub>30</sub>                                  | 5.5  | 226               |        |
|  | C <sub>13</sub> H <sub>28</sub> /C <sub>14</sub> H <sub>30</sub> | 2.6  | 212               |        |
|  | C <sub>13</sub> H <sub>28</sub> /C <sub>14</sub> H <sub>30</sub> | 0.7  | 148               |        |
|  | C <sub>13</sub> H <sub>28</sub> /C <sub>14</sub> H <sub>30</sub> | –0.5   | 138               |        |
|  | C <sub>13</sub> H <sub>28</sub> /C <sub>14</sub> H <sub>30</sub> | –1.5   | 110               |        |
|  | C <sub>12</sub> H <sub>26</sub> /C <sub>13</sub> H <sub>28</sub> | –5.4   | 126               |        |
|  | C <sub>12</sub> H <sub>26</sub> /C <sub>13</sub> H <sub>28</sub> | –8.0   | 147               |        |
|  | C <sub>12</sub> H <sub>26</sub> /C <sub>13</sub> H <sub>28</sub> | –9.1   | 145               |        |
|  | C <sub>12</sub> H <sub>26</sub> /C <sub>13</sub> H <sub>28</sub> | –9.7   | 159               |        |
|  | Dodecane   | –9.6   | 216               |        |
|  | Triethylene glycol   | –7   | 247               |        |
|  | Microencapsulated 94% tetradecane + 6% tetradecanol              | 5.1  | 202.1             |        |
|  | Microencapsulated 100% tetradecane                               | 5.2  | 215               |        |
|  | Microencapsulated 96% tetradecane + 4% tetradecanol              | 5.2  | 206.4             |        |

**Table 21 (continued)**

| Type                      | Material   | Melting point °C | Fusion heat kJ/kg |
|---------------------------|--|------------------|-------------------|
| Fatty acid                | Bulk 100% tetradecane                              | 5.5              | 215               |
|                           | Bulk 96% tetradecane + 4% tetradecanol             | 5.5              | 206.4             |
|                           | Bulk 94% tetradecane + 6% tetradecanol             | 5.5              | 202.1             |
|                           | Paraffin C <sub>14</sub>                           | 5.5              | 228               |
|                           | <i>n</i> -Tetradecane                              | 6                | 230               |
|                           | Polyglycol E400                                    | 8                | 99.6              |
|                           | Paraffin C <sub>15</sub> –C <sub>16</sub>          | 8                | 153               |
|                           | <i>n</i> -Pentadecane                              | 10               | –                 |
|                           | Paraffin C <sub>15</sub>                           | 10               | 205               |
|                           | Tetrabutyl ammoniumbromide (type A–type B)         | 10–12            | 193–199           |
|                           | KF 4H <sub>2</sub> O                               | 4.5              | 165               |
|                           | Paraffin C <sub>14</sub>                           | 4.5              | 165               |
|                           | Paraffin C <sub>15</sub> –C <sub>16</sub>          | 8                | 153               |
|                           | Polyglycol E400                                    | 8                | 99.6              |
|                           | No. of carbon atoms: 15                            | 10               | 205               |
| Inorganic (hydrated salt) | Formic acid  | 7.8              | 247               |
|                           | Propyl palmitate                                   | 10               | 186               |
| Salt hydrates             | LiClO <sub>3</sub> ·3H <sub>2</sub> O              | 8                | 253               |
|                           | ZnCl <sub>2</sub> ·3H <sub>2</sub> O               | 10               | –                 |
| Compound                  | K <sub>2</sub> HPO <sub>4</sub> ·6H <sub>2</sub> O | 4                | 109               |
|                           | H <sub>2</sub> O + polyacrylamide                  | 0                | 295               |

**Table 22**

Commercially available PCM for cold storage.

| PCM Type                    | Name                      | Melting temperature °C | Latent heat of fusion KJ/Kg | Company              |     |
|-----------------------------|---------------------------|------------------------|-----------------------------|----------------------|-----|
| Hydrated Salts-Eutectic PCM | Freezer salt Preservation | –16                    | 330                         | TEAP PCM             |     |
|                             |                           | 4                      | 105                         |                      |     |
|                             |                           | 7                      | 135                         |                      |     |
|                             |                           | 7                      | 300                         |                      |     |
|                             |                           | 10                     | 170                         |                      |     |
| Hydrated salts              |                           | 15                     | 175                         | PlusICE PCM Products |     |
|                             | S15                       | 15                     | 160                         |                      |     |
|                             | S13                       | 13                     | 160                         |                      |     |
|                             | S10                       | 10                     | 155                         |                      |     |
|                             | S8                        | 8                      | 150                         |                      |     |
|                             | S7                        | 7                      | 150                         |                      |     |
|                             | S15                       | 15                     | 130                         |                      |     |
| Organic                     | A9                        | 9                      | 140                         |                      |     |
|                             | A8                        | 8                      | 150                         |                      |     |
|                             | A6                        | 6                      | 150                         |                      |     |
|                             | A4                        | 4                      | 200                         |                      |     |
|                             | A3                        | 3                      | 200                         |                      |     |
| Eutectic                    | A2                        | 2                      | 200                         |                      |     |
|                             | E0                        | 0                      | 332                         |                      |     |
|                             | E–2                       | –2                     | 306                         |                      |     |
|                             | E–3                       | –3.7                   | 312                         |                      |     |
|                             | E–6                       | –6                     | 275                         |                      |     |
| Pure PCM                    | E–10                      | –10                    | 286                         |                      |     |
|                             | –                         | –30 to 56              | –                           |                      |     |
| Microencapsulated PCM       | –                         | –30 to 43              | –                           | Microteklabs         |     |
|                             | –                         | –30 to 43              | –                           |                      |     |
| Macroencapsulated PCM       | –                         | –30 to 43              | –                           |                      |     |
|                             | Paraffin                  | RT–20                  | 8                           |                      | 140 |
|                             |                           | RT–4                   | –4                          |                      | 179 |
|                             |                           | RT–3                   | 4                           |                      | 198 |
|                             |                           | RT–5                   | 9                           |                      | 205 |
| Inorganic salts             | RT2HC                     | –4 to 100              | –                           | Rubitherm GmbH       |     |
|                             | HS 7N                     | –7 to –5               | 230                         |                      |     |
|                             | SN06                      | –6                     | 284                         |                      |     |
| Salt solution               | SN03                      | –3                     | 328                         | Cristopia            |     |
|                             | STL–3                     | –3                     | 328                         |                      |     |
| Salt solution               | STL–6                     | –6                     | 284                         | Mitsubishi Chemical  |     |

considering (a) choice of equipment, (b) technique to characterize the PCM before/after testing, (c) number of cycles, and (d) heating rate and thermal cycling method [263]. Fatty acids composites can be stabilized by four methods [79] (a) adsorption, (b) polymer blends, (c) electrostatic spinning, and (d) microencapsulation. DSC and thermostatic chamber are used to perform cyclic stability tests with PCM [256]. A review of methodology used in thermally stable characterization of PCM can be found in [263]. Thermal stability is different from the form-stability where the latter is enhancing the performance and safety of PCM through encapsulation methods and shape stabilization procedures [33]. Health hazards and toxicity of PCM are also crucial characteristics of few PCMs. Paraffins release toxic vapor and salt hydrates need careful handling. A more detailed review in this direction can be found in [264].

#### 7.4. Corrosion

The use of PCM in solar absorption refrigeration is relatively new and has been investigated by very few researchers. Their observations were more focused on the effect of PCM with enhancements on the overall performance of the system, rather than continuous test to study specific effects such as corrosion on the containers used. Thus, the study performed with the use of PCM in solar absorption refrigeration application are low and need more exploration.

Corrosive properties of water are well known. It is also the most used hot and cold storage medium in solar absorption cooling systems. Corrosive properties of other materials with higher latent heat of fusion are needed for the applications. In terms of a non-corrosive containers, stainless steels has been much tested with impressive results. Moreno et al. [265] studied different metals (copper, stainless steel, carbon steel, aluminium) in contact with salt hydrate PCMs (S10, C10,  $\text{ZnCl}_2 \cdot 3\text{H}_2\text{O}$ ,  $\text{NaOH} \cdot 1.5\text{H}_2\text{O}$ ,  $\text{K}_2\text{HPO}_4 \cdot 6\text{H}_2\text{O}$ ). Of these,  $\text{ZnCl}_2 \cdot 3\text{H}_2\text{O}$  and  $\text{K}_2\text{HPO}_4 \cdot 6\text{H}_2\text{O}$  did not exhibit corrosive nature with copper; and almost all of them showed high corrosion rate with carbon steel after 12 weeks. They suggested stainless steel as suitable to all kind of studied PCM and rated copper and carbon steel to exhibit high corrosion in heating and cooling applications, respectively. Accordingly, they suggested that S10, C10, S46, C48,  $\text{MgSO}_4 \cdot 7\text{H}_2\text{O}$  and  $\text{Na}_2\text{S}_2\text{O}_3 \cdot 5\text{H}_2\text{O}$  can be encapsulated with stainless steel and aluminium (depending upon the application); and  $\text{ZnCl}_2 \cdot 3\text{H}_2\text{O}$  and  $\text{K}_2\text{HPO}_4 \cdot 6\text{H}_2\text{O}$  can be used with stainless steel and copper encapsulation. Ferrer et al. [266] also studied five selected metals (stainless steel 304, copper, aluminium, carbon steel and stainless steel 316) with one ester (PureTemp 23), one inorganic mixture and two fatty acid eutectics (Capric acid (73.5%) + myristic acid (26.5%), and Capric acid (75.2%) + palmitic acid (24.8%)). They too suggested stainless steel (304 and 316) and PureTemp 23 as corrosion resistant among the studied PCMs. Stainless steel (304 and 316) and copper showed resistance to inorganic salt SP21E. Fatty acids were corrosion resistant with all the metals. Rest of the combinations exhibited more or less corrosive nature during the testing.

#### 7.5. Phase segregation

The change in initial design composition of the microscopical separation of phases over thermal cycles is called phase segregation/phase separation/ incongruent melting. It is an important issue of cold thermal storage system and progressively reduces the energy storage capacity of the LHES system. Most organic PCMs (paraffins, fatty acids and sugar alcohols) do not exhibit phase segregation [267]. Paraffins, which are commonly used in solar heating and cooling applications, do not exhibit phase segregation. Ushak et al. [268] studied bischofite, a by-product of non-metallic industry, to replace  $\text{MgCl}_2 \cdot 6\text{H}_2\text{O}$  as a PCM suitable for solar thermal energy storage system with lower cost. They concluded that bischofite is a potential PCM for solar energy application with melting point of about 100 °C, one of the two main

**Table 23**

Strengths and weaknesses of two storage design used in [52].

| System            | Longitudinal finned  | Multitube  |
|-------------------|--|--|
| <b>Strengths</b>  | <ul style="list-style-type: none"> <li>• Most uniformly distributed temperature</li> <li>• No sub-cooling during discharge</li> <li>• Best discharge efficiency</li> </ul> | <ul style="list-style-type: none"> <li>• Highest final melt temperature</li> <li>• Highest output temperature</li> <li>• Most energy stored</li> <li>• Highest overall utilization efficiency</li> </ul> |
| <b>Weaknesses</b> | <ul style="list-style-type: none"> <li>• Slower charge rate compared to multitube</li> </ul>   | <ul style="list-style-type: none"> <li>• Sub-cooling during discharge</li> </ul>   |

concerning issues was phase segregation. An encapsulated PCM is a promising technique to deal with the issue of phase segregation along with the use of expanded graphite [269,270].

Salt or salt hydrates are used in solar applications operating at higher temperature (> 500 °C). A major issue with salt hydrates is phase segregation. A thickening agent or a polymer [269,271] with water is added to avoid settling of heavier particles in salt hydrates to stabilize. However, it lowers storage density [230]. Thickening agents are mostly super absorbent polymers, cellulose derivatives, or polyvinyle alcohols [270,272,273].

#### 7.6. Container design enhancements

Choosing the appropriate container size and heat exchanger is a crucial part of the storage design. The starting time of the chiller depends upon the volume of PCM charged. Similarly, the mass flow rate of the HTF (and its properties) plays an important role in overall steadiness of thermal storage unit. Shell and tube design is commonly used in solar absorption cooling systems; and the use of fins increase the heat transfer rate more uniformly [103]. Increasing the number of fins decreases the PCM volume, altering desired parametric observations along with energy storage capacity. Using helical coaxial tubes to melt the PCM can be more complex in design and much work is required to test this design on various system capacities. Nonetheless, scale analysis along with numerical simulation is proven approach to design a thermal energy storage system [105]. Agyenim [52] reported subcooling problems with a storage design (multi-tubes) with highest effectiveness. Therefore, he suggested to include longitudinal fins that performed the best in terms of satisfactory discharge. Table 23 shows strengths and weaknesses for using the two designs with best effectiveness and least subcooling effect. He only proposed modified equations for enhanced COP of LiBr-H<sub>2</sub>O system.

#### 7.7. Heat loss

Heat losses from the solar collector to the evaporator effectively influence the COP of the system. Choosing a container for the PCM is different from insulating it to reduce the heat losses. The overall energy capacity of the storage unit includes the sensible heat storage of the container metal. The heat storage capacity of the storage unit can be calculated accurately when heat losses are minimized to its largest extent. This will not only enhance the COP of the solar absorption system, but also its reliability during the night time. Heat loss can occur through the pipes depending upon the distance of the storage unit in the system. Heat loss can also occur due to improper insulation of the storage unit. Glass wool is generally applied (up to 250 °C) as an insulation around solar collectors and hot water piping. Rubber based elastomeric foam is used for hot/cold pipelines (−50 °C ~ +105 °C). In order to reduce the heat losses, Raja et al. [58] placed the generator inside the thermal storage unit; additionally saving the pumping power. Gil et al. [103] insulated the storage tank with a 24 cm thick rock wool on the sides and 45 cm of Foamglass™ underneath. If the

standby period increases, this can also lead to freezing problems which in turn affect the storage capacity of the unit [107].

### 7.8. Control

The thermal storage unit is charged and discharged according to the availability of the sun and the cooling demand. The fluctuation of the heat source cannot affect the output temperature of the evaporator in most of the applications, including SAR system with thermal storage. Choosing the most economic mode of cooling using the best parameters to maximize the exergy can be done with a meticulous control program. This depends upon the system and application demands. Godarzi et al. [274] optimized a LiBr-H<sub>2</sub>O absorption system with a latent heat thermal storage unit using exergoeconomic principles and genetic algorithm. They were able to reduce the exergy losses and raise the COP by 3.8%. Advanced control algorithms are also required to maximize energy saving in buildings while maintaining optimum thermal comfort.

### 7.9. Material selection

There are practically hundreds of phase change materials that can be employed at various desirable temperature ranges according to the applications. Only a couple of PCMs have been investigated in various thermal circuits of a solar absorption system. Moreover, selecting a material with its appropriate property is more difficult for any application. Commercially available PCMs like hydroquinone, erythritol, D-mannitol and other paraffins are investigated in abundance, but a clear picture of database of PCMs suitable for required application, their limitations, explored solutions etc are missing.

### 7.10. Thermal responses

New designs to investigate and enhance the performance of the solar absorption system are needed. Agyenim's [52] three cylindrical shells equipped with mechanical ways to enhance the heat transfer are worth mentioning. He tested circular and longitudinal fins on the HTF tube running from the center of the shell with a multi-tubes geometry. The longitudinal fins exhibited the most uniform melting (except for a small part at the bottom) during the charging (in hot circuit) and has the highest discharge efficiency (82.2%) with no sub-cooling. The highest energy discharged was in multitube system with 83.5% efficiency. Designs dictated by PCM thermal behavior are still under-researched.

## 8. System design for PCM integrated solar absorption cooling system

During the charging/discharging process, the phase change solid-liquid boundary constantly shifts and this rate is dependent upon various heat input parameters, PCM's thermophysical properties and the design of the heat storage container. It is difficult to exactly formulate the position of the boundary which forms the part of the solution [275]. Various experimental and numerical studies have been conducted to solve the energy formulated equation [276–287]. A detailed review of heat transfer and phase change problem formulation can be found in [288].

Design of PCM integrated solar absorption cooling system can be achieved by considering storage capacity, geometry, heat storage method, thermal behavior, total cost and application specifics. Heat storage can be done internally or externally. In an external storage system, storing of heat for the generator or cool energy for the cold storage is done with a TES system installed/attached outside the circuit, while the internal storage system is by using (slurry) heat transfer fluid in the system (solar circuit) to store and also transfer heat to the TES system [16].

Shell and tube LHS system was numerically analyzed for thermal behavior of two phase change materials by Adine and Qarnia [110]. To study the effect of operating and geometric parameters (HTF inlet temperature, mass flow rate and length of PCM section), they conducted several experimental iterations using volume control approach transformed to algebraic equations. Higher mass flow rate ( $\dot{m}_f = 10\text{--}2 \text{ kg/s}$ ) and partial storage resulted more efficient LHS unit with *n*-octadecane as a PCM. However, the maximum thermal storage efficiencies for both the storages were identical. Agyenim et al. [289] used another type of shell and tube heat exchanger where they tested two configurations (single and four tubes in a control unit) to study the temperature gradient (in Erythritol) along three directions (axial, radial and angular) and suggested that a four tube configuration suitable to power a LiBr-H<sub>2</sub>O absorption system. Medrano et al. [290] tested five small heat exchangers and commercially available paraffin RT35 and water as a HTF. Average thermal power values were evaluated and double pipe heat exchanger with PCM embedded in graphite matrix (DPHX-PCM matrix) was found to be the best option. Their model set-up consisted of a thermostatic bath to control the water inlet temperature, pump, valves and an easily replaceable heat storage system. They used to charge the system with solid PCM until no solid PCM is observed. Then discharging with cold water with HTF was started immediately until no liquid PCM is observed; taking readings at every 10 s. Trp et al. [291] numerically studied the transient heat transfer phenomenon in a shell and tube heat exchanger with water as HTF and paraffin as PCM. All the thermocouples were connected to a data acquisition system through LabView<sup>®</sup> software collecting data every 10 s. They deduced few guidelines for parametric designing of a LHTS system:

- Mass flow rate of the HTF has negligible effect on thermal energy stored. This can vary with thermal conductivity of the HTF.
- Parametric changes in temperature difference between the HTF inlet and PCM melting can be used to influence (linearly) the amount of stored and delivered thermal energy in the LHTS system.
- Parametric changes in geometry, like outer tube radii be 1.2–1.8 for melting, and 1.2–2 for solidification with a dimensionless length of the unit=40. Increasing the dimensionless tube length decreases the energy density and the ratio of the total to the latent energy.
- Energy density and the ratio of total to latent energy stored decrease significantly with the increasing of outer tube radius during charging and discharging process

The effects of the Reynolds number and the Stefan number on the charging and discharging behaviors in fixed geometry storage unit (at 5 degree tilt) was experimentally investigated by Akgün et al. [292] for three different paraffins. They concluded that the Reynolds number does not have a considerable effect on total melting time, but a lower value should be chosen for an energy efficient storage system. Increasing the Stefan number decreases the melting time drastically and an average of 0.04 increment in Stefan number with 5 °C increment in HTF inlet temperature was observed. Gil et al. [103] placed the shell and tube storage tank with an electrical boiler (24 kW<sub>e</sub>) and an air heat exchanger (20 kW<sub>e</sub>) to cool down the HTF (Therminol VP-01). Two containers with 49 bent tubes with/without (196) square fins and PCM (hydroquinone) on shell side were constructed. The containers size was 527×273×1273 mm with a heat transfer surface of 6.6 m<sup>2</sup> and PCM quantity of 155 kg and 170 kg, for with/without fins respectively. Raja et al. [58] placed the generator inside a hot water storage tank to reduce the heat losses. Ponshanmugakumar et al. [187] placed the vertical generator in a thermal storage tank with phase change material to decrease the heat demand at peak loads and low radiation periods, whereas Lorente et al. [105] numerically and analytically studied a vertical cylinder with PCM on the shell side and HTF in the helical tube inside the shell. They determined the optimum pitch and diameter of the helix for better performance of the

heat storage unit. Few new design options were suggested by Zhai et al. [293] with regards to solar collectors, auxiliary systems and cooling modes in single effect absorption cooling system. A review on influence of geometry and initial conditions on the performance of PCM based energy storages can be found at [294].

### 8.1. Cost analysis

The two most influential parameters affecting the economics of solar cooling options are the solar collection technology and the performance of the system [295]. Solar assisted absorption refrigeration system is more feasible than other conventional as well as solar powered cooling systems. The main factors affecting the techno-economic feasibility are cooling load, weather, system performance, and cost of components [296]. Building features like composite wall materials/layers, type of glazing, orientation, primary usage and number of working persons also play an important role in defining the total load. A suitable selection of solar collectors and storage tanks contribute to achieve the payback in shorter time period [297]. Although economic analysis for conventional systems (without thermal storage) [298,299] and systems with sensible storage (water) tanks are abundant [296,297,300–304], a comparative cost analysis on using PCM as latent heat thermal storage unit in solar absorption cooling system are rarely seen. Godarzi et al. [274] designed a PCM storage based on exergoeconomic analysis and genetic algorithm in a 45.4 kW LiBr-H<sub>2</sub>O system. Their analysis showed a payback period of 0.61 yr without PCM storage to 1.13 yr with PCM storage.

Other investigations analyzing cost of the system with a storage tank include Misra et al. [305] who optimized LiBr-H<sub>2</sub>O single-effect absorption system based on theory of exergetic cost and thermo-economic optimization technique. They suggested that the techniques provided cost-effective improvements. They also observed a reduction of 3.5% production cost with an increase of 12.58% investment cost. Later, they used the same technique to improve the COP and exergetic efficiency of the same system by 10.419% and 10.423%, respectively with an increase of 3.14% investment cost [306]. They later applied the same technique to NH<sub>3</sub>-H<sub>2</sub>O absorption system and were able to improve COP and exergetic efficiency by 44.2% and 44.6%, respectively by increasing the investment in evaporator assembly (19.1%) and RHX (100.6%) and decrease the cost of generator (64.4%), SHX (30.4%) and rectifier (70.5%) [307].

Calise [300] numerically investigated a LiBr-H<sub>2</sub>O system using thermo-economic and optimization techniques and 64% of primary energy saving was achieved with a payback period of 12 years. Later, Calise et al. [297] optimized the same system with the objective of finding the payback period and overall annual cost. They calculated three types of payback periods and the one with least value (14.8 years) includes public funding in capital cost.

Tsoutsos et al. [304] simulated and optimized the size of a complete LiBr-H<sub>2</sub>O system for a hospital building in Greece. They simulated four scenarios with varied collector area, solar fraction heating/cooling using two size of chiller units (70 kW and 121 kW). The least payback time (11.5 years) was found in their forth scenario with a combination of compression vapor pressure and absorption system of 50 kW and 70 kW, respectively. The collector area was 500 m<sup>2</sup> and the hot water storage tank volume was 15 m<sup>3</sup>. Koroneos et al. [170] calculated a payback period of 24 years for a 70 kW LiBr-H<sub>2</sub>O absorption system cooling a medical center in Greece. Mateus and Oliveira [308] evaluated the potential of solar absorption system for three types of buildings (office, hotel and single-family house) in three cities of various countries. Single-family house and hotel were two most economically feasible scenarios. They however concluded that the use of evacuated tube collectors, rather than flat plate collectors can reduce the collector area to 5–50%. Hang et al. assessed a 150 kW LiBr-H<sub>2</sub>O system for a midsized office building in California, USA. A payback of 13.8 years was estimated with 40% government subsidies. Al-Alili

[302] simulated a 10 kW NH<sub>3</sub>-H<sub>2</sub>O system for the weather conditions of Abu Dhabi, UAE. They reported a 47% energy saving by replacing the current system with conventional vapor compression evaporation system. They did not mention the payback period but inversely correlated it with electricity prices.

Al-Ugla et al. [296] calculated a payback period of 18.5 years for a 1500 kW LiBr-H<sub>2</sub>O solar absorption system working 10 h daily, and it reduced to 9 years with 50% government subsidy in the Kingdom of Saudi Arabia. It can also be reduced from 18.5 years to 16 years if the COP is increased to 0.7644.

## 9. Conclusions

A detailed review of phase change materials and their enhancement techniques suitable for solar absorption refrigeration system has been performed. A comprehensive review on latent heat thermal storage units, suitable materials selection, PCM challenges, enhancement techniques used, system and cost analysis is made. Concluding summaries on the basis of approach to the use of PCM in solar assisted absorption refrigeration systems have been made. Preferences in selecting a material according to the component heat balance, dissipation, operating temperature, and PCM challenges are suggested for an improved output. Design approaches, challenges faced and solutions in the container design, heat propagation, PCM behavior and effect on the system are described. Concluding remarks for future research in effective utilization of PCM selection basis and approach strategy in solar absorption cooling are as follows:

1. Melting temperature, latent heat of fusion and PCM thermophysical issues are three basic factors influencing the selection of PCM in any application. High heat of fusion, precise melting/solidification temperature (without subcooling) are two primary requirements in the selection approach.
2. Erythritol, Hydroquinone and D-mannitol are three much studied HTFs for the temperature range (140–200 °C) suitable for absorption refrigeration system. Next to melting point temperature, degree of subcooling (of inorganic materials) is also an important parameter that influence the thermal capacity of the system. Other eutectic mixtures are also suitable provided the challenges are explored and solutions are tried.
3. Storage tank design plays an important role in effectively maximizing the heat intake and output from the LHTSS. Shell and tube design has proven to be the best, but at the cost of low PCM volume capacity. Multitube design is another proved efficient design with complete charging and discharging observed. A good heat-exchanger considering the thermos-physical behavior of PCM has not been studied yet. Thermal behavior during charging and discharging is crucial parameter. This depends upon the container design and the heat transfer rate of the PCM.
4. PCM melting temperature is selected ~10 °C lower than operating temperature. The PCM enthalpy, heat of fusion and some negative PCM characteristics like, subcooling, phase segregation and corrosion are to be studied well before investing the time and money. Few commercial PCMs like PlusIce have smooth thermal behavior suitable for solar energy storage.
5. Numerous mechanical and nano-level enhancements have been done to increase the heat transfer rate and found promising. Microencapsulation increases the heat transfer surface area and is also a solution for phase segregation in salt hydrates. Nucleating agents are a good option to solve subcooling problem in inorganic salt hydrates. This method is largely investigated and its application has a definite positive impact on the storage capacity.
6. A good heat exchange in the generator can save a lot of input energy and increases the capacity of LHTES systems. Condenser, absorber and evaporator heat exchanger efficiencies affect the overall COP of the system. Application of PCM at generator and evaporator is quite



effective than using PCM at condenser or absorber.

7. Innovative techniques to integrate PCM in a flat plate or custom designed solar collector have proved efficient. However, this still requires the pump power which is not the case if the generator is submerged in the PCM of storage unit. PCM system integration methods are sparse.
8. PCM increases the initial cost, but saves energy in prolong operating periods. The added advantage of using PCM in any thermal system is that it thermally stabilizes the system making its transition between different modes (day, night and cloudy) smooth.
9. It largely depends upon the economic factor on how far adjustments can be made. High heat of fusion at precise melting temperature can come at a cost of PCM issues which might need expensive treatments like using nanoparticles or encapsulations, or completely changing the container material or using nucleating agents. The balance between these parameters depends upon discretion of the researcher's expertise and the economic viability.

## 10. Recommendations

Based on the diversity of topics, a few recommendations for future research in utilization of PCM in solar absorption cooling (and in general) are made as follows:

1. High temperature HTF are already in use, but high temperature latent heat storage has not been explored yet. Although materials are identified for higher temperatures, their reliable design and integration with the system is hardly seen. Very few pilot storage systems have been investigated to be commercially implemented. There are only few studies on the nano enhancement of HTF for high temperatures applications.
2. Empirical formulation for system design and integration; and energy-exergy analysis are two areas that needs more investigation. Study of melting/freezing layer movement in the PCM is hardly seen in the literature. This is useful in designing an efficient PCM storage unit.
3. Although optimum generator operating temperatures for single and multi-effect absorption cycles has been accurately determined through numerous experimental results, suitable integrated storage units have not been explored yet. Pumping heat from an external LHTSS consumes energy and if the generator and LHTS units are combined, this pumping energy can be saved. So far, only two attempts have been made in this direction. A more efficient system is expected with this type of integration.
4. In a cylindrical PCM storage unit, multi-tubes geometry was proven to be the most effective, but in order to reduce the subcooling, integration of longitudinal fins with multi-tubes has a promising scope for better performance. A combination or innovative design for storage unit is needed in this direction.
5. Absorber and condenser operate at almost same temperature. Yet, no attempt to combine them into one unit integrated with PCM is made. Use of PCM at condenser should be critically handled as thermal conductivity of the PCM is of the highest importance to dissipate energy in the process. PCM with condenser in hot weather conditions ( $> 40\text{ }^{\circ}\text{C}$ ) and its effect on compressor run-time has never been studied, especially considering how heavily refrigeration is used in hot countries.
6. In cold storage, materials with subzero temperatures are identified, but their thermal reliability, phase-segregation and subcooling issues are not deeply studied. Studies on industrial (large scale) level thermal cold storage phase change materials are hardly tested.
7. Application of nano-particles with various PCMs open the door to infinite possibilities and test that give out a new generation of enhanced PCM. Property customization is a great way to make application based PCM perfectly suitable for the system operating condition.

8. Work on phase segregation and high thermal cycling is less seen in the literature due to long time needed to investigate this phenomenon. But this property decides the reliability of the product and should be focused more. Many salt hydrates exhibit good and suitable thermal properties but need better ways to enhance their properties and avoid the issues they are known for.

## Acknowledgement

Authors would like to thank the Center of Research Excellence in Renewable Energy (CoRE-RE), King Fahd University of Petroleum & Minerals (KFUPM) for the support to conduct this research.

## References

- [1] Sørensen B. Chapter 3 - The Individual Energy Sources. In: Sørensen B, editor. *Renewable Energy* Third edition. Burlington: Academic Press; 2004. p. 210–317.
- [2] Noailly J, Smeets R. Directing technical change from fossil-fuel to renewable energy innovation: an application using firm-level patent data [7//]. *J Environ Econ Manag* 2015;72:15–37, [7//].
- [3] Kalogirou S. Parabolic trough collector system for low temperature steam generation: design and performance characteristics. *Appl Energy* 1996;55:1–19.
- [4] Eltawil MA, Zhengming Z, Yuan L. A review of renewable energy technologies integrated with desalination systems [12//]. *Renew Sustain Energy Rev* 2009;13:2245–62, [12//].
- [5] Chang M. The Present Situation and Prospects of Solar Photovoltaic Power Generation in China, In: 2015 Asia-Pacific Energy Equipment Engineering Research Conference; 2015.
- [6] Tabor H. Use of solar energy for cooling purposes [10//]. *Sol Energy* 1962;6:136–42, [10//].
- [7] Li ZF, Sumathy K. Technology development in the solar absorption air-conditioning systems [9/1//]. *Renew Sustain Energy Rev* 2000;4:267–93, [9/1//].
- [8] Henning H-M. Solar assisted air conditioning of buildings – an overview [7//]. *Appl Therm Eng* 2007;27:1734–49, [7//].
- [9] Löf GOG, Tybout RA. The design and cost of optimized systems for residential heating and cooling by solar energy," [8//]. *Sol Energy* 1974;16:9–18, [8//].
- [10] Wilbur PJ, Mitchell CE. Solar absorption air conditioning alternatives [7//]. *Sol Energy* 1975;17:193–9, [7//].
- [11] Ward DS. Solar absorption cooling feasibility [//]. *Sol Energy* 1979;22:259–68, [//].
- [12] Lamp P, Ziegler F. European research on solar-assisted air conditioning [3//]. *Int J Refrig* 1998;21:89–99, [3//].
- [13] Papadopoulos AM, Oxizidis S, Kyriakis N. Perspectives of solar cooling in view of the developments in the air-conditioning sector [10//]. *Renew Sustain Energy Rev* 2003;7:419–38, [10//].
- [14] Grossman G. Solar-powered systems for cooling, dehumidification and air-conditioning [1//]. *Sol Energy* 2002;72:53–62, [1//].
- [15] Balaras CA, Grossman G, Henning H-M, Infante Ferreira CA, Podesser E, Wang L, et al. Solar air conditioning in Europe—an overview [2//]. *Renew Sustain Energy Rev* 2007;11:299–314, [2//].
- [16] Chidambaram LA, Ramana AS, Kamaraj G, Velraj R. Review of solar cooling methods and thermal storage options [8//]. *Renew Sustain Energy Rev* 2011;15:3220–8, [8//].
- [17] Zalba B, Marin JM, Cabeza LF, Mehling H. Review on thermal energy storage with phase change: materials, heat transfer analysis and applications [2//]. *Appl Therm Eng* 2003;23:251–83, [2//].
- [18] Sharma A, Tyagi VV, Chen CR, Buddhi D. Review on thermal energy storage with phase change materials and applications [2//]. *Renew Sustain Energy Rev* 2009;13:318–45, [2//].
- [19] Zhou D, Zhao CY, Tian Y. Review on thermal energy storage with phase change materials (PCMs) in building applications [4//]. *Appl Energy* 2012;92:593–605, [4//].
- [20] Moreno P, Solé C, Castell A, Cabeza LF. The use of phase change materials in domestic heat pump and air-conditioning systems for short term storage: a review," [11//]. *Renew Sustain Energy Rev* 2014;39:1–13, [11//].
- [21] Tay NHS, Liu M, Belusko M, Bruno F. "Review on transportable phase change material in thermal energy storage systems," *Renewable and Sustainable Energy Reviews*.
- [22] Liu M, Saman W, Bruno F. Review on storage materials and thermal performance enhancement techniques for high temperature phase change thermal storage systems [5//]. *Renew Sustain Energy Rev* 2012;16:2118–32, [5//].
- [23] Zhai XQ, Wang XL, Wang T, Wang RZ. A review on phase change cold storage in air-conditioning system: materials and applications [6//]. *Renew Sustain Energy Rev* 2013;22:108–20, [6//].
- [24] Pintaldi S, Perfumo C, Sethuvenkatraman S, White S, Rosengarten G. A review of thermal energy storage technologies and control approaches for solar cooling [1//]. *Renew Sustain Energy Rev* 2015;41:975–95, [1//].
- [25] Tian Y, Zhao CY. A review of solar collectors and thermal energy storage in solar thermal applications [4//]. *Appl Energy* 2013;104:538–53, [4//].
- [26] Mastani Joybari M, Haghighat F, Moffat J, Sra P. Heat and cold storage using phase change materials in domestic refrigeration systems: the state-of-the-art

- review. *Energy Build* 2015.
- [27] Oró E, de Gracia A, Castell A, Farid MM, Cabeza LF. Review on phase change materials (PCMs) for cold thermal energy storage applications [11/]. *Appl Energy* 2012;99:513–33, [11/].
- [28] RBiradar N, CHOUGALE CA. Review on Thermal Energy Storage using Phase Change Materials and Applications; 2015.
- [29] Thakare KA, Bhawe A. Review on latent heat storage and problems associated with phase change materials. *Int J Res Eng Technol* 2015;4:176–82.
- [30] Sharma SD, Sagara K. Latent heat storage materials and systems: a review [2005/01/01]. *Int J Green Energy* 2005;2:1–56, [2005/01/01].
- [31] Nomura T, Okinaka N, Akiyama T. Technology of latent heat storage for high temperature application: a review. *ISIJ Int* 2010;50:1229–39.
- [32] Hasnain SM. Review on sustainable thermal energy storage technologies, Part I: heat storage materials and techniques. *Energy Convers Manag* 8/1/1998;39:1127–38.
- [33] Pielichowska K, Pielichowski K. Phase change materials for thermal energy storage [8/]. *Prog Mater Sci* 2014;65:67–123, [8/].
- [34] Pereira J, da Cunha , Eames P. Thermal energy storage for low and medium temperature applications using phase change materials – a review [9/1/]. *Appl Energy* 2016;177:227–38, [9/1/].
- [35] Alva G, Liu L, Huang X, Fang G. Thermal energy storage materials and systems for solar energy applications [2/]. *Renew Sustain Energy Rev* 2017;68(Part1):693–706, [2/].
- [36] Kim DS, Ferreira CA Infante. Solar refrigeration options – a state-of-the-art review [1/]. *Int J Refrig* 2008;31:3–15, [1/].
- [37] Srihirin P, Aphornratana S, Chungpaibulpatana S. A review of absorption refrigeration technologies [12/]. *Renew Sustain Energy Rev* 2001;5:343–72, [12/].
- [38] Ullah K, Saidur R, Ping H, Akikur R, Shuvo N. A review of solar thermal refrigeration and cooling methods. *Renew Sustain Energy Rev* 2013;24:499–513.
- [39] Sarbu I, Sebarchievici C. Review of solar refrigeration and cooling systems [12/]. *Energy Build* 2013;67:286–97, [12/].
- [40] Shirazi A, Pintaldi S, White SD, Morrison GL, Rosengarten G, Taylor RA. Solar-assisted absorption air-conditioning systems in buildings: control strategies and operational modes [1/5/]. *Appl Therm Eng* 2016;92:246–60, [1/5/].
- [41] Afshar O, Saidur R, Hasanuzzaman M, Jameel M. A review of thermodynamics and heat transfer in solar refrigeration system [10/]. *Renew Sustain Energy Rev* 2012;16:5639–48, [10/].
- [42] Wang SG, Wang RZ. Recent developments of refrigeration technology in fishing vessels [4/]. *Renew Energy* 2005;30:589–600, [4/].
- [43] Siddiqui MU, Said SAM. A review of solar powered absorption systems [2/]. *Renew Sustain Energy Rev* 2015;42:93–115, [2/].
- [44] Worsøe-Schmidt P. Solar refrigeration for developing countries using a solid-absorption cycle [1983/07/01]. *Int J Ambient Energy* 1983;4:115–24, [1983/07/01].
- [45] Brendel ZM Muller-Steinhagen T. H. Development of a small scale ammonia/water absorption chiller, presented at In: Proceedings of the Ninth IIR Gustav Lorentzen conference, Sydney; 2010.
- [46] Le Lostec B, Galanis N, Millette J. Experimental study of an ammonia-water absorption chiller [12/]. *Int J Refrig* 2012;35:2275–86, [12/].
- [47] Li ZF, Sumathy K. Experimental studies on a solar powered air conditioning system with partitioned hot water storage tank [11/]. *Sol Energy* 2001;71:285–97, [11/].
- [48] Syed A, Izquierdo M, Rodríguez P, Maidment G, Missenden J, Lecuona A, et al. "A novel experimental investigation of a solar cooling system in Madrid [9/]. *Int J Refrig* 2005;28:859–71, [9/].
- [49] Pongtornkulpanich A, Thepa S, Amornkitbamrung M, Butcher C. Experience with fully operational solar-driven 10-ton LiBr/H<sub>2</sub>O single-effect absorption cooling system in Thailand [5/]. *Renew Energy* 2008;33:943–9, [5/].
- [50] Asdrubali F, Grignaffini S. Experimental evaluation of the performances of a H<sub>2</sub>O–LiBr absorption refrigerator under different service conditions [6/]. *Int J Refrig* 2005;28:489–97, [6/].
- [51] Agyenim F, Knight I, Rhodes M. Design and experimental testing of the performance of an outdoor LiBr/H<sub>2</sub>O solar thermal absorption cooling system with a cold store [5/]. *Sol Energy* 2010;84:735–44, [5/].
- [52] Agyenim F. "The use of enhanced heat transfer phase change materials (PCM) to improve the coefficient of performance (COP) of solar powered LiBr/H<sub>2</sub>O absorption cooling systems [3/]. *Renew Energy* 2016;87(Part1):229–39, [3/].
- [53] Kherris S, Zebbar D, Makhlof M, Zebbar S. Etude et analyse d'une machine frigorifique à absorption-diffusion solaire NH<sub>3</sub>-H<sub>2</sub>O-H<sub>2</sub>. *Rev Energy Renouv* 2012;373–82.
- [54] Said SAM, El-Shaarawi MAI, Siddiqui MU. Alternative designs for a 24-h operating solar-powered absorption refrigeration technology [11/]. *Int J Refrig* 2012;35:1967–77, [11/].
- [55] Said SAM, El-Shaarawi MAI, Siddiqui MU. Analysis of a solar powered absorption system [6/]. *Energy Convers Manag* 2015;97:243–52, [6/].
- [56] Said SAM, Spindler K, El-Shaarawi MA, Siddiqui MU, Schmid F, Bierling B, et al., Design, construction and operation of a solar powered ammonia-water absorption refrigeration system in saudi arabia, *International Journal of Refrigeration*.
- [57] Balghouthi M, Chahbani MH, Guizani A. Investigation of a solar cooling installation in Tunisia [10/]. *Appl Energy* 2012;98:138–48, [10/].
- [58] Raja VSVB. Experimental analysis of newly designed solar assisted single effect absorption cooling system of 5.25 kW cooling capacity for domestic Use. *Appl Mech Mater* 2015;787:32–6.
- [59] Ozgoren M, Bilgili M, Babayigit O. Hourly performance prediction of ammonia-water solar absorption refrigeration [7/]. *Appl Therm Eng* 2012;40:80–90, [7/].
- [60] Pintaldi S, Sethuvenkatraman S, White S, Rosengarten G. Energetic evaluation of thermal energy storage options for high efficiency solar cooling systems [2/15/]. *Appl Energy* 2017;188:160–77, [2/15/].
- [61] Arias-Varela S-GW, Castillo-Lopez HD, Best-Brown R O. Thermodynamic design of a solar refrigerator to preserve sea products. *California* 2000;22370.
- [62] Abdulateef J, Alghoul M, Zaharim A, Sopian K. Experimental investigation on solar absorption refrigeration system in Malaysia, in: Proceedings of the 3rd Wseas International Conference On Renewable Energy Sources, pp. 1–3; 2009.
- [63] Boudéhenn F, Demasles H, Wyttenbach J, Jobard X, Chéze D, Papillon P. Development of a 5 kW cooling capacity ammonia-water absorption chiller for solar cooling applications [1/]. *Energy Procedia* 2012;30:35–43, [1/].
- [64] Albers J, Ziegler F. Analysis of the part load behaviour of sorption chillers with thermally driven solution pumps. In: Proceedings of the 21st International Congress of Refrigeration, IIR/IIF, WA, Paper No. ICR0570; 2003.
- [65] De Francisco A, Illanes R, Torres JL, Castillo M, De Blas M, Prieto E, et al. Development and testing of a prototype of low-power water-ammonia absorption equipment for solar energy applications. *Renew Energy* 2002;25:537–44.
- [66] Rivera CO, Rivera W. Modeling of an intermittent solar absorption refrigeration system operating with ammonia–lithium nitrate mixture [3/31/]. *Sol Energy Mater Sol Cells* 2003;76:417–27, [3/31/].
- [67] Rivera W, Moreno-Quintanar G, Rivera CO, Best R, Martínez F. Evaluation of a solar intermittent refrigeration system for ice production operating with ammonia/lithium nitrate [1/]. *Sol Energy* 2011;85:38–45, [1/].
- [68] Moreno-Quintanar G, Rivera W, Best R. Comparison of the experimental evaluation of a solar intermittent refrigeration system for ice production operating with the mixtures NH<sub>3</sub>/LiNO<sub>3</sub> and NH<sub>3</sub>/LiNO<sub>3</sub>/H<sub>2</sub>O [2/]. *Renew Energy* 2012;38:62–8, [2/].
- [69] Hernández JA, Rivera W, Colorado D, Moreno-Quintanar G. Optimal COP prediction of a solar intermittent refrigeration system for ice production by means of direct and inverse artificial neural networks [4/]. *Sol Energy* 2012;86:1108–17, [4/].
- [70] Tangka JK, Kamnang NE. Development of a simple intermittent absorption solar refrigeration system [April 1, 2006]. *Int J Low-Carbon Technol* 2006;1:127–38, [April 1, 2006].
- [71] Joseph A, Kabbara M, Groulx D, Allred P, White MA. Characterization and real-time testing of phase-change materials for solar thermal energy storage. *Int J Energy Res* 2016;40:61–70.
- [72] Al-abidi AA, Bin Mat S, Sopian K, Sulaiman MY, Mohammed AT. "CFD applications for latent heat thermal energy storage: a review [4/]. *Renew Sustain Energy Rev* 2013;20:353–63, [4/].
- [73] Ayyappan S, Mayilsamy K, Sreenarayanan VV. "Performance improvement studies in a solar greenhouse drier using sensible heat storage materials [2015/04/19]. *Heat Mass Transf* 2015;1–9, [2015/04/19].
- [74] Helm M, Keil C, Hiebler S, Mehling H, Schweigler C. Solar heating and cooling system with absorption chiller and low temperature latent heat storage: energetic performance and operational experience [6/]. *Int J Refrig* 2009;32:596–606, [6/].
- [75] Aydin D, Utlu Z, Kincay O. Thermal performance analysis of a solar energy sourced latent heat storage [10/]. *Renew Sustain Energy Rev* 2015;50:1213–25, [10/].
- [76] Laevemann E, Energiespeicher Thermische. Theoretische Grenzen und Beurteilungskriterien, presented at the Experten-Workshop Thermische Speicher: Potentiale und Grenzen der Steigerung der Energiespeicherdichten, Berlin, Germany; June 2010.
- [77] Dieckmann J. Latent heat storage in concrete, Technische Universität Kaiserslautern, Kaiserslautern, Germany, www.eurosolar.org, retrieved December, vol. 9; 2008.
- [78] Kuznik F, David D, Johannes K, Roux J-J. A review on phase change materials integrated in building walls [1/]. *Renew Sustain Energy Rev* 2011;15:379–91, [1/].
- [79] Yuan Y, Zhang N, Tao W, Cao X, He Y. Fatty acids as phase change materials: a review [1/]. *Renew Sustain Energy Rev* 2014;29:482–98, [1/].
- [80] del Barrio EP, Godin A, Duquesne M, Daranlot J, Jolly J, Alshaer W, et al. Characterization of different sugar alcohols as phase change materials for thermal energy storage applications [1/]. *Sol Energy Mater Sol Cells* 2017;159:560–9, [1/].
- [81] Gunasekara SN, Pan R, Chiu JN, Martin V. Polyols as phase change materials for surplus thermal energy storage [1/15/]. *Appl Energy* 2016;162:1439–52, [1/15/].
- [82] Mohamed SA, Al-Sulaiman FA, Ibrahim NI, Zahir MH, Al-Ahmed A, Saidur R, et al., A review on current status and challenges of inorganic phase change materials for thermal energy storage systems, *Renewable and Sustainable Energy Reviews*.
- [83] Ge H, Li H, Mei S, Liu J. Low melting point liquid metal as a new class of phase change material: an emerging frontier in energy area [5/]. *Renew Sustain Energy Rev* 2013;21:331–46, [5/].
- [84] Su W, Darkwa J, Kokogiannakis G. Review of solid–liquid phase change materials and their encapsulation technologies [8/]. *Renew Sustain Energy Rev* 2015;48:373–91, [8/].
- [85] Sharma RK, Ganesan P, Tyagi VV, Metselaar HSC, Sandaran SC. Developments in organic solid–liquid phase change materials and their applications in thermal energy storage. *Energy Convers Manag* 5/1/2015;95:193–228.
- [86] Kalogirou SA. Solar thermal collectors and applications [1/]. *Prog Energy Combust Sci* 2004;30:231–95, [1/].
- [87] Sabiha MA, Saidur R, Mekhilef S, Mahian O. Progress and latest developments of evacuated tube solar collectors [11/]. *Renew Sustain Energy Rev* 2015;51:1038–54, [11/].

- [88] Lecuona A, Ventas R, Venegas M, Zacarias A, Salgado R. Optimum hot water temperature for absorption solar cooling. *Sol Energy* 10/2009;83:1806–14.
- [89] Praene JP, Marc O, Lucas F, Miranville F. Simulation and experimental investigation of solar absorption cooling system in Reunion Island [3//]. *Appl Energy* 2011;88:831–9, [3//].
- [90] Rabin Y, Bar-Niv I, Korin E, Mikic B. Integrated solar collector storage system based on a salt-hydrate phase-change material [12//]. *Sol Energy* 1995;55:435–44, [12//].
- [91] Mettawee E-BS, Assassa GMR. Experimental study of a compact PCM solar collector [11//]. *Energy* 2006;31:2958–68, [11//].
- [92] Eames PC, Griffiths PW. Thermal behaviour of integrated solar collector/storage unit with 65 °C phase change material [12//]. *Energy Convers Manag* 2006;47:3611–8, [12//].
- [93] Xue HS. Experimental investigation of a domestic solar water heater with solar collector coupled phase-change energy storage [2//]. *Renew Energy* 2016;86:257–61, [2//].
- [94] Naghavi MS, Ong KS, Badruddin IA, Mehrali M, Silakhori M, Metselaer HSC. Theoretical model of an evacuated tube heat pipe solar collector integrated with phase change material [11//]. *Energy* 2015;91:911–24, [11//].
- [95] Höhne G, Hemminger , Wolfgang F, Flammersheim H-J. *Differential scanning calorimetry*, 2 ed.. Heidelberg: Springer-Verlag Berlin; 2003.
- [96] Brancato V, Frazzica A, Sapienza A, Freni A. Identification and characterization of promising phase change materials for solar cooling applications [2//]. *Sol Energy Mater Sol Cells* 2017;160:225–32, [2//].
- [97] Gil A, Oró E, Peiró G, Álvarez S, Cabeza LF. Material selection and testing for thermal energy storage in solar cooling [9//]. *Renew Energy* 2013;57:366–71, [9//].
- [98] Agyenim F, Smyth M, Eames P. A review of phase change material energy storage; selection of materials suitable for energy storage in the 100–130 C temperature range. In: *World Renewable Energy Congress (WREC 2005)*, Aberdeen, UK, pp. 384–389; 2005.
- [99] Agyenim MRF. "The use of phase change material (PCM) to improve the coefficient of performance of a chiller for meeting domestic cooling in Wales," presented at In: *Proceedings of the 2nd PALENC Conference and 28th AIVC Conference on Building Low Energy Cooling and Advanced Ventilation Technologies in the 21st Century*, Crete island, Greece; 2007.
- [100] Schweigler C, Hiebler S, Keil C, Köbel H, Kren C, Mehling H. *Low-Temperature Heat Storage for Solar Heating and Cooling Applications*. ASHRAE Trans 2007;113:89–96.
- [101] Serale G, Baronetto S, Goia F, Perino M. Characterization and Energy Performance of a Slurry PCM-based Solar Thermal Collector: a Numerical Analysis [//]. *Energy Procedia* 2014;48:223–32.
- [102] Elbahjaoui, H REQ. "Numerical study of solar latent heat storage unit using Paraffin Wax P116," presented at the *Renewable and Sustainable Energy Conference (IRSEC)*, 2014 International, Morocco, 2014.
- [103] Gil A, Oró E, Miró L, Peiró G, Ruiz Á, Salmerón JM, et al. "Experimental analysis of hydroquinone used as phase change material (PCM) to be applied in solar cooling refrigeration [3//]. *International J Refrig* 2014;39:95–103, [3//].
- [104] He LJ, Tang LM, Chen GM. Performance prediction of refrigerant-DMF solutions in a single-stage solar-powered absorption refrigeration system at low generating temperatures [11//]. *Sol Energy* 2009;83:2029–38, [11//].
- [105] Lorente S, Bejan A, Niu JL. "Constructal design of latent thermal energy storage with vertical spiral heaters [2//]. *Int J Heat Mass Transf* 2015;81:283–8, [2//].
- [106] Assilzadeh F, Kalogirou SA, Ali Y, Sopian K. Simulation and optimization of a LiBr solar absorption cooling system with evacuated tube collectors [7//]. *Renew Energy* 2005;30:1143–59, [7//].
- [107] Suárez C, Iranzo A, Pino FJ, Guerra J. Transient analysis of the cooling process of molten salt thermal storage tanks due to standby heat loss [3/15//]. *Appl Energy* 2015;142:56–65, [3/15//].
- [108] Al-Abidi AA, Mat S, Sopian K, Sulaiman MY, Mohammad AT. Experimental study of melting and solidification of PCM in a triplex tube heat exchanger with fins [1//]. *Energy Build* 2014;68(Part A):33–41, [1//].
- [109] Murray RE, Groulx D. Experimental study of the phase change and energy characteristics inside a cylindrical latent heat energy storage system: part 2 simultaneous charging and discharging [3//]. *Renew Energy* 2014;63:724–34, [3//].
- [110] Qarnia H El. Numerical analysis of a coupled solar collector latent heat storage unit using various phase change materials for heating the water. *Energy Convers Manag* 2//2009;50:247–54.
- [111] Dhaidan NS, Khodadadi JM. Melting and convection of phase change materials in different shape containers: a review [3//]. *Renew Sustain Energy Rev* 2015;43:449–77, [3//].
- [112] Uber SJ. einge problem der theoric der wärmeleitung. S B Wein, Acad Mat Nat 1989;98:173–484.
- [113] Raam Dheep G, Sreekumar A. Influence of nanomaterials on properties of latent heat solar thermal energy storage materials – a review [7//]. *Energy Convers Manag* 2014;83:133–48, [7//].
- [114] Vakalotajjar SM, Saman W. Analysis and modelling of a phase change storage system for air conditioning applications [2/1//]. *Appl Therm Eng* 2001;21:249–63, [2/1//].
- [115] Liu L, Alva G, Huang X, Fang G. Preparation, heat transfer and flow properties of microencapsulated phase change materials for thermal energy storage [12//]. *Renew Sustain Energy Rev* 2016;66:399–414, [12//].
- [116] Hawlader MNA, Uddin MS, Khin MM. Microencapsulated PCM thermal-energy storage system [1//]. *Appl Energy* 2003;74:195–202, [1//].
- [117] Jacob R, Bruno F. Review on shell materials used in the encapsulation of phase change materials for high temperature thermal energy storage [8//]. *Renew Sustain Energy Rev* 2015;48:79–87, [8//].
- [118] Khadiran T, Hussein MZ, Zainal Z, Rusli R. Encapsulation techniques for organic phase change materials as thermal energy storage medium: a review [12//]. *Sol Energy Mater Sol Cells* 2015;143:78–98, [12//].
- [119] Su W, Darkwa J, Kokogiannakis G. Development of microencapsulated phase change material for solar thermal energy storage [2/5//]. *Appl Therm Eng* 2017;112:1205–12, [2/5//].
- [120] Giro-Paloma J, Martínez M, Cabeza LF, Fernández AI. Types, methods, techniques, and applications for microencapsulated phase change materials (MPCM): a review [1//]. *Renew Sustain Energy Rev* 2016;53:1059–75, [1//].
- [121] Yataganbaba A, Ozkahraman B, Kurtbas I. Worldwide trends on encapsulation of phase change materials: a bibliometric analysis (1990–2015) [1/1//]. *Appl Energy* 2017;185(Part1):720–31, [1/1//].
- [122] Tiari S, Qiu S, Mahdavi M. Numerical study of finned heat pipe-assisted thermal energy storage system with high temperature phase change material [1/1//]. *Energy Convers Manag* 2015;89:833–42, [1/1//].
- [123] Hosseini MJ, Ranjbar AA, Rahimi M, Bahrampoury R. Experimental and numerical evaluation of longitudinally finned latent heat thermal storage systems [7/15//]. *Energy Build* 2015;99:263–72, [7/15//].
- [124] Rathod MK, Banerjee J. Thermal performance enhancement of shell and tube Latent Heat Storage Unit using longitudinal fins [1/22//]. *Appl Therm Eng* 2015;75:1084–92, [1/22//].
- [125] Prabhakar SSM, Saha SK, Heat Transfer Enhancement in Latent Heat Thermal Energy Storage System using Fins for Solar Thermal Power Plant, presented at the *Third Southern African Solar Energy Conference SASEC*. 2015, Kruger National Park, South Africa, 2015.
- [126] Tao YB, He YL. Numerical study on performance enhancement of shell-and-tube latent heat storage unit [10//]. *Int Commun Heat Mass Transf* 2015;67:147–52, [10//].
- [127] Horbaniuc B, Dumitrascu G, Popescu A. Mathematical models for the study of solidification within a longitudinally finned heat pipe latent heat thermal storage system [10//]. *Energy Convers Manag* 1999;40:1765–74, [10//].
- [128] Zhang Y, Faghri A. Heat transfer enhancement in latent heat thermal energy storage system by using the internally finned tube [10//]. *Int J Heat Mass Transf* 1996;39:3165–73, [10//].
- [129] Velraj R, Seeniraj RV, Hafner B, Faber C, Schwarzer K. Experimental analysis and numerical modelling of inward solidification on a finned vertical tube for a latent heat storage unit [6//]. *Sol Energy* 1997;60:281–90, [6//].
- [130] Ismail KAR, Alves CLF, Modesto MS. Numerical and experimental study on the solidification of PCM around a vertical axially finned isothermal cylinder [1/1//]. *Appl Therm Eng* 2001;21:53–77, [1/1//].
- [131] Ermiş K, Ereğ A, Dincer I. Heat transfer analysis of phase change process in a finned-tube thermal energy storage system using artificial neural network [7//]. *Int J Heat Mass Transf* 2007;50:3163–75, [7//].
- [132] Agyenim F, Eames P, Smyth M. A comparison of heat transfer enhancement in a medium temperature thermal energy storage heat exchanger using fins [9//]. *Sol Energy* 2009;83:1509–20, [9//].
- [133] Trelles JP, Dufly JJ. Numerical simulation of porous latent heat thermal energy storage for thermoelectric cooling [9//]. *Appl Therm Eng* 2003;23:1647–64, [9//].
- [134] Hoogendoorn CJ, Bart G CJ, Performance and modelling of latent heat stores, *Solar Energy*, vol. 48, pp. 53–58, 1992/01/01 1992.
- [135] Hamada Y, Ohtsu W, Fukai J. Thermal response in thermal energy storage material around heat transfer tubes: effect of additives on heat transfer rates [10//]. *Sol Energy* 2003;75:317–28, [10//].
- [136] Fan L, Khodadadi JM. Thermal conductivity enhancement of phase change materials for thermal energy storage: a review [1//]. *Renew Sustain Energy Rev* 2011;15:24–46, [1//].
- [137] Halder SSS, Saha SK Effect of Metal Matrix and Foam Porosity on Thermal Performance of Latent Heat Thermal Storage for Solar Thermal Power Plant, presented at the *Third Southern African Solar Energy Conference SASEC*. 2015, Kruger National Park, South Africa, 2015.
- [138] Mahian O, Kianifar A, Kalogirou SA, Pop I, Wongwises S. A review of the applications of nanofluids in solar energy [2//]. *Int J Heat Mass Transf* 2013;57:582–94, [2//].
- [139] Hajare V, Gawali B, Experimental Study of Latent Heat Storage System using Nano-Mixed Phase Change Material."
- [140] Chaichan MT, Kamel SH, Al-Ajeely A-MN. Thermal conductivity enhancement by using nano-material in phase change material for latent heat thermal energy storage systems.
- [141] Otanicar TP, Phelan PE, Prasher RS, Rosengarten G, Taylor RA. Nanofluid-based direct absorption solar collector. *J Renew Sustain Energy* 2010;2:033102.
- [142] Mettawee E-BS, Assassa GMR. Thermal conductivity enhancement in a latent heat storage system [7//]. *Sol Energy* 2007;81:839–45, [7//].
- [143] Soochan L, Robert AT, Lenore D, Ravi P, Patrick EP. The effective latent heat of aqueous nanofluids. *Mater Res Express* 2015;2:065004.
- [144] Liu J, Chen L, Fang X, Zhang Z. Preparation of graphite nanoparticles-modified phase change microcapsules and their dispersed slurry for direct absorption solar collectors [1//]. *Sol Energy Mater Sol Cells* 2017;159:159–66, [1//].
- [145] Narayanan SS, Kardam A, Kumar V, Bhardwaj N, Madhwal D, Shukla P, et al., Development of sunlight-driven eutectic phase change material nanocomposite for applications in solar water heating, *Resource-Efficient Technologies*.
- [146] Li Y, Guo B, Huang G, Kubo S, Shu P. Characterization and thermal performance of nitrate mixture/SiC ceramic honeycomb composite phase change materials for thermal energy storage [4/25//]. *Appl Therm Eng* 2015;81:193–7, [4/25//].



- [147] Abdollahzadeh M, Esmailpour M. Enhancement of phase change material (PCM) based latent heat storage system with nano fluid and wavy surface [1//]. *Int J Heat Mass Transf* 2015;80:376–85, [1//].
- [148] Kardam A, Narayanan SS, Bhardwaj N, Madhwal D, Shukla P, Verma A, et al. Ultrafast thermal charging of inorganic nano-phase change material composites for solar thermal energy storage. *RSC Adv* 2015;5:56541–8.
- [149] Karaipekli A, Biçer A, Sari A, Tyagi VV. Thermal characteristics of expanded perlite/paraffin composite phase change material with enhanced thermal conductivity using carbon nanotubes [2/15//]. *Energy Convers Manag* 2017;134:373–81, [2/15//].
- [150] Jin Y, Wan Q, Ding Y. PCMs heat transfer performance enhancement with expanded graphite and its thermal stability [//]. *Procedia Eng* 2015;102:1877–84, [//].
- [151] Taylor R, Phelan P, Otanicar T, Adrian R, Prasher R. Nanofluid optical property characterization: towards efficient direct absorption solar collectors. *Nanoscale Res Lett* 2011;6:225.
- [152] Bozorgan N, Shafahi M. Performance evaluation of nanofluids in solar energy: a review of the recent literature. *Micro Nano Syst Lett* 2015;3:1–15.
- [153] Luo Z, Wang C, Wei W, Xiao G, Ni M. Performance improvement of a nanofluid solar collector based on direct absorption collection (DAC) concepts. *Int J Heat Mass Transf* 2014;75:262–71.
- [154] Sardarabadi M, Passandideh-Fard M, Heris SZ. Experimental investigation of the effects of silica/water nanofluid on PV/T (photovoltaic thermal units). *Energy* 2014;66:264–72.
- [155] Vishwakarma V, Singhal N, Khullar V, Tyagi H, Taylor RA, Otanicar TP, et al., Space Cooling Using the Concept of Nanofluids-Based Direct Absorption Solar Collectors. In: ASME 2012 International Mechanical Engineering Congress and Exposition,, p. 2769–2777; 2012.
- [156] Saidur R, Meng T, Said Z, Hasanuzzaman M, Kamyar A. Evaluation of the effect of nanofluid-based absorbers on direct solar collector. *Int J Heat Mass Transf* 2012;55:5899–907.
- [157] Said Z, Saidur R, Rahim N, Alim M. Analyses of exergy efficiency and pumping power for a conventional flat plate solar collector using SWCNTs based nanofluid. *Energy Build* 2014;78:1–9.
- [158] Faizal M, Saidur R, Mekhilef S, Alim M. Energy, economic and environmental analysis of metal oxides nanofluid for flat-plate solar collector. *Energy Convers Manag* 2013;76:162–8.
- [159] Zhang H, Chen H-J, Du X, Lin G, Wen D. Dependence of photothermal conversion characteristics on different nanoparticle dispersions. *J Nanosci Nanotechnol* 2015;15:3055–60.
- [160] Subramaniyan A, Priya SL, Ilangovan R. Energy Harvesting Through Optical Properties of TiO<sub>2</sub> and C-TiO<sub>2</sub> Nanofluid for Direct Absorption Solar Collectors.
- [161] Fedele L, Colla L, Bobbo S, Barison S, Agresti F. Experimental stability analysis of different water-based nanofluids. *Nanoscale Res Lett* 2011;6:1–8.
- [162] Hordy N, Meunier J-L, Coulombe S. High Temperature Stability of Plasma Functionalized Carbon Nanotube Nanofluids for Direct Solar Thermal Absorption.
- [163] Phelan P, Otanicar T, Taylor R, Tyagi H. Trends and opportunities in direct-absorption solar thermal collectors. *J Therm Sci Eng Appl* 2013;5:021003.
- [164] Gupta HK, Agrawal G, Mathur J. Assessment of energy and economic advantages by proposing nanofluid based direct absorption in solar collectors for India [in]. *Recent Adv Innov Eng (ICRAIE)*, 2014 2014:1–8.
- [165] Ni G, Miljkovic N, Ghasemi H, Huang X, Boriskina SV, Lin C-T, et al. Volumetric solar heating of nanofluids for direct vapor generation. *Nano Energy* 2015;17:290–301.
- [166] Liu L, Su D, Tang Y, Fang G. Thermal conductivity enhancement of phase change materials for thermal energy storage: a review [9//]. *Renew Sustain Energy Rev* 2016;62:305–17, [9//].
- [167] Yadav A, Barman B, Kumar V, Kardam A, Shankara Narayanan S, Verma A, et al. A Review on Thermophysical Properties of Nanoparticle-Enhanced Phase Change Materials for Thermal Energy Storage. In: Jain VK, Rattan S, Verma A, editors. *Recent Trends in Materials and Devices: Proceedings ICRTMD 2015*. Cham: Springer International Publishing; 2017. p. 37–47.
- [168] Mahfuz MH, Kamyar A, Afshar O, Sarraf M, Anisur MR, Kibria MA, et al. Exergetic analysis of a solar thermal power system with PCM storage [2//]. *Energy Convers Manag* 2014;78:486–92, [2//].
- [169] Koca A, Oztop HF, Koyun T, Varol Y. Energy and exergy analysis of a latent heat storage system with phase change material for a solar collector [4//]. *Renew Energy* 2008;33:567–74, [4//].
- [170] Koroneos C, Nanaki E, Xydis G. Solar air conditioning systems and their applicability—an exergy approach. *Resour, Conserv Recycl* 2010;55:74–82.
- [171] Yanbing K, Yinping Z, Yi J, Yingxin Z. A general model for analyzing the thermal characteristics of a class of latent heat thermal energy storage systems. *J Sol Energy Eng* 1999;121:185–93.
- [172] Chua HT, Toh HK, Ng KC. Thermodynamic modeling of an ammonia–water absorption chiller [11//]. *Int J Refrig* 2002;25:896–906, [11//].
- [173] Gordon JM, Ng KC. A general thermodynamic model for absorption chillers: theory and experiment [1//]. *Heat Recovery Syst CHP* 1995;15:73–83, [1//].
- [174] Kim B, Park J. Dynamic simulation of a single-effect ammonia–water absorption chiller [5//]. *Int J Refrig* 2007;30:535–45, [5//].
- [175] Bulgan AT. Optimization of the thermodynamic model of aqua-ammonia absorption refrigeration systems [2//]. *Energy Convers Manag* 1995;36:135–43, [2//].
- [176] Zheng D, Chen B, Qi Y, Jin H. Thermodynamic analysis of a novel absorption power/cooling combined-cycle [4//]. *Appl Energy* 2006;83:311–23, [4//].
- [177] Lee S-F, Sherif SA. Thermodynamic analysis of a lithium bromide/water absorption system for cooling and heating applications. *Int J Energy Res* 2001;25:1019–31.
- [178] Sun D-W. Thermodynamic design data and optimum design maps for absorption refrigeration systems [3//]. *Appl Therm Eng* 1997;17:211–21, [3//].
- [179] Tozer RM, James RW. Fundamental thermodynamics of ideal absorption cycles [3//]. *Int J Refrig* 1997;20:120–35, [3//].
- [180] Abdulateef KSJ, Yahya M, Zaharim A, Alghoul M. Optimization of the thermodynamic model of a solar driven Aqua-ammonia absorption refrigeration system. presented at In: *Proceedings of the 2nd WSEAS/IASME International Conference on RENEWABLE ENERGY SOURCES (RES'08)*, Corfu, Greece; 2008.
- [181] Raghuvanshi S, Maheshwari G. Analysis of ammonia–water (NH<sub>3</sub>-H<sub>2</sub>O) apor absorption refrigeration system based on first law of thermodynamics. *Int J Sci Eng Res* 2011;2:1–7.
- [182] Arun Bangotra AM. Design analysis Of 3 TR aqua ammoniavapour absorption refrigeration system. *Int J Eng Res Technol* 2012;1:1–6.
- [183] Caciula B, Popa V, Costiuc L. Theoretical study on solar powered absorption cooling system. *Termotehnica* 2013;1:130–4.
- [184] Chen W, Liang S, Guo Y, Tang D. Thermodynamic analysis of an absorption system using [bmim]Zn<sub>2</sub>Cl<sub>5</sub>/NH<sub>3</sub> as the working pair [9//]. *Energy Convers Manag* 2014;85:13–9, [9//].
- [185] Kaynakli O, Kilic M. Theoretical study on the effect of operating conditions on performance of absorption refrigeration system [2//]. *Energy Convers Manag* 2007;48:599–607, [2//].
- [186] Sözen A. Effect of heat exchangers on performance of absorption refrigeration systems [9//]. *Energy Convers Manag* 2001;42:1699–716, [9//].
- [187] Ponsanmugakumar SBA, Deepak P, Sivaraman H, Vignesh Kumar R. Numerical investigation on vertical generator integrated with phase change materials in vapour absorption refrigeration system. *Appl Mech Mater* 2015;766–767:468–73.
- [188] Celata GP, Cumo M, Setaro T. "Forced convective boiling in binary mixtures [1993/09/01]. *Int J Heat Mass Transf* 1993;36:3299–309, [1993/09/01].
- [189] Bennett DL, Chen JC. Forced convective boiling in vertical tubes for saturated pure components and binary mixtures. *AIChE J* 1980;26:454–61.
- [190] Rivera W, Best R. Boiling heat transfer coefficients inside a vertical smooth tube for water/ammonia and ammonia lithium nitrate mixtures [3/1//]. *Int J Heat Mass Transf* 1999;42:905–21, [3/1//].
- [191] He Q, Zhang W. A study on latent heat storage exchangers with the high-temperature phase-change material. *Int J Energy Res* 2001;25:331–41.
- [192] Charach C, Zemel A. Thermodynamic analysis of latent heat storage in a shell-and-tube heat exchanger. *J Sol Energy Eng* 1992;114:93–9.
- [193] Medrano M, Yilmaz MO, Nogués M, Martorell I, Roca J, Cabeza LF. Experimental evaluation of commercial heat exchangers for use as PCM thermal storage systems [10//]. *Appl Energy* 2009;86:2047–55, [10//].
- [194] Jeong S AL, Sang K, Koo J, Kee-Kahb J, Ziegler , Felix , et al. Heat transfer performance of a coiled tube absorber with working fluid of ammonia/water / discussion. *ASHRAE Trans* 1998;104:1577.
- [195] Matsuda A, Choi KH, Hada K, Kawamura T. Effect of pressure and concentration on performance of a vertical falling-film type of absorber and generator using lithium bromide aqueous solutions [//]. *Int J Refrig* 1994;17:538–42, [//].
- [196] Fong KF, Chow TT, Lee CK, Lin Z, Chan LS. Solar hybrid cooling system for high-tech offices in subtropical climate – Radiant cooling by absorption refrigeration and desiccant dehumidification [8//]. *Energy Convers Manag* 2011;52:2883–94, [8//].
- [197] Macriss RA, Gutraj J, Zawacki T. Absorption fluids data survey: final report on worldwide data. Chicago, IL (USA): Oak Ridge National Lab., TN (USA); Institute of Gas Technology; 1988.
- [198] El-Ghalban AR. Operational results of an intermittent absorption cooling unit. *Int J Energy Res* 2002;26:825–35.
- [199] Rasul MG MA. Solar powered intermittent absorption refrigeration unit, presented at the Australasian Power Engineering Conference, Australia; 2006.
- [200] Aman J, Ting DSK, Henshaw P. Residential solar air conditioning: energy and exergy analyses of an ammonia–water absorption cooling system [1/25//]. *Appl Therm Eng* 2014;62:424–32, [1/25//].
- [201] Abbaspour M, Saraei A. Thermoeconomic analysis and multi-objective optimization of a LiBr-Water absorption refrigeration system. *Int J Environ Res* 2015;9:61–8.
- [202] Cheng W-L, Mei B-J, Liu Y-N, Huang Y-H, Yuan X-D. A novel household refrigerator with shape-stabilized PCM (Phase Change Material) heat storage condensers: an experimental investigation [10//]. *Energy* 2011;36:5797–804, [10//].
- [203] Cheng W-L, Yuan X-D. Numerical analysis of a novel household refrigerator with shape-stabilized PCM (phase change material) heat storage condensers [9/15//]. *Energy* 2013;59:265–76, [9/15//].
- [204] Cheng W-l, Zhang R-m, Xie K, Liu N, Wang J. Heat conduction enhanced shape-stabilized paraffin/HDPE composite PCMs by graphite addition: preparation and thermal properties [10//]. *Sol Energy Mater Sol Cells* 2010;94:1636–42, [10//].
- [205] Wang F, Maidment G, Missenden J, Tozer R. The novel use of phase change materials in refrigeration plant. Part 1: experimental investigation [12//]. *Appl Therm Eng* 2007;27:2893–901, [12//].
- [206] Wang F, Maidment G, Missenden J, Tozer R. The novel use of phase change materials in refrigeration plant. Part 2: dynamic simulation model for the combined system [12//]. *Appl Therm Eng* 2007;27:2902–10, [12//].
- [207] Wang F, Maidment G, Missenden J, Tozer R. The novel use of phase change materials in refrigeration plant. Part 3: pcm for control and energy savings [12//]. *Appl Therm Eng* 2007;27:2911–8, [12//].
- [208] Sonnenrein G, Elsner A, Baumhögger E, Morbach A, Fieback K, Vrabec J. Reducing the power consumption of household refrigerators through the integration of latent heat storage elements in wire-and-tube condensers [3//]. *Int J*

- Refrigeration 2015;51:154–60, [3/].
- [209] Sonnenrein G, Baumhögger E, Elsner A, Fieback K, Morbach A, Paul A, et al. Copolymer-bound phase change materials for household refrigerating appliances: experimental investigation of power consumption, temperature distribution and demand side management potential [12/]. *Int J Refrig* 2015;60:166–73, [12/].
- [210] Zhao D, Tan G. Numerical analysis of a shell-and-tube latent heat storage unit with fins for air-conditioning application [1/15/]. *Appl Energy* 2015;138:381–92, [1/15/].
- [211] Hassan HZ, Mohamad AA. A review on solar cold production through absorption technology [9/]. *Renew Sustain Energy Rev* 2012;16:5331–48, [9/].
- [212] Osterman E, Tyagi VV, Butala V, Rahim NA, Strith U. Review of PCM based cooling technologies for buildings [6/]. *Energy Build* 2012;49:37–49, [6/].
- [213] Mehling H, Cabeza LF. Heat and cold storage with PCM. Springer; 2008.
- [214] Wang F, Maidment G, Missenden J, Tozer R. A review of research concerning the use of PCMs in air conditioning and refrigeration engineering. In: Anson M, Ko JM, Lam ESS, editors. *Advances in building technology*. Oxford: Elsevier; 2002. p. 1273–80.
- [215] Gin B, Farid MM. The use of PCM panels to improve storage condition of frozen food. *J Food Eng* 9/2010;100:372–6.
- [216] Azzouz K, Leducq D, Gobin D. Enhancing the performance of household refrigerators with latent heat storage: an experimental investigation [11/]. *Int J Refrig* 2009;32:1634–44, [11/].
- [217] Azzouz K, Leducq D, Gobin D. Performance enhancement of a household refrigerator by addition of latent heat storage [8/]. *Int J Refrig* 2008;31:892–901, [8/].
- [218] Khan MIH, Afroz HMM. Effect of phase change material on performance of a household refrigerator. *Asian J Appl Sci* 2013;6:56–67.
- [219] Marques AC, Davies GF, Evans JA, Maidment GG, Wood ID. Theoretical modelling and experimental investigation of a thermal energy storage refrigerator. *Energy* 6/15/2013;55:457–65.
- [220] Marques AC, Davies GF, Maidment GG, Evans JA, Wood ID. Novel design and performance enhancement of domestic refrigerators with thermal storage [2/22/]. *Appl Therm Eng* 2014;63:511–9, [2/22/].
- [221] Oró E, Miró L, Farid MM, Cabeza LF. Improving thermal performance of freezers using phase change materials [6/]. *Int J Refrig* 2012;35:984–91, [6/].
- [222] Li G, Hwang Y, Radermacher R. Cold thermal energy storage materials and applications toward sustainability. In: Zhang X, Dincer I, editors. *Energy solutions to combat global warming*. Cham: Springer International Publishing; 2017. p. 67–117.
- [223] Khan I, Afroz HM. Effect of phase change material on performance of a household refrigerator. *Asian J Appl Sci* 2013;6:56–67.
- [224] Dominguez-Inzunza LA, Hernández-Magallanes JA, Sandoval-Reyes M, Rivera W. Comparison of the performance of single-effect, half-effect, double-effect in series and inverse and triple-effect absorption cooling systems operating with the NH<sub>3</sub>–LiNO<sub>3</sub> mixture [5/]. *Appl Therm Eng* 2014;66:612–20, [5/].
- [225] Kaushik SC, Arora A. Energy and exergy analysis of single effect and series flow double effect water-lithium bromide absorption refrigeration systems. *Int J Refrig* 2009;32:1247–58.
- [226] Wan Z, Shu S, Hu X. Novel high-efficient solar absorption refrigeration cycles. *Huazhong Keji Daxue Xuebao (Ziran Kexue Ban)/J Huazhong Univ Sci Technol (Nat Sci Ed)* 2006;34:85–7.
- [227] Gebreslassie BH, Medrano M, Boer D. Exergy analysis of multi-effect water–LiBr absorption systems: from half to triple effect. *Renew Energy* 2010;35:1773–82.
- [228] Gomri R. Investigation of the potential of application of single effect and multiple effect absorption cooling systems [8/]. *Energy Convers Manag* 2010;51:1629–36, [8/].
- [229] Darkwa J, Fraser S, Chow DHC. Theoretical and practical analysis of an integrated solar hot water-powered absorption cooling system [3/]. *Energy* 2012;39:395–402, [3/].
- [230] Li G, Hwang Y, Radermacher R. Review of cold storage materials for air conditioning application [12/]. *Int J Refrig* 2012;35:2053–77, [12/].
- [231] Lazaridis A. A numerical solution of the multidimensional solidification (or melting) problem. *Int J Heat Mass Transf* 1970;13:1459–77.
- [232] Saitoh T. Numerical method for multi-dimensional freezing problems in arbitrary domains. *J Heat Transf* 1978;100:294–9.
- [233] Kouskousou T, Bruel P, Jamil A, El Rhafiki T, Zeraoui Y. "Energy storage: applications and challenges [1/]. *Solar Energy Mater Sol Cells* 2014;120(Part A):59–80, [1/].
- [234] Cerri G, Palmieri A, Monticelli E, Pezzoli D. Identification of domestic refrigerator models including cool storage. In: *International Congress of refrigeration*. Washington DC; 2003.
- [235] Rahman M, Hossain A, Das SK, Adnan Hasan R. Performance Improvement of a Domestic Refrigerator by using PCM (Phase Change Material)". *Glob J Res Eng* 2014;13.
- [236] Abhat A. Low temperature latent heat thermal energy storage: heat storage materials [7/]. *Sol Energy* 1983;30:313–32, [7/].
- [237] Kemink R, Sparrow E. Heat transfer coefficients for melting about a vertical cylinder with or without subcooling and for open or closed containment. *Int J Heat Mass Transf* 1981;24:1699–710.
- [238] Barreneche C, Gil A, Sheth F, Inés Fernández A, Cabeza LF. Effect of d-mannitol polymorphism in its thermal energy storage capacity when it is used as PCM [8/]. *Sol Energy* 2013;94:344–51, [8/].
- [239] Pitkänen I, Perkkäläinen P, Rautiainen H. Thermooanalytical studies on phases of D-mannitol. *Thermochim Acta* 1993;214:157–62.
- [240] Abhat A, Heine D, Heinisch M, Malatidis N, Neuer G. Development of a modular heat exchanger with an integrated latent heat storage, Report no. BMFT FBT, p. 81–050; 1981.
- [241] Heine D. The chemical compatibility of construction materials with latent heat storage materials. In: *Proceedings of the International Conference on Energy Storage*. Brighton, UK; 1981.
- [242] Li G, Hwang Y, Radermacher R, Chun H-H. Review of cold storage materials for subzero applications [3/1/]. *Energy* 2013;51:1–17, [3/1/].
- [243] Farid MM, Khudhair AM, Razack SAK, Al-Hallaj S. A review on phase change energy storage: materials and applications. *Energy Convers Manag* 2004;45:1597–615.
- [244] Telkes M. Nucleation of supersaturated inorganic salt solutions. *Ind Eng Chem* 1952;44:1308–10.
- [245] Wu Q, Zhao D, Jiao X, Zhang Y, Shea KJ, Lu X, et al. Preparation, Properties, and supercooling prevention of phase change material n-Octadecane microcapsules with peppermint fragrance scent [2015/08/26]. *Indust Eng Chem Res* 2015;54:8130–6, [2015/08/26].
- [246] Abhat A. Short term thermal energy storage. *Rev De Phys Appl* 1980;15:477–501.
- [247] Safari A, Saidur R, Sulaiman FA, Xu Y, Dong J. A review on supercooling of Phase Change Materials in thermal energy storage systems. *Renewable and Sustainable Energy Reviews*.
- [248] Yamagishi Y, Sugeno T, Ishige T, Takeuchi H, Pyatenko AT. An evaluation of microencapsulated PCM for use in cold energy transportation medium. In: *Energy Conversion Engineering Conference, 1996. IECEC 96., Proceedings of the 31st Intersociety, 1996*, p. 2077–2083.
- [249] Zhang X-x, Fan Y-f, Tao X-m, Yick K-l. Crystallization and prevention of supercooling of microencapsulated n-alkanes. *J Colloid Interface Sci* 2005;281:299–306.
- [250] Fan Y, Zhang X, Wang X, Li J, Zhu Q. Super-cooling prevention of microencapsulated phase change material. *Thermochim Acta* 2004;413:1–6.
- [251] Androsch R, Monami A, Kucera J. Effect of an alpha-phase nucleating agent on the crystallization kinetics of a propylene/ethylene random copolymer at largely different supercooling [12/15/]. *J Cryst Growth* 2014;408:91–6, [12/15/].
- [252] Yudong L, Chuangjian S, Pengfei H, Quanguai P, Liuzhu W, Jiangqing W. Containerless nucleation behavior and supercooling degree of acoustically levitated graphene oxide nanofluid PCM [12/]. *Int J Refrig* 2015;60:70–80, [12/].
- [253] Al-Shannaq R, Kurdi J, Al-Muhtaseb S, Dickinson M, Farid M. Supercooling elimination of phase change materials (PCMs) microcapsules [7/1/]. *Energy* 2015;87:654–62, [7/1/].
- [254] Cao F, Yang B. Supercooling suppression of microencapsulated phase change materials by optimizing shell composition and structure [1/]. *Appl Energy* 2014;113:1512–8, [1/].
- [255] Chandrasekaran P, Cheralathan M, Velraj R. Effect of fill volume on solidification characteristics of DI (deionized) water in a spherical capsule – an experimental study [10/]. *Energy* 2015;90(Part1):508–15, [10/].
- [256] Solé A, Neumann H, Niedermaier S, Martorell I, Schossig P, Cabeza LF. Stability of sugar alcohols as PCM for thermal energy storage [7/]. *Sol Energy Mater Sol Cells* 2014;126:125–34, [7/].
- [257] Behzadi S, Farid MM. Long term thermal stability of organic PCMs [6/1/]. *Appl Energy* 2014;122:11–6, [6/1/].
- [258] Zhang X-x, Tao X-m, Yick K-l, Wang X-c. Structure and thermal stability of microencapsulated phase-change materials. *Colloid Polym Sci* 2004;282:330–6.
- [259] Tang B, Wu C, Qiu M, Zhang X, Zhang S. PEG/SiO<sub>2</sub>-Al<sub>2</sub>O<sub>3</sub> hybrid form-stable phase change materials with enhanced thermal conductivity. *Mater Chem Phys* 2014;144:162–7.
- [260] Cai Y, Zong X, Zhang J, Du J, Dong Z, Wei Q, et al. The improvement of thermal stability and conductivity via incorporation of carbon nanofibers into electrospun ultrafine composite fibers of lauric acid/polyamide 6 phase change materials for thermal energy storage. *Int J Green Energy* 2014;11:861–75.
- [261] Fauzi H, Metselaar HSC, Mahlia TMI, Silakhori M, Ong HC. Thermal characteristic reliability of fatty acid binary mixtures as phase change materials (PCMs) for thermal energy storage applications [4/5/]. *Appl Therm Eng* 2015;80:127–31, [4/5/].
- [262] Rathod MK, Banerjee J. Thermal stability of phase change materials used in latent heat energy storage systems: a review [2/]. *Renew Sustain Energy Rev* 2013;18:246–58, [2/].
- [263] Ferrer G, Solé A, Barreneche C, Martorell I, Cabeza LF. Review on the methodology used in thermal stability characterization of phase change materials [10/]. *Renew Sustain Energy Rev* 2015;50:665–85, [10/].
- [264] Chandel SS, Agarwal T. Review of current state of research on energy storage, toxicity, health hazards and commercialization of phase changing materials [1/]. *Renew Sustain Energy Rev* 2017;67:581–96, [1/].
- [265] Moreno P, Miró L, Solé A, Barreneche C, Solé C, Martorell I, et al. Corrosion of metal and metal alloy containers in contact with phase change materials (PCM) for potential heating and cooling applications [7/15/]. *Appl Energy* 2014;125:238–45, [7/15/].
- [266] Ferrer G, Solé A, Barreneche C, Martorell I, Cabeza LF. Corrosion of metal containers for use in PCM energy storage [4/]. *Renew Energy* 2015;76:465–9, [4/].
- [267] Noël JA, Allred PM, White MA. Life cycle assessment of two biologically produced phase change materials and their related products. *Int J Life Cycle Assess* 2015;20:367–76.
- [268] Ushak S, Gutierrez A, Galleguillos H, Fernandez AG, Cabeza LF, Grágeda M. Thermophysical characterization of a by-product from the non-metallic industry as inorganic PCM. *Sol Energy Mater Sol Cells* 1/2015;132:385–91.
- [269] Byung Chul S, Sang Done K, Won-Hoon P. Phase separation and supercooling of a latent heat-storage material [12/]. *Energy* 1989;14:921–30, [12/].
- [270] Shin HK, Park M, Kim H-Y, Park S-J. Thermal property and latent heat energy



- storage behavior of sodium acetate trihydrate composites containing expanded graphite and carboxymethyl cellulose for phase change materials [1/22/]. *Appl Therm Eng* 2015;75:978–83, [1/22/].
- [271] Dannemand M, Schultz JM, Johansen JB, Furbo S. Long term thermal energy storage with stable supercooled sodium acetate trihydrate [12/5/]. *Appl Therm Eng* 2015;91:671–8, [12/5/].
- [272] Garay Ramirez BML, Glorieux C, San Martin Martinez E, Cuautle JJA Flores. Tuning of thermal properties of sodium acetate trihydrate by blending with polymer and silver nanoparticles [1/25]. *Appl Therm Eng* 2014;62:838–44, [1/25/].
- [273] Ryu HW, Woo SW, Shin BC, Kim SD. Prevention of supercooling and stabilization of inorganic salt hydrates as latent heat storage materials. *Sol Energy Mater Sol Cells* 1992;27:161–72.
- [274] Godarzi AA, Jalilian M, Samimi J, Jokar A, Vesaghi MA. Design of a PCM storage system for a solar absorption chiller based on exergoeconomic analysis and genetic algorithm [1//]. *Int J Refrig* 2013;36:88–101, [1//].
- [275] Li H, Hsieh C, Goswami D. Conjugate heat transfer analysis of fluid flow in a phase-change energy storage unit. *Int J Numer Methods Heat Fluid Flow* 1996;6:77–90.
- [276] Solomon A. Melt time and heat flux for a simple PCM body. *Sol Energy* 1979;22:251–7.
- [277] Lacroix M. Numerical simulation of a shell-and-tube latent heat thermal energy storage unit. *Sol Energy* 1993;50:357–67.
- [278] Gong Z-X, Mujumdar AS. Finite-element analysis of cyclic heat transfer in a shell-and-tube latent heat energy storage exchanger. *Appl Therm Eng* 1997;17:583–91.
- [279] Zongqin Z, Bejan A. The problem of time-dependent natural convection melting with conduction in the solid. *Int J Heat Mass Transf* 1989;32:2447–57.
- [280] Velraj R, Seeniraj R, Hafner B, Faber C, Schwarzer K. Experimental analysis and numerical modelling of inward solidification on a finned vertical tube for a latent heat storage unit. *Sol Energy* 1997;60:281–90.
- [281] Inaba H, Dai C, Horibe A. Natural convection heat transfer of microemulsion phase-change-material slurry in rectangular cavities heated from below and cooled from above. *Int J Heat Mass Transf* 2003;46:4427–38.
- [282] Morgan K. A numerical analysis of freezing and melting with convection. *Comput Methods Appl Mech Eng* 1981;28:275–84.
- [283] Raj V Antony Aroul, Hariharan C, Velraj R, Seeniraj R. Numerical investigations of outward solidification in cylindrical PCM storage Unit [in]. *Appl Mech Mater* 2015:177–81.
- [284] Tao YB, He YL. Effects of natural convection on latent heat storage performance of salt in a horizontal concentric tube [4/1/]. *Appl Energy* 2015;143:38–46, [4/1/].
- [285] Sharifi N, Faghri A, Bergman TL, Andraka CE. Simulation of heat pipe-assisted latent heat thermal energy storage with simultaneous charging and discharging [1//]. *Int J Heat Mass Transf* 2015;80:170–9, [1//].
- [286] Tao YB, He YL, Liu YK, Tao WQ. Performance optimization of two-stage latent heat storage unit based on entransy theory [10//]. *Int J Heat Mass Transf* 2014;77:695–703, [10//].
- [287] Tao Y-B, Li M-J, He Y-L, Tao W-Q. Effects of parameters on performance of high temperature molten salt latent heat storage unit [11/5/]. *Appl Therm Eng* 2014;72:48–55, [11/5/].
- [288] Agyenim F, Hewitt N, Eames P, Smyth M. A review of materials, heat transfer and phase change problem formulation for latent heat thermal energy storage systems (LHTESS) [2//]. *Renew Sustain Energy Rev* 2010;14:615–28, [2//].
- [289] Agyenim F, Eames P, Smyth M. Heat transfer enhancement in medium temperature thermal energy storage system using a multitube heat transfer array. *Renew Energy* 2010;35:198–207.
- [290] Medrano M, Yilmaz M, Nogués M, Martorell I, Roca J, Cabeza LF. Experimental evaluation of commercial heat exchangers for use as PCM thermal storage systems. *Appl Energy* 2009;86:2047–55.
- [291] Trp A, Lenic K, Frankovic B. Analysis of the influence of operating conditions and geometric parameters on heat transfer in water-paraffin shell-and-tube latent thermal energy storage unit [11//]. *Appl Therm Eng* 2006;26:1830–9, [11//].
- [292] Akgün M, Aydın O, Kaygusuz K. Thermal energy storage performance of paraffin in a novel tube-in-shell system. *Appl Therm Eng* 4//2008;28:405–13.
- [293] Zhai XQ, Qu M, Li Y, Wang RZ. A review for research and new design options of solar absorption cooling systems. *Renew Sustain Energy Rev* 2011;15:4416–23.
- [294] Shinde G, Suresh P. A Review on Influence of Geometry and Other Initial Conditions on the Performance of a PCM Based Energy Storage System 2014.
- [295] Mokhtar M, Ali MT, Bräuniger S, Afshari A, Sgouridis S, Armstrong P, et al. Systematic comprehensive techno-economic assessment of solar cooling technologies using location-specific climate data. *Appl Energy* 2010;87:3766–78.
- [296] Al-Ugla AA, El-Shaarawi MAI, Said SAM, Al-Qutub AM. Techno-economic analysis of solar-assisted air-conditioning systems for commercial buildings in Saudi Arabia [2//]. *Renew Sustain Energy Rev* 2016;54:1301–10, [2//].
- [297] Calise F, d'Accadia MD, Vanoli L. Thermoeconomic optimization of solar heating and cooling systems. *Energy Convers Manag* 2011;52:1562–73.
- [298] Tsoutsos T, Anagnostou J, Pritchard C, Karagiorgas M, Agoris D. Solar cooling technologies in Greece. An economic viability analysis. *Appl Therm Eng* 2003;23:1427–39.
- [299] Kızılkan Ö, Şencan A, Kalogirou SA. Thermoeconomic optimization of a LiBr absorption refrigeration system. *Chem Eng Process: Process Intensif* 2007;46:1376–84.
- [300] Calise F. Thermoeconomic analysis and optimization of high efficiency solar heating and cooling systems for different Italian school buildings and climates. *Energy Build* 2010;42:992–1003.
- [301] Eicker U, Pietruschka D. Design and performance of solar powered absorption cooling systems in office buildings. *Energy Build* 2009;41:81–91.
- [302] Al-Alili A, Islam M, Kubo I, Hwang Y, Radermacher R. Modeling of a solar powered absorption cycle for Abu Dhabi. *Appl Energy* 2012;93:160–7.
- [303] Hang Y, Qu M, Zhao F. Economical and environmental assessment of an optimized solar cooling system for a medium-sized benchmark office building in Los Angeles, California. *Renew Energy* 2011;36:648–58.
- [304] Tsoutsos T, Aloumpi E, Gkouskos Z, Karagiorgas M. Design of a solar absorption cooling system in a Greek hospital. *Energy Build* 2010;42:265–72.
- [305] Misra R, Sahoo P, Gupta A. Application of the exergetic cost theory to the LiBr/H<sub>2</sub>O vapour absorption system. *Energy* 2002;27:1009–25.
- [306] Misra R, Sahoo P, Sahoo S, Gupta A. Thermoeconomic optimization of a single effect water/LiBr vapour absorption refrigeration system. *Int J Refrig* 2003;26:158–69.
- [307] Misra R, Sahoo P, Gupta A. Thermoeconomic evaluation and optimization of an aqua-ammonia vapour-absorption refrigeration system. *Int J Refrig* 2006;29:47–59.
- [308] Mateus T, Oliveira AC. Energy and economic analysis of an integrated solar absorption cooling and heating system in different building types and climates. *Appl Energy* 2009;86:949–57.